



**POLITÉCNICO
DE LISBOA**

Instituto Politécnico de Lisboa



ISEL
INSTITUTO SUPERIOR DE
ENGENHARIA DE LISBOA



ESCOLA SUPERIOR DE
TECNOLOGIA DA SAÚDE
DE LISBOA
INSTITUTO POLITÉCNICO DE LISBOA

Instituto Superior de Engenharia de Lisboa

Escola Superior de Tecnologia de Saúde de Lisboa

Effect of pulsed electric fields on cell viability and metabolism

Viviana Modesto Caldeira

Thesis to obtain the Master Degree in

Biomedical Engineering

Supervisors:

Luís Redondo (ISEL)

Cecília Ribeiro da Cruz Calado (ISEL)

February 2020



**POLITÉCNICO
DE LISBOA**

Instituto Politécnico de Lisboa



ISEL
INSTITUTO SUPERIOR DE
ENGENHARIA DE LISBOA



ESCOLA SUPERIOR DE
TECNOLOGIA DA SAÚDE
DE LISBOA
INSTITUTO POLITÉCNICO DE LISBOA

Instituto Superior de Engenharia de Lisboa

Escola Superior de Tecnologia de Saúde de Lisboa

Effect of pulsed electric fields on cell viability and metabolism

Viviana Modesto Caldeira

Thesis to obtain the Master Degree in

Biomedical Engineering

Supervisors:

Prof. Dr. Luís Redondo (ISEL)

Prof. Dr. Cecília Ribeiro da Cruz Calado (ISEL)

Examination Committee

Chairperson: Prof. Dr. Manuel Matos

Supervisor: Prof. Dr. Luís Redondo

Member of the Committee Prof. Dr. Luís Freire

Member of the Committee: Prof. Dr. Edna Ribeiro

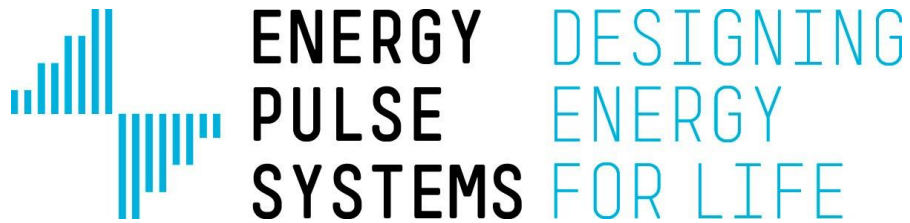
February 2020

[This page is intentionally left blank]

“The present is theirs. The future, for which I really worked, is mine.”

Nikola Tesla

[This page is intentionally left blank]



Effect of pulsed electric field on cell viability and metabolism

Viviana Modesto Caldeira

February 2020

This work was partially supported by *Instituto Politécnico de Lisboa, IDI&CA/IPL/2017/DrugsPlatf/ISEL, 2018/RenalProg/ISEL e 2020/NephroMD.*, in close cooperation with *Energy Pulse Systems*. The present work was conducted in the *Research & Development Laboratory in Health and Engineering at ISEL*, with all the Pulsed Electric Field Equipment provided by *Energy Pulse Systems*.

[This page is intentionally left blank]

Acknowledgments

I have been a dreamer for as long as I can remember, always full of ideas and always very eager to achieve them. Someone once said to me, that the idea can be really good but the best way to implement it is not always a straight line, we often have to make detours along the way, but in these detours, we learn more and make the idea even better. This person was Professor Luís Redondo.

Along the way numerous difficulties have arisen, which often seem to make the idea more difficult to achieve. I have also learned that in the big turning points of our lives it is natural for these difficulties to arise throughout evolution, but that they only strengthen our resilience and make us tougher. The person from whom I learned this was Professor Cecília Calado.

So, to Professor Luís Redondo, amazing professor, amazing human being, a true visionary, a scientist, an inspiration for me. I will always remember our first meeting and your openness while I was presenting this idea. Thank you for accepting this idea, for believing in me, for giving me the opportunity to work with you and your team.

Regarding Professor Cecília Calado, she is a true role model for all women in science. Thank you for accepting me in Biomedical Engineering Master's degree and for opening the door to your laboratory. Thanks for believing in me and for supporting me in the most difficult times.

To EPS and its team, especially to Duarte Rego for helping me and working by my side.

To ISEL, where from the moment I walked through those gates, it became my home, allowing me to learn and to evolve with a new scientific family. Thanks to this institution, which I am so proud to belong to, for giving equal opportunities to those who want to learn, proving that people should be valued due to their true worth, despite status, gender, or race.

I always said that, in this work, would be a special acknowledgement to João Mendes and Pedro Fernandes, because they represent a turning point in my life. Pedro Fernandes introduced me to ISEL and João Mendes led my steps to Professor Luis Redondo and helped me in so many ways.

To special professors:

To Manuel Matos, for helping me in so many moments, with ideas and materials. To Lina Vieira and Margarida Ribeiro, hope to work with you both in the future. To Luis Freire and Pedro Ferreira for teaching me about mechanics and for guiding me in the quest for physics knowledge.

To my friends at the lab, Maria João, Hélder, Bernardo, Ana, Pedro and Paulo, with a special thanks to Rúben Araújo and Luís Ramalhete for all the support.

To my best friend and partner in crime Marta Catarino, who was always by my side during so many nights in the lab and outside of it, along with our friend Sara Gomes. Thank you both. To my family inside ISEL, Pedro and Sofia. To all my friends and family outside ISEL, my cousins Pedro, Carlos, Sandra, Ana, Inês, Alexandre and Ana Margarida. To my friends Alexandre, Rafaela, Joana, Filipa, Mafalda, Vera, Bruno, Marco, Pedro, Fraga, João, Fátima, Ricardo, Carlos, Sofia and Tiago. Thank you for letting me belong to your lives and understanding my absence during this Master's degree. To my nephews from the heart, Francisca Garcia Massas, Francisca Fernandes, Beatriz, and Artur, you are the future, so please, do science.

To CVP Foz do Tejo's team for all the support. To my patients, for all the tolerance. To my students, hope to inspire you to see further.

And above all, thanks to my parents Bia Caldeira and Sidónio Caldeira, for giving me everything, including love and education, and for giving me the most important of all the heritage: vision. Thank you for being such visionaries, for seeing not only further, but beyond all things. You two are my true inspiration, and your intelligence and strength will always live in me.

Thank you all.

[This page is intentionally left blank]

Abstract

Pulsed Power (PP) is used in industry and biotechnology research due to its high voltage singularities. In biological systems, electroporation based on Pulsed Electric Fields (PEF) is an effective way of energy delivery, allowing controlled pulses with specific electrical parameters. Electroporation is the name given to the phenomenon where occurs a permeabilization of the plasma membrane and this process could be reversible or irreversible.

PEF on mammalian cells promotes diverse biological processes based on non-ligand agonists, that bypass receptors at plasma membrane while inducing diverse intracellular signalling pathways. The final biological effect will depend on the quantity and type of the targeted cells and PEF conditions and can be as diverse as the enhancement of cells proliferation capacity or in opposition, on cells death.

The main goal of this experimental work, based on *in vitro* techniques using fibroblast L929 cell line, was to evaluate three different conditions under PEF applications that may influence fibroblast metabolism. Firstly, the impact of electric fields magnitude (between 10 and 15kV/cm) with different pulses, secondly the effect of different fibroblasts concentration on the assay (between 50,000 to 1500 x10³ cells per 800µL of Dulbecco's Phosphate-Buffered Saline - DPBS) and finally to evaluate the effect of repeated PEF applications (between 1 to 3 repetitions) on cells viability and proliferative capacity. To achieve the latter, three experiments were designed. The first experiment evaluated the impact of PEF on cell viability immediately, at 48 hours and at 72 hours after the assay. The second experiment studied the influence of cell density and its interference on the electric field applied, on cell lysis and on cell viability immediately and 72 hours after the assay. The third experiment entails three assays which assessed the weight of applying consecutively PEF with 48 hours intervals on different cell density samples and the maintenance of cell viability upon each application – immediately, at 48 hours and 96 hours after the assay.

The specific energy (*Ws*) and temperature increase (ΔT) of each biological sample were calculated after each experiment to guarantee that was no cell overheating. The DPBS used as conductive solution, the cell pellet and the culture medium of all samples after PEF application were submitted to Fourier Transformed Infrared (FTIR) spectroscopy, the data obtain was then processed by Unscrambler X software and submitted to Principal Component Analysis (PCA). Regarding cell count and cell viability common statistical analysis (average and standard deviation) and Analysis of Variance – ANOVA – single factor evaluation was performed.

The data obtained demonstrates that a high electric field (15kV/cm with 1 pulse) promoted almost whole cell lysis, representing a non-thermal irreversible electroporation (NTIRE), where the lowest electric field (10kV/cm with 2 pulses or 10 pulses) did not affected with stactical significance cell viability. In addition, the lowest field with 5 pulses (10kV/cm with 5 pulses) was the most promising since the cells showed acceptable FTIR spectroscopy signals without major effects on initial cell viability. Moreover, it was observed that larger cells densities during PEF application guarantee a higher cell viability, being the ideal number between 1,500x10³ and 500x10³ cells per 800µL of assay. Furthermore, the repeated application of PEF in fibroblasts affected cell viability, being acceptable one or two repetitions with intervals not inferior to 48h between applications.

According to statistical data the assays are verifiable and reproducible, but in the future, more control samples are needed. This work confirms the potential of PEF in mammalian cells research, since it avoids overheating in living matter, showing that further studies are needed, in this area.

Keywords

Pulsed power, pulsed electric fields, electroporation, metabolic state, cell culture

Resumo

A Potência Pulsada (PP) é amplamente usada na indústria e também em investigação biotecnológica devido às suas singularidades de alta tensão. Em sistemas biológicos, a eletroporação baseada em Campos Elétricos Pulsados (CEP) é uma forma eficaz de aplicar energia, permitindo pulsos controlados com parâmetros elétricos específicos. Eletroporação é o nome dado ao fenômeno onde ocorre uma permeabilização da membrana citoplasmática e este processo pode ser reversível ou irreversível.

Os CEP em células animais promovem diversos processos biológicos baseados em agonistas não ligantes, que contornam os recetores na membrana plasmática enquanto induzem diversas vias de sinalização intracelular. O efeito biológico final dependerá da quantidade e tipo de células-alvo e das condições do campo elétrico pulsado e pode ser tão distinto quanto o aumento da capacidade da proliferação celular ou, pelo contrário, a morte celular.

O principal objetivo deste trabalho experimental, baseado em técnicas *in vitro* utilizando a linha celular de fibroblastos L929, foi avaliar três condições diferentes com aplicações de CEP que podem influenciar o metabolismo dos fibroblastos.

Primeiro, foi avaliado o impacto dos campos elétricos (entre 10 e 15kV/cm) com diferentes impulsos, seguidamente, o efeito de diferentes concentrações de fibroblastos no ensaio (entre 50000 a 1500×10^3 células por 800 μ L de *Dulbecco's Phosphate-Buffered Saline Dulbecco - DPBS*) e, finalmente o efeito de aplicações repetidas de PEF (entre 1 a 3 repetições) na viabilidade e capacidade proliferativa das células. Para isto, desenharam-se três experiências. A primeira experiência avaliou o impacto do CEP na viabilidade celular imediatamente, 48 horas e 72 horas após o ensaio. A segunda experiência estudou a influência da densidade celular e sua interferência no campo elétrico aplicado, na lise celular e na viabilidade celular imediatamente e 72 horas após o ensaio. A terceira experiência envolve três ensaios que avaliaram o impacto da aplicação consecutiva de CEP com intervalos de 48 horas em diferentes amostras de densidade celular e a manutenção da viabilidade celular em cada aplicação - imediatamente, 48 horas e 96 horas após o ensaio.

A energia específica (Ws) e o aumento da temperatura (ΔT) de cada amostra biológica foram calculados após cada experiência para garantir a ausência de sobreaquecimento celular. O *DPBS* utilizado como solução condutora, o *pellet* celular e o meio de cultura de todas as amostras após a aplicação do PEF foram submetidos à espectroscopia de infravermelho por transformada de Fourier (*FTIR*), os dados obtidos foram então processados pelo software *Unscrambler X* e submetidos a Análise de Componentes Principais (*PCA*). Em relação à contagem e viabilidade celular, foram realizadas, estatística comum (média e desvio padrão) e análise de variância - *ANOVA - single factor evaluation*.

Os dados obtidos demonstraram que, um campo elétrico elevado (15kV/cm com 1 impulso) promoveu quase por completo a lise celular, representando uma eletroporação não térmica irreversível (*NTIRE*) e o menor campo elétrico (10kV/cm com 2 impulsos e 10 impulsos) não afetou pertinentemente a viabilidade celular, mas ocorreu libertação de componentes intracelulares para o meio condutor. Consequentemente, o campo mais baixo (10kV/cm com 5 impulsos) foi o mais promissor, uma vez que as células mostraram sinais de espectroscopia *FTIR* aceitáveis sem grande impacto na viabilidade celular inicial. Além disso, observou-se ainda que um maior número de células tem um efeito relevante nas aplicações CEP, observando-se que maior densidade celular garante uma melhor viabilidade, sendo o número ideal entre 1500×10^3 e 500×10^3 (em 800 μ L de *DPBS*). A aplicação repetida de CEP em células animais também afeta a viabilidade celular, sendo aceitável uma ou duas repetições com intervalos não inferiores a 48h entre aplicações.

De acordo com os dados estatísticos, os ensaios são verificáveis e reprodutíveis, mas no futuro, mais amostras de controlo serão necessárias. Este trabalho confirma o potencial do CEP na investigação em células animais, uma vez que evita o supraaquecimento na matéria viva, mas revelando que mais estudos são necessários, nesta área.

Palavras-chave

Potência pulsada, campos elétricos pulsados, eletroporação, estado metabólico, cell culture

Contents

Acknowledgments	viii
Abstract	x
<u>Resumo</u>	xi
List of Figures	xv
List of Tables	xxi
List of Abbreviations	xxii

Chapter 1

1. Aims & Thesis Structure	1
----------------------------------	---

Chapter 2

2. Introduction	3
2.1. Importance of plasma membrane	3
2.2. Why use fibroblasts?	4
2.3. Why use Pulsed Electric Fields based on Pulsed Power?	5
2.4. Why use the electroporation phenomenon?	6

Chapter 3

3. Cell culture & PEF	8
3.1. Cell culture	8
3.1.1. Basics on cell culture	8
3.1.1.1. Culture room – How to work with cells	8
3.1.1.2. Primary culture – How to obtain cells	9
3.1.1.3. Subculture – How to grow cells	9
3.1.1.4. Cell cycle inside a culture	10
3.1.1.5. Cell types, lines and strains	12
3.1.1.6. Culture media and other solutions	13
3.1.2. How to grow and maintain Fibroblasts L929	16
3.2. Pulsed Electric Fields (PEF) and Electroporation	17
3.2.1. Pulsed Electric Fields generation	17
3.2.2. The electroporation phenomenon	19
3.2.3. Electroporation and Biotechnology	21
3.2.3.1. Biotechnological applications	21
3.2.3.2. Biomedical applications	24
3.3. Analytical methods	28
3.3.1. Trypan blue exclusion assay for cell viability and density	28
3.3.2. FTIR spectroscopy for component analysis	29

Chapter 4

4. Materials & Methodologies	35
4.1. Preliminary tests	35
4.2. Cell line and cryopreservation	35
4.3. Cell culture – thaw and expansion	36
4.4. PEF experiments	38
4.4.1. Experiment 1 – Effect of PEF variations	40
4.4.2. Experiment 2 – Effect of cell density	43

4.4.3. Experiment 3 – Effect of repeated PEF	46
4.4.3.1. First Assay (t=0h)	46
4.4.3.2. Second Assay (t=48h)	48
4.4.3.3. Third Assay (t=96h)	51

Chapter 5

5. Results & Discussion	55
5.1. Preliminary tests	55
5.2. Experiment 1 – Effect of PEF variations	59
5.2.1. Overview	59
5.2.2. Variations in electrical parameters and temperature increase	60
5.2.3. Cells microscope observation and cell viability	61
5.2.4. FTIR spectroscopy	63
5.2.5. Conclusions on experiment 1	69
5.3. Experiment 2 – Effect of cell density	70
5.3.1. Overview	70
5.3.2. Variations in electrical current and temperature increase for different cell density	70
5.3.3. Cell counting and cell viability	73
5.3.4. FTIR spectroscopy	76
5.3.5. Conclusions on experiment 2	80
5.4. Experiment 3 – Effect of repeated PEF applications	81
5.4.1. A Brief Overview of the experiment	81
5.4.2. First Assay (t=0h)	81
5.4.2.1. Variations in electrical current and temperature increase during PEF application.....	82
5.4.2.2. Cell counting and cell viability	83
5.4.2.3. FTIR spectroscopy	83
5.4.3. Second Assay (t=48h)	84
5.4.3.1. Variations in electrical current and temperature increase during PEF application.....	84
5.4.3.2. Cell counting and cell viability	85
5.4.3.3. FTIR spectroscopy	86
5.4.4. Third Assay (t=96h)	87
5.4.4.1. Variations in electrical current and temperature increase during PEF application.....	87
5.4.4.2. Cell counting and cell viability	88
5.4.4.3. FTIR spectroscopy	89
5.4.5. Conclusions on experiment 3	90

Chapter 6

6. Conclusions, Challenges & Future Work	93
--	----

Chapter 7

7. Bibliography	95
-----------------------	----

[This page is intentionally left blank]

List of Figures*

Figure 2.1. Schematic diagram of a Typical Mammalian Cell [4].	3
Figure 2.2. Schematic diagram of cell membrane [9].	4
Figure 2.3. Left: Active Fibroblasts in adherent phase [2]. Right: Active Fibroblasts observed by fluorescence technique under the microscope [11].	4
Figure 2.4. Marx generator circuit with several levels.	5
Figure 2.5. Cell membrane and phospholipid structure (a) [18] and Phospholipid behavior to electroporation (b) [17].	6
Figure 2.6. Example of Industrial PEF equipment from the Portuguese company <i>Energy Pulse Systems</i> .	6
Figure 3.1. Scheme of how to obtain a cell line.	9
Figure 3.2. Growth curve of adherent cells. (A) Lag phase; (B) Logarithmic phase, where the arrow represents the end of this exponential phase; (C) Stationary phase. The arrow represents the ideal moment of passage. Adapted from [23].	11
Figure 3.3. Graphics representing the ideal point for the first passage in the end of Generation 2 (G2) and for the second passage in the end of generation 4 (G4). Adapted from [23].	11
Figure 3.4. Graphic representing the typical cell senescence curve in cells with finite growth. The subculture is viable until Fifty generations, which corresponds to approximately 4 months. Adapted from [23].	12
Figure 3.5. Graphic representing the moment of crisis, in which will result cell death or the establishment of the cell line with infinite growth. D represents the diploid characteristics of the cells and, H the heteroploidy characteristics of the cells with infinite growth. Adapted from [23].	13
Figure 3.6. L929 fibroblastic cells above 80% confluence, image obtain under the optical microscope.	16
Figure 3.7. Simplified negative Marx generator topology, where Cn represents the capacitor, Dn represents the diode and Scn represents the switch [34].	17
Figure 3.8. Typical voltage waveform in PEF application [34].	17
Figure 3.9. Illustrations of the batch treatment chamber [36].	17
Figure 3.10. Electroporation cuvettes. Left: 90 μL capacity, 1 mm gap between electrodes, used for bacteria. Middle: 400 μL capacity, 2 mm gap between electrodes, suitable for yeast. Right: 800 μL capacity, 4 mm gap between electrodes, appropriate for mammalian cells [37].	19
Figure 3.11. Left: space-filling model and structural formula of the SOPC (1-stearoyl-2-oleoyl-phosphatidylcholine) molecule, a typical membrane lipid. Right: a bilayer of such lipids in an aqueous electrolyte solution [17].	20
Figure 3.12. Left: change in lipid bilayer energy caused by formation of an aqueous pore, plotted as a function of the pore radius and voltage across the bilayer. Right: bilayer without pores (A), with a hydrophobic pore (B), its reversible transition into a metastable hydrophilic pore (C), and its irreversible transition into an unstable self-expanding hydrophilic pore (D; at membrane voltages above ~ 500 mV) [17].	20

Figure 3.13. A molecular dynamics simulation of an aqueous pore forming in a lipid bilayer exposed to an electric field perpendicular to the bilayer plane. Left: the intact bilayer. Middle: water molecules penetrate the bilayer, forming a “water wire.” Right: the adjacent lipids reorient with their heads toward the water molecules in the bilayer, stabilizing the aqueous pore and allowing the ions to enter [13].	20
Figure 3.14. The induced transmembrane voltage (ITV) and electroporation of an irregularly shaped Chinese-hamster-ovary (CHO) cell: (A) changes in fluorescence of di-8-ANEPPS reflecting the ITV, with dark regions corresponding to membrane depolarization and bright regions corresponding to membrane hyperpolarization; (B) fluorescence of propidium iodide (PI), reflecting transport of PI across the membrane; (C) ITV along the path shown in (A) as measured (black) and as predicted by numerical computation (gray); (D) fluorescence of PI along the path shown in (A) [17].	21
Figure 3.15. Microbial deactivation [38].	21
Figure 3.16. Selective release of bacteria proteins using electroporation [19].	22
Figure 3.17. Gene electrotransfer technique [42].	24
Figure 3.18. Direct microscopical observation of electrotransfer of PI, siRNA and pDNA into murine melanoma cell [42].	25
Figure 3.19. ECT steps [55].	26
Figure 3.20. PDGF concentration ($\mu\text{g}/\text{mL}$) in different processing conditions [64].	27
Figure 3.21. Hemocytometer – Neubauer chamber, and the area for cell counting [67].	28
Figure 3.22. a) The harmonic oscillator models. B) Table illustrating the relationship between vibrations of some functional groups, atomic masses, and bond strength. C) Fundamental vibrational modes of a free water molecule detectable at specific frequency values of the electromagnetic spectrum [72].	30
Figure 3.23. Above, the transfectance technique that couple’s absorption and reflection through the sample, and below, the attenuated total reflectance (ATR) technique [72].	31
Figure 3.24. Summary of the vibrational frequencies of some functional groups, associated with a wavenumber, in molecules in the mid-IR region of the electromagnetic spectrum [72].	32
Figure 3.25. Spectra obtained by FTIR, identifying the peaks where each type of biochemical component belongs. In the image is visible three different regions; the stretching region, where are Amide A and B and Lipids; the double bonds stretching region, where are Amide I and II and phospholipid esters; and the Fingerprint region, where are Amide III, diverse proteins like collagen and others, DNA and RNA.	33
Figure 4.1. Summary scheme of all preliminary tests.	35
Figure 4.2. Left: Laminar vertical flow cabinet. Right: Work inside the laminar flow cabinet, using the automatic motorized pipette to remove culture medium.	36
Figure 4.3. Cell culture in T-flask observed by the inverted phase microscope Zeiss Axiovert 40 CFL.	36
Figure 4.4. Hemocytometer (before assembly) improved Neubauer chamber from Hirschmann-Laborgeräte.	37
Figure 4.5. Two different T25-Flasks (25cm^2 of adhesion surface) with Nunclon Delta treated surface for cell culture.	37

Figure 4.6. EPULSOS-LPM 1B-10 equipment inside culture room for PEF applications.	38
Figure 4.7. Electroporation cuvette from VWR with a capacity of 0.8 to 1mL.	38
Figure 4.8. 24-well adherent Nunc culture plate.	39
Figure 4.9. Si microplates of 96-well (left) and 384-well (right) for FTIR analysis.	39
Figure 4.10. FTIR equipment: VERTEX 70 spectrometer from Bruker equipped with an HTS-XT module, also from Bruker, connected to a computer for data acquisition obtained by OPUS software, from Bruker.	39
Figure 4.11. PEF equipment display to set the electrical parameters.	40
Figure 4.12. Digital oscilloscope, from Lecroy model WaveAce 224 – 200MHz, to show graphically varying signals and control the waveform of each pulse.	40
Figure 4.13. Schematic image of the sown cells in a Nunc® 24-well adherent culture plate.	42
Figure 4.14. Schematic image of the Si 96-well microplate for FTIR analysis in experiment 1, immediately after PEF. A1 to E3 are the samples of DPBS without the cells. From A(P) to E(P) there are samples of cells pellet. PBS is pure DPBS without contacting cells, for control of single DPBS signal versus DPBS that contacted with cells.	42
Figure 4.15. Schematic image of the sown cells in the two Nunc® 24-well adherent culture plate, in experiment 2.	45
Figure 4.16. Schematic image of the Si 384-well microplate for FTIR analysis in experiment 2, immediately after PEF. A1 to E3 are the samples of DPBS without the cells. A1(P) to E+(P) are the samples of cell pellet. PBS is the DPBS pure with no cell contact for spectra comparison with the supernatant experimental groups.	45
Figure 4.17. Schematic image of the sown cells in a Nunc® 12-well adherent culture plate, in 1 st assay in experiment 3.	47
Figure 4.18. Schematic image of the sown cells in a Nunc® 12-well adherent culture plate, in 2 nd assay of experiment 3.	50
Figure 4.19. Schematic image of the Si 384-well microplate for FTIR analysis in the 2 nd assay of experiment 3, immediately after PEF: A1 to C- are the samples of DPBS without the cells. A1(P) to C-(P) are the samples of cell pellet, and analysis of the culture medium of cells from 1 st assay at 48h: blue A1 to C-. PBS is the DPBS pure and blue CM is complete medium with no cell contact, both for spectra comparison with the experimental groups.	50
Figure 4.20. Schematic image of the sown cells in a Nunc® 12-well adherent culture plate, in the 3 rd assay of experiment 3.	53
Figure 4.21. Summary scheme of all experiences.	54
Figure 5.1. Schematic image of a cuvette used in the electroporation test.	55
Figure 5.2. Growth expansion curves. The top curve is the normal curve of adherent cells compared with the growth expansion curve for fibroblasts L929 (bottom curve), when starting with a seeding of 1×10^5 in a T-25 flask (25cm^2). In the first 12 hours it can be seen the lag phase (A), and then a logarithmic phase of exponential growth that starts after 12 hours culture and stops at 96 hours, giving rise to the stationary phase (C). In a T-25 flask with L929 cells, at 48h they were already 10 times more than the initial number, at 72h they reached approximately 2,5 to 4 million with a confluence of 85% -98% (lack of adherent surface and space) at 96 hours they reached approximately 4.5 million.	57

Figure 5.3. Comparing spectra from different types of media analyzed in a 96 well plate. Blue spectra: DPBS by Lonza; Green spectra FBS inactivated; Yellow spectra: Lonza DMEM; Purple spectra: Sigma DMEM; Orange spectra: Lonza DMEM with FBS; Pink spectra: Sigma DMEM with FBS.	58
Figure 5.4. Spectra analysis (DPBS) in a 96-well plate.	58
Figure 5.5. Comparing different types of medium with spectra analysis in a 384-well plate. Blue spectra: DPBS by Lonza; Green spectra FBS inactivated; Yellow spectra: Lonza DMEM; Purple spectra: Sigma DMEM; Orange spectra: Lonza DMEM with FBS; Pink spectra: Sigma DMEM with FBS.	58
Figure 5.6. Spectra of supernatant (DPBS) in a 384-well plate.	58
Figure 5.7. Image obtained by Picoscope6, representing the real pulse applied. The controlled pulse represents a well-defined area, almost a rectangle, that shows an application time of 5 μ s with a controlled Voltage and Current.	59
Figure 5.8. Cells image obtained by the inverted phase microscope, of group A, or negative control group, 72h after experiment 1. Left: well A1 with confluence over 98%. Middle: well A3 with confluence over 99%. Right: well A2 overconfluent.	61
Figure 5.9. Cells image obtained by the inverted phase microscope, immediately after PEF application ($t=0$ h). Left: Group D (D1) where is observed an increase of ECM density, making it almost gelatinous to the eye. This shows the result of exposure to a higher energy field (15kV/cm) where almost 90% of cells are non-viable by plasma membrane lysis. Right: Group B (B2) there was a change in cell size, making it smaller, due to reversible electroporation where there was a loss of intracellular water. This last process was reversible, and the cells start recovering their shape at 48h.	61
Figure 5.10. Cells image obtained by the inverted phase microscope, 48h after PEF application, well B2 from group B, recovered cell shape, being an example of reversible electroporation, where cells open pores in their membranes and in the one hand can release some components to extracellular environment turning themselves shrunken or in the other hand can let the passage of some components into the intracellular medium turning themselves turgid, but in both phenomena, the recovery of membrane is possible.	62
Figure 5.11. Cells image obtained by the inverted phase microscope, at 72h where is visible a migration of almost all cells of group B (B2) to a unique spot, placing themselves on top of each other.	62
Figure 5.12. Cells image obtained by an optical microscope, to perform a blue trypan exclusion method assay. It can be seen, the hemocytometer geometrical lines with the counting squares, and living cells correspondent to blue circles and dead cells corresponding to dark blue dots.	62
Figure 5.13. Left: Spectra of supernatant (DPBS) of different groups, with different electrical parameters, immediately after PEF application, only group A is the control group without any PEF application. Right: Typical spectra of DPBS. All spectra were submitted to atmospheric compensation and baseline correction.	64
Figure 5.14. Left: Spectra analysis of the culture medium of the cells 48 hours after PEF application. Middle: Spectrum of DMEM. Right: Spectra analysis of the culture medium of the cells 72 hours after PEF application. All spectra were submitted to atmospheric compensation and baseline correction.	65
Figure 5.15. IR spectra of supernatant (A) and cell pellet (B) of the assay after PEF, respectively, and the spectra of culture media after plating cells after the PEF experiment and grown for 48 h (C) or 72h (D).	66

Figure 5.16. Average and corresponding standard deviation of the sum of absorbances of whole IR spectra of triplicated PEF assays, concerning the supernatant (A) and the cell pellet (B) of the assay immediately after PEF, respectively, and the IR spectra of culture media from , and the spectra of culture media after plating cells after the PEF experiment, and grown for 48h (C) or 72h (D). The spectra relative to cell pellet was not conducted in triplicate.	66
Figure 5.17. PCA of baseline corrected spectra of supernatant (A) and cell pellet of PEF assays (B). The Hotelling's ellipse at 5% is represented. Graph A, symbols corresponds to: blue square, pure PBS; red circle, negative control, i.e. without PEF; green triangle, 6000KV/cm; light blue lozenge, 4000 KV/cm 2P; brown inverted triangle, 4000 KV/cm 10P; grey lozenge, 4000 KV/cm 20P. Graph B, symbols corresponds to: blue square, negative control; red circle, 6000KV/cm ; green triangle, 4000 KV/cm 2P; light blue lozenge, 4000 KV/cm 10P; brown inverted triangle, 4000 KV/cm 20P.	67
Figure 5.18. PCA of baseline corrected spectra of culture media of cells plated and grown for 48h (Top) and 72h (Bottom). The Hotelling's ellipse at 5% is represented. Symbols correspond to: blue square, DMEM media; red circle, negative control, i.e. without PEF; green triangle, 6000KV/cm; light blue lozenge, 4000 KV/cm 2P; brown inverted triangle, 4000 KV/cm 10P; grey lozenge, 4000 KV/cm 20P. Graph B, symbols correspond to: blue square, negative control; red circle, 6000KV/cm ; green triangle, 4000 KV/cm 2P; light blue lozenge, 4000 KV/cm 10P; brown inverted triangle, 4000 KV/cm 20P.	68
Figure 5.19 Average number of cells and cells viability of assays conducted with different cells density in relation to the assay without PEF. Data are due to assays immediately after PEF or after 72htrs of culture after PEF. The error bars are the average value of standard deviations of all assays.	75
Figure 5.20. Left: Spectra of supernatant (PBS) of the 1,000,000 cells group, immediately after PEF application, and the corresponding positive and negative control. Middle: Spectrum of a typical spectra of PBS. Right: Spectra of supernatant (PBS) of the 50,000 cells group, immediately after PEF application and the corresponding positive and negative control.	76
Figure 5.21. Left: Spectra of culture medium of 1000,000 cells, 72H after PEF application, and the corresponding positive and negative control. Middle: Spectrum of non-consumed culture medium. Right: Spectra of culture medium of 50,000 cells, 72H after PEF application, and the corresponding positive and negative control.	77
Figure 5.22. Left: IR spectra of supernatant (A) and cell pellet (B) of the assay after PEF, respectively, and the spectra of culture media after plating cells after the PEF experiment and grown for 72h (C). Right: Average of the sum of absorbances of whole IR spectra of triplicated PEF assays, concerning the supernatant (A) and the cell pellet (B) of the assay immediately after PEF, respectively, and the IR spectra of culture media from after plating cells from the PEF experiment, and grown for 72h (C).	77
Figure. 5.23. PCA of normalized second derivative spectra of supernatant (A, B) and cell pellet (C, D) immediate after PEF. The Hotelling's ellipse at 5% is represented.	79
Figure. 5.24. PCA of normalized second derivative FTIR spectra of culture media from cultures grown for 72hrs, in function if cells were submitted or not to PEF or lysed through cycles of freezing and defrost (A) or in function of the number of cells considered in the PEF assay (B). The Hotelling's ellipse at 5% is represented.	80
Figure. 5.25. Left: Spectra of DPBS immediately after PEF, when compared with the control groups and DPBS not exposed to cells or PEF. Right: Spectra of culture media immediately after PEF, when compared with the control groups and medium not exposed to cells or PEF.	83
Figure. 5.26. Left: Spectra of DPBS immediately after the 2 nd repetition of PEF, when compared with the control groups and DPBS not exposed to cells or PEF. Right: Spectra of culture media of the 2 nd assay, when compared with the control groups and medium not exposed to cells or PEF.	86

Figure. 5.27. Left: Spectra of DPBS immediately after the 3rd repetition of PEF, when compared with the control groups and DPBS not exposed to cells or PEF. Right: Spectra of culture media of the 3rd assay, when compared with the control groups and medium not exposed to cells or PEF. 89

Figure. 5.28. PCA of normalized second derivative FTIR spectra of supernatant DPBS, pellet and Culture medium of 1st assay, 2nd assay and 3rd assay. 91

*All figure captions are preceded by the chapter number in which the figure appears in.

List of Tables**

Table 3.1. Main compositions of saline solutions. Adapted from [23].	14
Table 3.2. Different types of media for cell culture [23].	15
Table 3.3. Example of different dilution factors in trypan blue exclusion method assay.	28
Table 5.1. Electrical parameters and calculations for Groups A, B, C, D and E.	60
Table 5.2. Cell viability immediately after PEF application, after 48hours and 72 hours.	63
Table 5.3. Group A (1,000,000 cells/800 μ L PBS).	71
Table 5.4. Group B (500,000 cells/800 μ L PBS).	71
Table 5.5. Group C (250,000 cells/800 μ L PBS).	71
Table 5.6. Group D (100,000 cells/800 μ L PBS).	72
Table 5.7. Group E (50,000 cells/800 μ L PBS).	72
Table 5.8. Cell counting by a trypan blue exclusion assay, immediately after PEF and 72h after.	73
Table 5.9. Statistical data for cell counting and cells viability, showing Average and Standard Deviation for each group of experiment 2 in relation to the negative control (i.e. conducted without PEF).	74
Table 5.10. Average and standard deviation of the sum of absorbances of whole IR spectra of triplicated PEF assays, concerning the supernatant and the cell pellet of the assay immediately after PEF, and from culture media grown for 72h.	78
Table 5.11. First Assay. Groups A; B; C (1,500,000; 1,000,000; 500,000 cells/800 μ L PBS).	82
Table 5.12. Cell counting by a trypan blue exclusion method, immediately after PEF and 48h after.	83
Table 5.13. Second Assay. Groups A; B; C (1,500,000; 1,000,000; 500,000 cells/800 μ L PBS).	84
Table 5.14. Cell counting by a trypan blue exclusion method, immediately after PEF and 48h after.	85
Table 5.15. Third Assay. Groups A; B; C (1,500,000; 1,000,000; 500,000 cells/800 μ L PBS).	87
Table 5.16. Cell counting by a trypan blue exclusion method, immediately after PEF and 48h after.	88
Table 5.17. Average number of cells and cells viability of assays conducted with different cells density in relation to the assay without PEF.	89

**The numbering of all tables is preceded by the numerical chapter in which they appears.

List of Abbreviations

ANOVA	Analysis of Variance
ATP	Adenosine Triphosphate
AV	Average (when applied for statistical data)
BME	Eagle Basal medium
BHK	Human hamster kidney cells
CAM	Cell adhesion molecules
Cas9	CRISPR associated protein 9
CMRL	Connaught Medical Research Laboratories medium
CRISPR	Clustered Regularly Interspaced Short Palindromic Repeats
DF	Dilution factor
DMEM	Dulbecco's Modified Eagle Medium
DMSO	Dimethyl Sulfoxide
DNA	Deoxyribonucleic Acid
DNase	Deoxyribonuclease (enzyme)
DPBS	Dulbecco's Phosphate Buffered Saline
DT	Doubling Time
ECM	Extracellular Matrix
ECT	Electrochemotherapy
EDTA	Ethylenediamine tetraacetic acid
EGTA	Ethylene glycol-bis(2-aminoethylether)
FBS	Fetal Bovine Serum tetraacetic acid
FTIR	Fourier-Transform Infrared
GET	Gene electrotransfer
GMEM	Glasgow minimum essential medium
HeLa	Henrietta Lacks
HEPES	(4-(2-hydroxyethyl)-1-piperazineethanesulfonic acid)
HV	High Voltage
IDPEF	Intermittently delivered pulsed electric fields
MEM	Minimum essential medium
nsEP	nanosecond high-voltage electrical pulses
NTIRE	Nonthermal irreversible electroporation
PCA	Principal Component Analysis
PBS	Phosphate Buffered Saline
PEF	Pulsed electric field
PP	Pulsed Power
RNA	RiboNucleic Acid
RPMI 1640	Roswell Park Memorial Institute Medium
SD	Saturation Density
SD	Standard Deviation (when applied for statistical data)
sgRNA	single guide RNA
SUM	Summation (when applied for statistical data)
TALENS	Transcription activator-like effector nucleases

Chapter 1

1. Aims & thesis structure

This work, which represents an *in vitro* study, aims to take a specific cell line - L929 Fibroblasts – and study their behaviour when exposed to specific pulsed electric fields (PEF).

This topic is, therefore, a challenge since it was a self-proposed work and is quite interdisciplinary. The application of PEF to biological systems, called Bioelectrics, is fraught with complexity and its interaction and complementarity will, in the end, be the perfect interface between electricity and biology, which in itself could be a raw definition of what biomedical engineering is all about. However, this interaction requires a very well-structured work, both in the development of laboratory protocols and in the presentation of all data, but also in its explanation. Thus, this dissertation will be divided in the following Chapters:

- **Chapter 1** is the present page and represents the aims of the thesis, as well as its structure, explaining briefly what is discussed in each chapter.
- **Chapter 2** is the theoretical introduction to the theme.
- **Chapter 3** is the theoretical foundation and *State-of-the-art* – “Cell culture and Pulsed Electric Fields” - presenting the *state-of-the-art* of all techniques used in the present work, as such as PEF characterization and its interaction with mammalian cells. This Chapter also meant to explore the *state-of-the-art* on cell culture in general but targeting fibroblasts, as part of the connective tissue, specifically the L929 line; and to explore the *state-of-the-art* of Pulsed Power, electroporation, and their main applications. There is also a brief overview on trypan blue exclusion method assay and FTIR analysis.
- **Chapter 4** regards the materials and methodologies used in this *in vitro* study. Here three different experiments, with different protocols, are described to give relevant information about PEF applications. The first experiment is called the “Effect of PEF variations”, the second experiment is the “Effect of cell density” and the third experiment is the “Effect of repeated PEF applications” and consists of three different assays. For all PEF experiments, two analytical methods are chosen; one is trypan blue exclusion method assay of cells, before and after PEF exposure, and then in culture; the other one is FTIR Spectroscopy using *OPUS* software and then processing the data in *Unscramber X*. Before these experiments, the protocols for thawing and expansion of the cryopreserved line in question, are presented.
- **Chapter 5** is the chapter dedicated to presenting results analysis and its discussion for the three different experiments. This chapter also has a description of all calculations and preparatory tests carried out before the three experiments, as well as the characterization of the spectra for different solutions and media.
- **Chapter 6** represents the final conclusions of this work, presenting limitations, possible *bias*, and a personal reflexion about this research as well as ideas for future work.
- **Chapter 7** presents the bibliographic references and scientific readings, that supported this work.

At the end, it is the principal aim of this work to innovate, hoping to contribute to a better understanding of the interaction between PEF and Biology.

[This page is intentionally left blank]

Chapter 2

2. Introduction

The cell is the basic unit of life and can be found in living beings in different forms and types. It constitutes the smallest portion that an organism can be reduced to, while maintaining the characteristics of life [1]. As such, mammalian cells are constantly used, in *in vitro* studies, for all different purposes and areas, like health investigation research or technology.

Cells provide protection and support, allow movement (muscle cells are examples), provide means of communication, metabolize, and release energy and ensure heredity [1-2].

Cells are constituted by a cytoplasmic membrane, also called plasma membrane, which controls the exchanges between the interior and exterior of the cell, with antagonists and agonists receptors, by the cytoplasm, which contains all the material found between the nucleus and the plasma membrane, by the centrioles, where the formation of microtubules occurs, by the rough endoplasmic reticulum and the ribosomes, where protein synthesis occurs and protein transport to the Golgi complex; by the smooth endoplasmic reticulum, responsible for the production of lipids and carbohydrates, neutralization of noxious chemicals and storage of calcium, by the Golgi complex, where the modification, organization and distribution of proteins and lipids for internal use of the cell occurs, by the mitochondria, which are the main ATP synthesis site, and finally, the nucleus that contains practically all the genetic information of the cell containing DNA and the cell's hereditary material inside [1-3] as can be seen in figure 1.1.

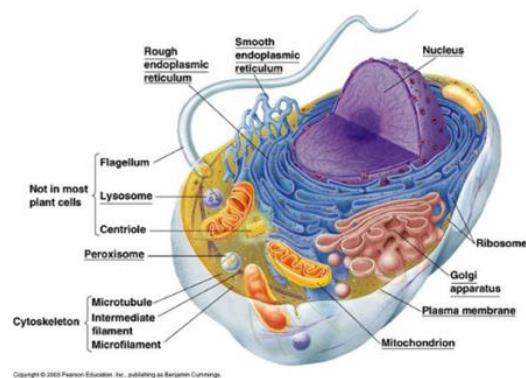


Figure 2.1. Schematic diagram of a typical mammalian cell [4].

For this work is very important to characterize the plasma membrane, so that the electroporation phenomenon can be understood, which is the pulsed electric field interaction with the cell membrane.

2.1. Importance of the plasma membrane

The cell membrane, also called plasmalemma, cytoplasmic membrane or plasma membrane, is the physiological barrier that separates the intracellular or cytoplasmic medium from the extracellular or interstitial medium. This barrier is dynamic, allowing component changes that are indispensable for the multiplication of cell structures. It consists of phospholipids – a link between a phosphate head and two lipid tails – arranged in two parallel, mirror-oriented layers, in which one contacts the intracellular medium and the other contact the extracellular medium through the hydrophilic phosphate heads, while inside this bilayer reside the hydrophobic lipid tails [2-5].

The permeability of the membrane depends on the type of substance with which it interacts but depends above all on ionic concentrations and action potentials, that change in the face of various internal and external factors, such as an electric field. This change can increase the porosity of the

membrane, thus allowing components to leave or enter the cell, which otherwise would not be able to do so or would take a longer period [5-7]. This interaction between cell membrane and electric fields justifies why cell membrane understanding is so important for this work.

Due to the polymorphic characteristics of eukaryotic cells (characterized by cells of different shapes, sizes, and volumes, as well as different organelles and structures), the plasma membrane and cytoplasm are the structures that present major morphological modifications, being differentiated by the different specific functions that a cell can perform in multicellular organisms or by the different environments in unicellular organisms [2-5].

Structural modifications of the membrane are adapted to the specific functions that cells perform or according to the environment in which they live, and the degree of specialization is proportional to the different degrees of differentiation of certain areas of ECM. Fibroblasts' main components of synthesis are collagen (of various types), elastin, in addition to the glycosaminoglycans and multi-adhesive glycoproteins that are part of the extracellular matrix [2][8].

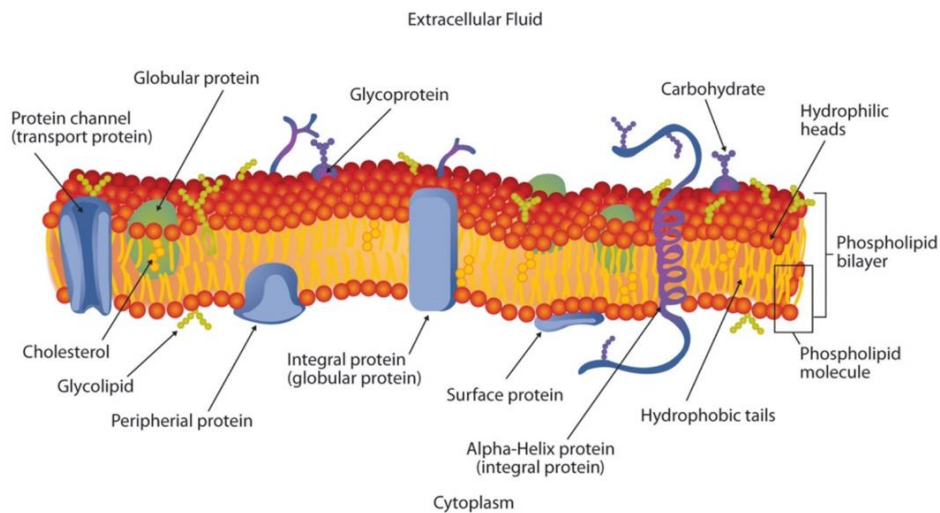


Figure 2.2. Schematic diagram of cell membrane [9].

2.2. Why use Fibroblasts?

The cells are differentiated according to their characterization and origin, for example, the connective tissue cells to which the fibroblasts belong. Fibroblasts are mesenchymal in origin and, when in an adherent phase, have an elongated spindle with numerous cytoplasmic projections [2][7] (Figure 1.3). When in suspension (non-adherent phase) fibroblasts are round cells, whose size could be between 10 to 15 μ m [10].

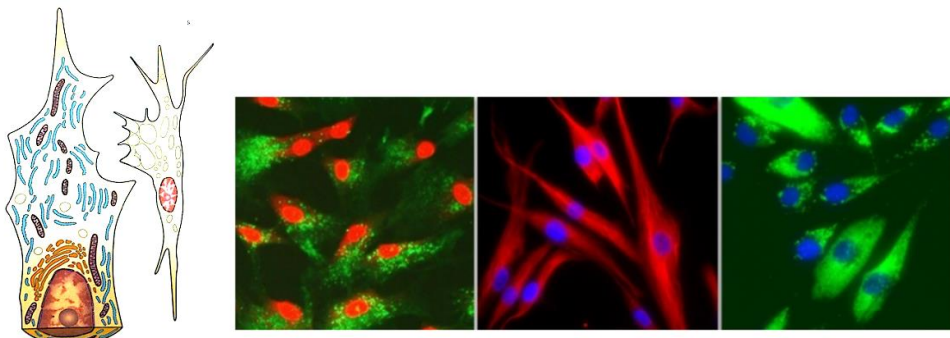


Figure 2.3. Left: Active Fibroblasts in adherent phase [2]. Right: Active Fibroblasts observed by fluorescence technique under the microscope [11].

Fibroblasts are the least specialized cells in the connective tissue cell family and are also the most common and abundant, however they are the most versatile cells in this group as they, in extreme conditions, could differentiate into other members of this cell family [2][11], such as chondroblasts and osteoblasts, so that's why fibroblasts were the chosen cells for this work.

They are of great value due to their high capacity to produce extracellular matrix components, such as several types of proteins, including almost 30 different types of collagens, elastin, and other components of high added value [2][12]. In fact, fibroblasts produce a diverse group of products, besides collagen, like proteoglycans, fibronectin, glycosaminoglycans, metalloproteinases and prostaglandins [2][12].

Fibroblasts can renovate functional tissue, so they play a pivot role in healing, tissue repair and remodelling. The process begins with an inflammatory response, the formation of a clot begins at the lesion site formed by a fibrin-fibronectin matrix, the fibroblasts act on the structure to initiate the deposition and remodelling process, move up to the injury site after chemotactic stimulation. Fibroblast migration is a dynamic process that involves the synthesis of the extracellular matrix. The collagenases produced by the fibroblast destroy the surrounding interstitial matrix and collaborate in the migratory process [6][13]. Fibroblasts proliferate at the lesion site mediated by a large number of cytokines and growth factors and are also needed to synthesize the skeleton of the ECM to replace damaged tissue [10][12-13].

So, when tissue damage occurs, fibroblasts proliferate, migrate to the injury and produce large amounts of collagen matrix that will help to isolate and to repair damaged tissue [6][11]. This ability may explain why fibroblasts are easy cells to grow in culture, justifying, once more, the choice of cell type for this work.

2.3. Why use Electric Fields based on Pulsed Power?

Pulsed electric fields (PEF) are produced from the application of high voltage short pulses based on pulsed power (PP) circuits and electronics. This technology has its origin in 1923 when Erwin Marx proposed the Marx's generator (Figure 1.4.) that acts as a transient voltage multiplier circuit. Its principle consists in storing energy for a relatively long period of time, in parallel capacitors, and its subsequent release in a short time, by placing the capacitors in series [14-16].



Figure 2.4. Marx generator circuit with several levels.

This method of energy manipulation allows the application of considerable peak powers, in well controllable energy packages during some time, by controlling frequencies and pulse times, with relatively low average power consumption, lowering the risk of overheating when applied to organic or cellular matter [16].

The reason why pulsed electric fields were chosen for this work is due to their advantage of reducing the thermal load applied to the material, making it possible to apply intense fields in the order of KV/cm to biological samples, but without thermal load, keeping these alive.

2.4. Why use the electroporation phenomenon?

The exposure of biological lipid bilayers to an external electric field of enough intensity causes an increase of their permeability, i.e. the pores formation in cell membrane, in order to distribute the electrical charges of the cells in the two sides of the phospholipidic bilayer [17]. This effect called electroporation is achieved by the intermittent delivery of short pulses of high voltage (kV) to a biological medium located between two electrodes (Pulsed Electric Fields).

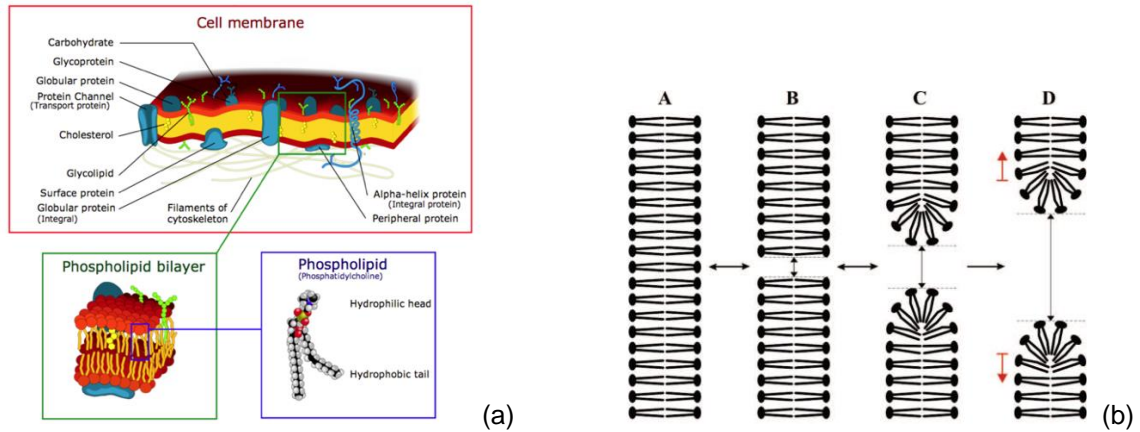


Figure 2.5. Cell membrane and phospholipid structure (a) [18] and Phospholipid behavior to electroporation (b) [17].

The formation of pores in the cell membrane occurs through the application of electric fields that cause water molecules to penetrate the phospholipid bilayer, forming a "water wire", inducing a reorganization of phospholipids and a change in the orientation of the hydrophilic head towards the water molecules, thus forming stable channels (pores) for the passage of ions [17].

Depending on the treatment conditions the electroporation can be either reversible or irreversible. The transient or permanent increment of the permeability of the cell membrane by application of an external electric field has numerous applications in different disciplines such as medicine, biotechnology, or food processing [19-21].



Figure 1.6. Example of Industrial PEF equipment from the Portuguese company *Energy Pulse Systems*.

For example, it is shown in Figure 1.6 an industrial PEF system, comprising the pulse generator and the continuous treatment chamber, to be assembled in the industrial pipes, used in the food industry for enhancing the extraction of juice, polyphenols, and colours, in the wine, olive oil and apple juice sectors [19-21].

[This page is intentionally left blank]

Chapter 3

3. Cell culture & PEF

3.1. Cell culture

3.1.1. Basics on cell culture

Despite limitations, the cell culture technique undoubtedly is proven to be effective, during its wide use in the last 50 years [22].

Currently it is a relatively accessible technique to be performed, allowing the analysis, in the same experience, of a large number of cell samples, this is mainly due to the evolution of the new materials and methods for cell maintenance, such as the physical-chemical conditions of cultures that are ensured by the precise formulation of culture media, laminar flow cabinets, developed for cultures under sterile conditions, and incubators that keep temperature, O₂ and CO₂ tension and pH constant in optimal conditions, or the possibility of preserving the cell samples in liquid nitrogen. In addition, cell culture also has the advantage of reducing the use of animals for experimental tests [22-23].

3.1.1.1. Culture Room - How to work with cells

It is important to realize that to work with cells, whether to obtain primary culture or to maintain cells in subculture, very specific conditions are required.

First, the culture room, also called the white room, due to its level of sterilization, is restricted to researchers who are working with mammalian cells, and they must use appropriate equipment to prevent possible contamination. The use of a white coat is mandatory, this should have long sleeves with elastic cuffs, and it is personal, non-transferable, and only used in the culture room, as well as the use of a disposable face mask, disposable gloves, foot protectors and hair burrow.

All the material inside the culture room must be sterile and well counted by prior inventory, avoiding the use of paper or cardboard material, as these are more susceptible to contamination than plastic or glass. All material, such as flasks, bottles or plates should be rightfully tagged.

When going to work with the culture or make observations under the microscope, the flasks containing the T-flask culture cells must be grasped by the cap, just as the culture plates must be grasped by the lid, without exposing the cellular content to air [22][24].

All work where cells may be exposed to air must be carried out in a laminar flow cabinet (vertical or horizontal flow), and when inside it, the opening of bottles, flasks or removing of plate lids, must be careful, as such, hands never must go over the material, thus, contamination is avoided. Before starting the work in the laminar flow cabinet, it must be cleaned with 70° ethanol and pre-sterilized with ultraviolet light, such as the non-organic material used for that specific work that cannot be autoclaved [24].

When in culture, the cells are inside a pre-sterilized CO₂ incubator, that guarantees optimum pH, O₂, temperature and humidity levels, keeping the culture at 37°C with 5% CO₂ conditions [22].

Each time the incubator is opened, it loses CO₂, temperature, and humidity, which requires some time to stabilize the conditions once more, for that same reason, openings and closings of the incubator must be fast and strictly necessary.

Culture media and other solutions or reagents, which are frequently used, must be kept in the refrigerator at 4°C and removed the volume strictly necessary to work, to heat it in a 37°C incubator or in a warm bath in order to the cells do not suffer a thermal shock [22][24].

Penicillin and streptomycin, Trypsin and EDTA and Fetal bovine serum (FBS) and other growth factors should be kept at -20°C [24].

In case of contamination, the cell culture must be discarded, the laminar flow cabinet and the incubators must be cleaned with bleach diluted in water and later disinfected with ethanol and, after

this procedure, sterilized with ultraviolet light cycles (in the case of the laminar flow cabinet) or with high temperature cycles (in the case of the CO₂ incubator). Material such as glass, some plastics such as micropipette tips, reagents such as sterile water and PBS must be autoclaved at temperatures above 137°C, for no less than 15 minutes [22][24].

3.1.1.2. Primary culture - How to obtain cells

There are several types of culture in Biology, organ culture, tissue culture and cell culture, becoming the last one better known since 1955.

Cell culture is the name given to the methodology in which cells are seeded in a dispersed way. This technique complies with certain standards approved since 1990 by the Tissue Culture American Association [22-23].

Currently, obtaining cells can be performed in two ways, a mechanical cell detachment that is used for soft tissues, such as the brain or liver, but it reduces the viability of the cells obtained, and, an enzymatic cell detachment, through a proteolytic enzyme - trypsin - that act breaking the peptide bond between lysine and arginine [22][24].

The obtaining and removal of cells from a tissue by trypsin is one of the most used methods for cell detachment and was first demonstrated, in a very primitive form, in 1916 by Rous & Jones. But it is since the 1950s that the methodology has become more developed and perfected, mostly due to Earle and Moscana in 1952 and Rinaldi in 1959 [23].

Trypsin has several advantages over the mechanical method since it does not have the level of mechanical trauma to the cell, but it also has disadvantages that are related to the fact that when exposed to the enzyme for long periods of time, cells can suffer irreparable damage in their membrane proteins, thereby killed by trypsin induction [22-23].

Blend with trypsin, it is common to see a mixture of trypsin and EDTA (ethylenediamine tetraacetic acid) in laboratories, which is a very effective chelating agent in adhesion molecules that have a calcium-dependent activity, or EGTA (ethylene glycol tetraacetic acid), which is also a chelating agent but not the most widely used [22][25]. In addition to trypsin, other enzymes can be used for the cell detachment process, such as pronase (with similar action to trypsin, pronase promotes almost complete detachment but may also represents a risk to cell membrane), elastase, hyaluronidase, collagenase and dispase, the last one less efficient in disaggregation but safer in cell viability. Hyaluronidase is normally used in conjunction with collagenase to disintegrate the extracellular matrix (when made up mostly of collagen and elastin fibers) and DNase is used to destroy the residual DNA of lysed cells that remains in the matrix [22].

It is after this detachment that a primary culture is obtained, which will give rise to cell lines (Figure 3.1).

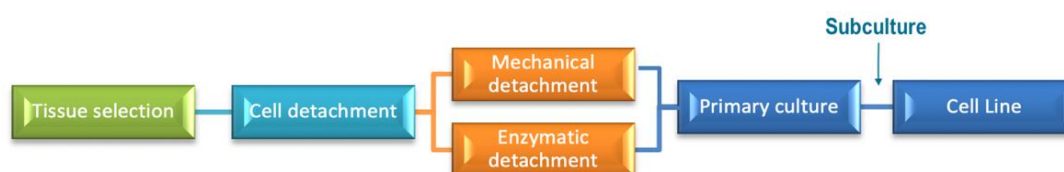


Figure 3.1. Scheme of how to obtain a cell line.

3.1.1.3. Subculture - How to grow cells

The primary culture consists of a heterogeneous cell population and is a vital step for final cell line achievement [22][25].

The cells removed from the tissue are seeded in a sparsely form on an appropriate medium inside culture flasks (further designated as T-flasks), where they remain in suspension (with a rounded shape) and then settle, establishing a connection with the surface of the T-flask [22].

The adherent culture flask (made of glass or polystyrene) itself has a substrate, that is the result of the previous treatment with ionizing radiation or chemicals, that give a negative charge to the contact surface, this allows the cell to adhere to the surface through specific receptors on its membrane and extracellular matrix molecules. The process occurs in the first stage through the cellular secretion of matrix proteins that adhere to the substrate, and then, the interaction of cells with these proteins. This phenomenon could explain why some types of cells bind more easily to surfaces that have previously been treated with matrix proteins, such as collagen or fibronectin. In turn, the cells maintain bonds between them through adhesion proteins such as CAM (independent of calcium Ca^{2+}), cadherins (dependent of Ca^{2+}) and proteoglycans, which are transmembrane proteins that interact with the components of ECM [22-23].

After several passages, cells in culture tends to become uniform due to the selective pressure imposed by the culture conditions, this strain, then, starts to present characteristics that define it as a cell strain and that remains permanent after several generations.

The term subculture, passages and transfers are referred to designate the procedure that is carried out in maintenance and propagation. The passage of a primary culture gives rise to secondary culture, third and so on, in practice this nomenclature is used only up to third culture, indicating from this point only the number of times the culture has been subcultured, to which is given the name of passages (P4, P5, P6, etc.) [22-25].

When a primary culture is subcultured, it is called a cell strain, which is formed by a heterogeneous population containing the different types of cells that formed the original tissue, with successive passages it is possible to obtain a more homogeneous cell line. If a specific cell in this population has been isolated or cloned, the new culture originating from this single cell is then called a cell sample or cell strain [22][25-26].

In cultures that proliferate forming layers of cells, subculture is normally carried out by enzymatic detachment (trypsin), followed by dispersion of cells in culture medium (in twice the volume of trypsin initial volume). In suspension cells, the subculture requires only the addition of the new culture medium to the pellet after centrifugation and disposal of the old medium, which is advantageous as it avoids the traumatic action of trypsin on the cells [22][25][27].

For each strain it is advisable to build a growth curve appropriate for the subculture (explained further in *Cell cycle inside a culture*), an important procedure for carrying out experiments, since cells in different growth phases behave differently in relation to enzymatic and metabolic activity [22].

The cells must be subcultured as soon as they reach 80% to 90% of cell density or confluence (cells/cm² of the substrate or per milliliter of culture medium) which corresponds to the end of the exponential growth phase of the culture [22-25][27].

Subculture in the stationary phase should be avoided due to the presence of non-viable cells and also because in this phase the cells synthesize a greater amount of matrix proteins, making the disintegration process difficult [25][27].

In general, in most strains, the subculture can be done with a sowing of 1×10^4 or 5×10^4 per milliliter, or in adherent cells 1×10^4 or 5×10^4 per cm², and in cultures with slow proliferation, this number should be increased to 100,000 per milliliter [23-24].

3.1.1.4. Cell cycle inside a culture

The growth of an animal cell culture has a kinetic profile like microorganisms. The cell cycle for adherent cells proceeds as follows, after seeding the cells in culture medium, there is a delayed initial phase called lag phase, which corresponds to an adaptation period in which the cells synthesize important components necessary to initiate the cell cycle and that, corresponds approximately to the first 12 to 14 hours. Then, between 12 and 72 hours, there is a period of exponential growth, which depends largely on the number of cells sown and placed in culture, called the logarithmic phase. When the cell density, also called confluence, reaches its maximum, usually after 72 or 96 hours, the growth of the culture is reduced or stops completely, and the time of the stationary phase appears [22-23][28] (Figure 3.2).

In non-adherent or cells in suspension, the number of cells must be determined and compared with the culture growth curve [23][27].

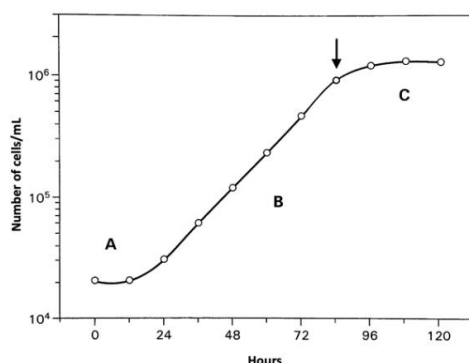


Figure 3.2. Growth curve of adherent cells. (A) Lag phase; (B) Logarithmic phase, where the arrow represents the end of this exponential phase; (C) Stationary phase. The arrow represents the ideal moment of passage. Adapted from [23].

Still in the exponential phase, the proliferative capacity of the different strains depends on the minimum number of cells sown per milliliter of the culture medium, the lower this ratio is, the less is the possibility of cells entering into division, this parameter is called plating efficiency and can be defined as the number of viable colonies formed in relation to the number of cells sown [22][27-28].

Primary cultures and finite cell lines have much lower plating efficiency than continuous or immortalized lines. In the stationary phase, in addition to proliferation stoppage, there is also a marked change in mobility and cell morphology. The growth cessation of the culture is due to the inactivation of nutrients and essentially of growth factors whose level is reduced to values between 0 and 10% of the initial concentration. After the maximum confluence, and if the culture medium is renewed, some cultures continue to proliferate, but in a less and reduced way, then forming several cell layers in addition to the layer already adhering to the substrate [22-23].

The exponential and stationary phases provide important data on the characteristics of cultural growth. Among these parameters, the doubling time called DT stands out. It is determined in the middle of the exponential phase and corresponds to the time that the culture takes to double the number of cells, the value can vary from 12 to 15 hours in cultures with fast growth and 24 to 36 hours in most continuous strains, however, it can reach 60 to 72 hours in slow-growing cells. This measure is used to quantify the cellular response to substances that stimulate or inhibit cultural growth, such as nutrients, hormones, and toxic substances. Population and the saturation density called SD, corresponds to the number of cells per cm² of the substrate surface, which is commonly called confluence, and is considered an important value, being variable according to the cell type, however it is a difficult measure to be obtained with precision mainly in cultures kept in suspension, since the growth is not limited by the substrate area but by the aging of the culture medium [22-23][28].

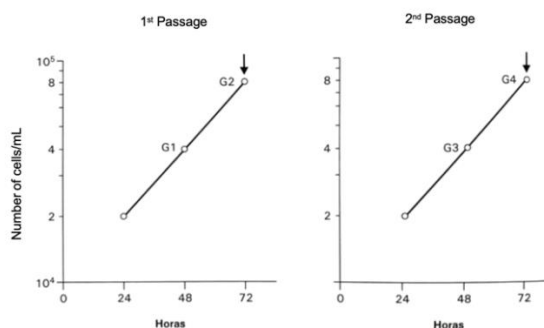


Figure 3.3. Graphics representing the ideal point for the first passage in the end of Generation 2 (G2) and for the second passage in the end of generation 4 (G4). Adapted from [23]

When the culture reaches the final stage, at 72 hours for example, the adherent cells are treated with trypsin and again divided into flasks, if the cultural conditions were kept constant, such as the type of seeding, culture medium and time, the cells should reach the end of the exponential phase

with the same number in each cycle of growth. For example, it can be observed that the number of cells per millimeter increased from 2×10^4 to 4×10^4 after 48 hours, in the middle of the exponential phase, thus forming the first generation G1 and later to 8×10^4 at 72 hours of the exponential phase, thus forming the second generation G2. After new subculture or passage, forming a new growth cycle with the G3 and G4 generations [22-23][28] (Figure 3.3).

3.1.1.5. Cell lines, strains, and types

Cells with finite growth

Cell lines originating from normal tissues generally proliferate only for a limited number of generations, this condition was initially studied by Hayflick & Moorhead in 1961, in an experiment later repeated by other researchers, who showed that normal human cells, from adult tissue or embryonic tissue, remains in culture only for about 50 generations, these authors characterized the cultural growth in 3 phases, the phase 1 that corresponds to the formation of initial primary and secondary cultures, the phase 2 where the vigorous growth of the culture during 50 generations is observed and the phase 3, which is characterized by a drastic reduction in cell growth and death, the cells from phase 2 form cell lines with finite growth [22-23][28] (Figure 3.4).

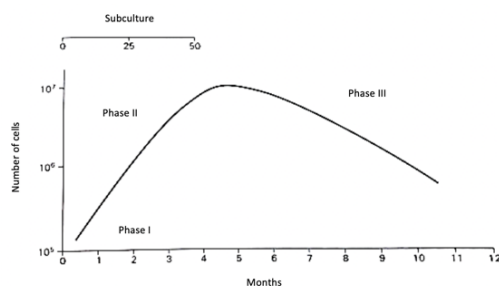


Figure 3.4. Graphic representing the typical cell senescence curve in cells with finite growth. The subculture is viable until Fifty generations, which corresponds to approximately 4 months. Adapted from [23].

It was thus shown that *in vitro* cell proliferation of normal tissues was also limited and formed cultures with finite growth. This limited culture process is called senescence and occurs partly due to a failure in the replication process in the terminal portion of the DNA that is called telomere. Therefore, due to the progressive shortening of the telomeres, the cell becomes unfit for division. However, germ cells, stem cells and transformed cells are considered an exception, these cells express the telomerase enzyme that could replicate the terminal DNA sequence in the telomeres, thus enabling cells for an infinite proliferation condition [22][28].

Cell lines with infinite growth – immortalized lines

One of the first experiments on the establishment of cell lines with infinite growth was carried out by Todaro and Green in 1963 with 3T3 cells from *Mus musculus* mouse (type of genetically modified rat for laboratory experiments), they showed that these cells regularly proliferated with successive passages for 30 or 45 days, that is, 15 to 30 generations, after this period the growth rate was reduced and the cells entered a phase called crisis, in which a large part of the cells died [23].

The surviving cells acquired a vigorous growth potential and formed established cultures with infinite growth that were called immortalized strains (Figure 3.5).

They also showed that during the crisis, the cells remained diploid but acquired heteroploidy characteristics, after the establishment of continuous or infinite cultural growth. It is now known that the capacity of a cell line to grow infinitely reflects the capacity for genetic variation and involves the mutation or deletion of the B53 gene that participates in the regulation of the cell cycle (Figure 3.5).

In the observation of the inverted phase optical microscope in the biology of cells in culture, with phase contrast is the simplest and most direct way to characterize the morphology of the cells, but it

should be noted that cells subcultured *in vitro* acquire shapes that are not always like the ones of the source tissue [22-23][27].

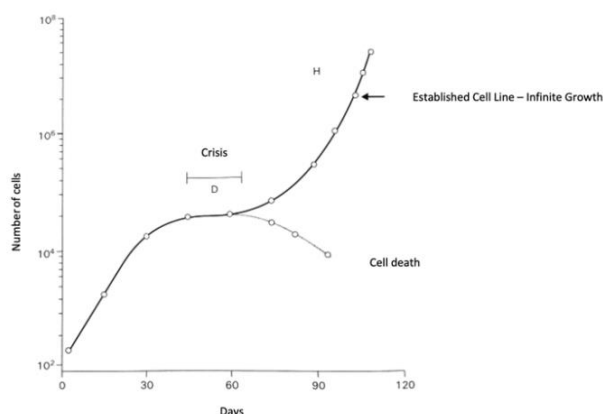


Figure 3.5. Graphic representing the moment of crisis, in which will result cell death or the establishment of the cell line with infinite growth. D represents the diploid characteristics of the cells and, H the heteroploidy characteristics of the cells with infinite growth. Adapted from [23].

In general, the cells of the tissues classically characterized as epithelial, muscular, connective and a specialization of this - lymphatic - when placed in culture have only 3 distinct shapes, called: epithelial (polygonal shape with regular dimensions and discrete separation between them, generally forming a single cell layer), lymphoid (do not proliferate adhered to the artificial substrate, although they have satisfactory growth in suspension, in isolated form or in clusters) and fibroblast [26].

Fibroblasts have a bipolar or multipolar shape with great mobility in the substrate, they have a fusiform aspect, forming several layers of cells [27].

The form that the cells acquire in culture derive in part from the morphological plasticity in response to the culture conditions, such as, composition of the medium, the type of substrate and the growth phase of the culture, as an example the HeLa cell line can be mentioned, it is typically epithelial, but when maintained in high serum concentration, takes on an elongated shape characteristic of fibroblasts. The 3T3 *Mus musculus* mouse cell line has the form of a fibroblast when kept in low population density but, acquire the epithelial form when the culture is in a stationary phase. BHK or human hamster kidney cells (lung and skin) when subconfluent have the form of multipolar fibroblasts, when they reach the confluence, they become bipolar and are distributed in an elongated form in parallel bundles [22-23][27].

For the reasons described above, some researchers prefer the designation epithelioid or fibroblastoid to distinguish these cellular forms. However, despite the limited value, the morphological identification of cells cultured *in vitro* is still in common use in laboratories. Currently, in addition to morphology, other methods are used to identify and authenticate a specific cell line, including karyotype, isoenzyme analysis, immunocytochemistry, and DNA analysis by restriction enzymes [22][27].

3.1.1.6. Culture media and other solutions

Natural culture media and saline solutions

During the initial period of development of the tissue technique, saline solutions were used in order to maintain the fragment of animal tissue in an aqueous medium containing mineral salts considered important for cellular activity, the physiological saline solutions were derived from the original formula described by English physiologist Sidney Ringer, in 1895, in his work on animal perfusion, years later this formula was modified by the American pharmacologist Maurice Vijuex Tyrod, in 1910, by adding glucose in order to maintain metabolic activity, it is assumed that success from the first experiments carried out with tissue culture, either due to the presence of biological fluids and cell debris from the tissue removed from the animal, which, when diffused into the saline solution, formed a medium that

contributed to increase cell survival. In fact, years later it was observed that some preparations of animal origin, such as frog lymph, chicken plasma, tissue extracts obtained from chicken and mouse embryos, bovine amniotic fluid, umbilical cord serum, serum bovine and horse serum, of animal origin when added to saline solutions significantly stimulated cultural growth. Table 3.1 shows the main compositions of saline solutions used in cell culture [23].

Table 3.1. Main compositions of saline solutions. Adapted from [23]

Substance (g/L)	Dulbecco	Dulbecco PBS as diluent of trypsin	Earle	Hanks
NaCl	8	8	6,8	8
KCl	0,2	0,2	0,4	0,4
CaCl ₂	0,1	-	0,25	0,14
MgSO ₄ ·7H ₂ O	-	-	0,1	0,1
MgCl ₂ ·6H ₂ O	0,1	-	-	0,1
NaH ₂ PO ₄ ·H ₂ O	-	-	0,125	-
NaH ₂ HPO ₄ ·2H ₂ O	1,15	1,15	-	0,006
KH ₂ PO ₄	0,2	0,2	-	0,006
NaHCO ₃	-	-	2,2	0,35
Glycose	-	-	1	1
Gas Phase	Air	Air	5% CO ₂	Air

In the 1940s, the media used in bacteriology were also tested in animal tissue culture, showing some success, although inefficient for the prolonged maintenance of cells. Some components of these media have been identified as excellent supplements that stimulate cell proliferation, among which can be mentioned hydrolyzed peptone, lactalbumin or casein. Tryptose-phosphate broth as a source of amino acids and yeast extract as a source of vitamins. The use of these supplements remains in several laboratories, assisting in the maintenance of cell lines considered difficult in terms of propagation [23][29].

Synthetic culture medium

It is since 1941, in the studies developed by Albert Fisher, a pioneer in the formulation of culture media, that the first attempts to develop synthetic media emerged.

These media had such a complex composition, that is, they were formed by mixing a large number of compounds, amino acids, vitamins, carbohydrates, nucleotides, intermediate metabolites of the cycle of tricarboxylic and lipid acids, later considered unnecessary and in excessive quantity. In the first defined synthetic medium it was called V605 medium, in 1948, soon after, White, in 1949, described another synthetic medium that was described efficient for the maintenance of chicken embryo cardiac muscle cells. At that time, cell lines had not been established and as such these media were used only to prolong the average life of cells in culture. Continuing these studies, Morgan et al, in 1950, described the Medium 199 which in the presence of serum was efficient in the proliferation of different cell types, of all the mediums described, medium 199 is the only one produced commercially, being widely used for maintenance of cells for vaccine production and virus titration. A less complex version of Medium 199 was the medium developed at *Connaugh Medical Research Laboratories* prepared in formulas CMRL1415, used for mouse cells, and CMRL1969 for human and monkey cells [22-23].

Among the complex media it is important to mention the 858 Medium described by Parker et al, the NCTC medium described by Evans and the Waymouth Medium. It is worth mentioning that these were the first media that proved to be efficient for cell proliferation in the absence of serum or other biological fluids [22-23].

A great advance in the use of synthetic culture media was achieved after the publications of Swin & Parker, in 1958, and Hayflick et al., in 1964, who described a method of preparing media that enabled industrialization in powder form. These studies demonstrated the advantages of these preparations in terms of homogeneity, stability, and economy, leading to large-scale industrial production [22-23].

Eagle medium and modifications

Although the synthetic medium developed in the decades from the 1940s to the 1950s represented a major advance for the culture of cells, they were extremely complex, and their formulas contained several substances that were possibly not necessary for cell proliferation [24][30].

A simplified formula for these mediums was obtained in 1955 by Harry Eagle, who precisely determined, at the National Institute of Health, the substances that participated in the metabolism of cells in culture. It thus identified the composition and the optimal concentration of amino acids, vitamins, and inorganic salts necessary for cell proliferation. Starting from a known medium, Eagle removed one by one, at a time, the components of the medium and observed the behavior of the culture under a microscope, observing the cytopathic effect. From this procedure, Eagle determined, in 1955, the optimum concentration of all substances necessary for the proliferation of cell lines L (*Mus musculus* mouse) and HeLa (human carcinoma) in a medium known as the basal medium of Eagle (BME). Later Eagle made several changes to the BME, developing another formula called Minimum essential medium (MEM). Of the various modifications to the Eagle medium since the publication of the original formula, the Dulbecco's medium is the most well-known and currently used in many laboratories. DMEM (Dulbecco's modified Eagle's medium) is a richer variation of BME, stimulating the culture of a huge variety of cell strains (table 3.2) [25][30].

Table 3.2. Different types of medium for cell culture [23].

Medium	Designation	Characteristics
BME	Basal Medium of Eagle, by Eagle, in 1955	13 amino acids were considered essential: arginine, cysteine, glutamine, histidine, isoleucine, leucine, lysine, methionine, phenylalanine, threonine, tryptophan, tyrosine and valine. 7 vitamins were identified as necessary: choline, folic acid, nicotinamide, pantothenate, pyridoxal, riboflavin and thiamine). Other substances were also necessary to avoid the cytopathic effect, glucose, ions Na^+ , K^+ , Mg^{2+} , Cl^- , PO_4^{3-} and of bovine or horse serum.
MEM	Minimum Essential Medium, by Eagle, in 1959	A variation from BME, which involved a higher concentration of existing amino acids and a supplement of non-essential amino acids, Ca^{2+} was omitted to prevent the formation of cell clumps and allowed to increase the concentration of sodium phosphate, which results in better buffering of the medium and without the formation of calcium phosphate crystals.
DMEM	Dulbecco's modified Eagle's Medium	A variation of BME but with four times the concentration of amino acids and vitamins and a higher dose of bicarbonate and a higher concentration of glucose 4,500mg / L.
GMEM	Glasgow Minimum Essential Medium, by Ian MacPherson and Michael Stoker, in 1962	Consists of yet another variation of BME, containing twice the original concentration of amino acids and vitamins, in addition to tryptose phosphate at 10 %. Which in addition to the MEMs that express BME variations and that are suitable for cultures such as L929, BHK-21 or HeLa fibroblasts.
RPMI-1640 Medium	Roswell Park Memorial Institute, by Moore et al. (1967)	Corresponds to a modification of the McCoy 5A medium and was developed for lymphoblastoid and human leukemia lines.
McCoy 5A Medium	By McCoy (1959)	Developed for the cultivation of Novikoff hepatoma cells but is now modified and used in the cultivation of primary cells, derived from the skin, bone marrow, suprarenal, lung and testicles.
IMDM	Iscove's modified Dulbecco's medium	It has selenium, pyruvate, HEPES, potassium nitrate instead of ferric nitrate, it is used in cultures of rodent lymphocytes and a wide variety of hybrid cells.
Ham Medium	By Richard Ham (1963)	Was developed for the cloning of Chinese hamster ovary cells and HeLa human tumor cells. Ham F-12 medium is used for the cultivation of hybrid cells and for primary cultures of human cells from the liver. This medium also contains a double concentration of amino acids and the addition of pyruvate, ascorbic acid and zinc sulfate.
Alfa-MEM	-	Medium enriched with more non-essential amino acids.
L-15 Medium	-	Medium with high concentration of amino acids, formulated for the proliferation of cells in the absence of the bicarbonate-CO ₂ system. As the amino acids have a low buffering capacity, the pH of this medium is kept stable due to the presence of phosphate buffer. Galactose replaces glucose to decrease acidification of the medium from the formation of lactic acid. it is a means used to transport cells over short distances and to grow cells in the absence of CO ₂ .
MCDB Medium	Molecular, Cellular and Developmental Biology	Series of means developed for the cloning of cells, which can be used with different amounts of serum. MCDB 104 and 105 are specific for human cells, MCDB 202 is chicken embryo specific, MCDB 401 and MCDB 501 are specific for mice.

3.1.2. How to grow and maintain Fibroblasts L929

Fibroblasts L929 represent an immortalized line of clone cells of the strain L, from mouse. And these cells can be obtained from subcutaneous connective tissue, areolar or adipose, or from lung [24].

Fibroblasts act like any adherent cell, but they are one of the most adherent cells that exists. They adhere to flasks or culture plates through the glycoprotein fibronectin. In the natural environment, fibronectin forms a bridge between the integrins present in the cell membrane and the extracellular matrix itself. So, when they have just been seeded, the fibroblasts appear like floating shiny spheres under a microscopic form, but after a few hours they begin to change their shape due to adhesion proteins, such as fibronectin and vitronectin, and therefore, these cells are only resuspended by the enzyme trypsin [31-32].

For cell culture with fibroblasts it is recommended to seed between 2500 to 5000 cells per cm^2 , ideally 4000 cells/ cm^2 (recommended by the research group from Instituto Superior Técnico), in T25 or T75 flasks in DMEM (Dulbecco's Modified Eagle Medium with 4.5 g/L Glucose, with L-Glutamine) supplemented with 10% FBS (Fetal Bovine Serum previously deactivated) and 1% Streptomycin and Penicillin, stored in the CO_2 incubator at 37°C and 5% of CO_2 , and the medium changed every 48 hours, when cells are above 80% of confluence [24].

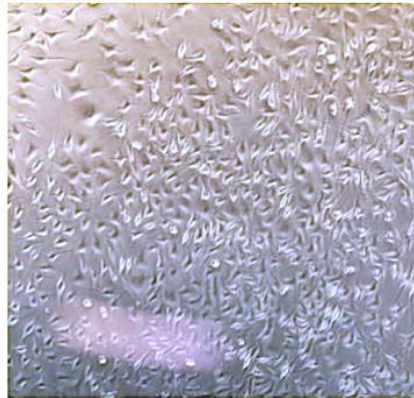


Figure 3.6. L929 fibroblastic cells above 80% confluence, image obtain under the optical microscope.

When fibroblasts have an acceptable confluence and viability, they should be subcultured (figure 3.6).

For this, the T-flask is placed vertically in the laminar flow cabinet and the medium consumed and discarded with the automatic pipette, taking caution not to touch the adherent wall of the flask where the cells are attached [24]. Then, cells are gently rinsed with DPBS, previously heated in a warm bath until 37°C (to avoid a thermal shock on the cells), to remove any remaining proteins from the FBS added to the DMEM medium, this DPBS is also discarded with the help of the automatic pipette. To enzymatically disaggregate the cells, trypsin-EDTA solution is used, which must also be heated in a warm bath until 37°C , and placed carefully in the flask, in a ratio of 25% of the total volume of medium. At this moment, the bottle should be horizontalized and placed in the CO_2 incubator for 2 minutes. At the end of this time, the flask is observed in an inverted phase microscope, and the cells must appear spherical and completely loose and therefore in motion, at that time it is placed in the flask complete medium (with FBS) that represents twice the volume of the trypsin-EDTA solution and the flask is slightly shaken, and with the help of the automatic pipette, the solution is stirred, releasing cells that may still be attached to the flask adherent wall. This solution is aspirated with an automatic pipette and taken to centrifuge at 1400RPM for 9 minutes [24][33].

At the end of this time, the supernatant is discarded, and the pellet is kept, where the cells are counted and seeded in new flasks [24].

3.2. Pulsed Electric Fields (PEF) and Electroporation

3.2.1. Pulsed Electric Fields Generation

Pulsed electric fields (PEF), used to produce electroporation in biologic cells, are, normally, generate between two electrodes, by the application of high-voltage (HV) pulses to one electrode, while the other is at ground potential.

The HV pulses are created by a Pulsed Power (PP) generator, in this work a semiconductor-based Marx generator, shown schematically in Figure 3.7. In this generator, a relatively low voltage dc power supply, U_{dc} , connected to the mains, charges n capacitors C_n in parallel, during a relatively long time, normally ms, and then these capacitors are connected in series with a load, applying a voltage of about $v_0 \approx nU_{dc}$, during short period, such as μs . The charging and pulse times are controlled the semiconductor switches S , where the S_{ci} command the charging and the S_{pi} the pulsing period, [34-35], as shown in Figure 3.7.

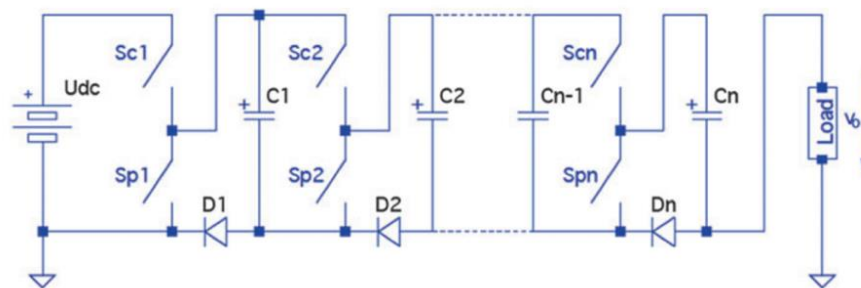


Figure 3.7. Simplified negative Marx generator topology, where C_n represents the capacitor, D_n represents the diode and S_{cn} represents the switch [34].

The pulse method in PEF lowers the average power delivery in the cell medium, enhancing the electric field effect efficiency, when compared to traditional direct current, DC, electric fields, without increasing the temperature, making this a non-thermal method. A typical electric pulse application is presented in Figure 3.8 [34-35].

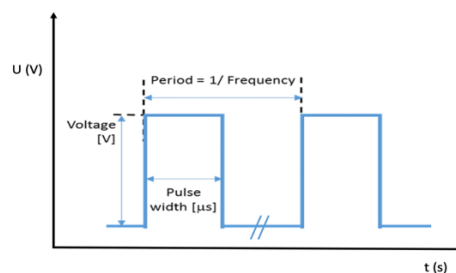


Figure 3.8. Typical voltage waveform in PEF application [34].

As mentioned before, PEF is applied between two electrodes, connected by an insulated material, in a treatment chamber, in this work a batch system known as cuvette, as seen in Figure 3.9.

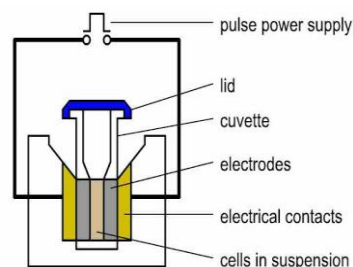


Figure 3.9. Illustrations of the batch treatment chamber [36].

To successfully apply PEF, it is important to know and define some of its parameters, such as the electric field strength, E , treatment time, t , and the specific energy, W_s , which are also used in the comparison between the results from several authors. The general idea of PEF application is to deliver an electric field strength, E , given by,

$$E = \frac{U}{d} \quad (1)$$

Where E is normally given in kV/cm , U refers to the voltage applied, in kV and d the distance between the electrodes of the treatment chamber, in cm .

The electric field is applied in n discrete pulses τ with μs width, giving a treatment time of

$$t = n \cdot \tau \quad (2)$$

Each pulse has an energy, in J, of

$$W = U \cdot I \cdot \tau \quad (1)$$

Where I is the current in A. The mixture inside the treatment chamber, for this specific study will be water and plant material, will have an electrical conductivity, σ , that can change slightly during the treatment time, as the plant material infuses in the water. Because of this slight change throughout the treatment time, it is important to use an average value for σ , as it will influence the value of the current applied, I , as can be seen [34-35].

$$I = \frac{U \cdot A_c \cdot \sigma}{d} \quad (4)$$

Where A_c refers to the electrode humid area, in cm^2 .

The total energy applied is, in J,

$$W_t = W \cdot n \quad (5)$$

The total energy is important to calculate the specific energy, W_s , given by,

$$W_s = \frac{W_t}{V \cdot \rho} \quad (6)$$

Where W_s is given in kJ/kg , and V the volume of the treatment chamber in ml , or kg .

From Equation (6) one can calculate the increase in temperature, ΔT in $^{\circ}C$, from the application of PEF, by

$$\Delta T = \frac{W_s}{C_p} \quad (7)$$

Where C_p is the Specific Heat Capacity ($kJ/(kg \cdot ^{\circ}C)$) of the treated material, which was the same as water, $4.18 kJ/(kg \cdot ^{\circ}C)$.

Having the most relevant parameters defined, to apply PEF to a treatment mixture, one has to define the desired voltage, U , pulse width, τ , pulse frequency, f , and, finally, either define the pulse number to be applied, n , or the operation time, t_{op} , in s . While the pulses are being applied, it is also important to control the electrical conductivity to ensure the specific energy delivered does not deviate from the desired value [14-16][34-35].

3.2.2. The Electroporation Phenomenon

Electroporation is the permeabilization of the biological cell membrane induced by application of electric fields. This method commonly uses electroporation cuvettes (Figure 3.10) placed in a Pulsed Power Field (PEF) generator equipment powered by Pulsed Power (PP) Energy.

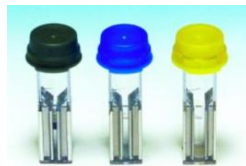


Figure 3.10. Electroporation cuvettes. Left: 90 μL capacity, 1 mm gap between electrodes, used for bacteria. Middle: 400 μL capacity, 2 mm gap between electrodes, suitable for yeast. Right: 800 μL capacity, 4 mm gap between electrodes, appropriate for mammalian cells [37].

The first successful work with electric field induction for Medical or biological applications was in 1958, when a group study the influence of electricity in a node of Ranvier, from a neuron axon. Almost fourteen years later the same influence was study in vesicle membranes and their permeability increase because of exposure to an external electric field. This method was named electroporation and two major branches appear, the reversible electroporation, in which cells integrity its maintained, and, an irreversible electroporation, where the cell membrane disrupts, letting out its organelles and, as such, inducing death. Irreversible electroporation is used in microbiology to annihilate bacteria (microbial deactivation) and in medicine to make nonthermal tissue ablation. In its turn, reversible electroporation, can enhance permeability of the membrane but the passage of the molecules is nonselective, as such, molecules can pass in out according to concentration gradients [38].

As already mentioned in chapter 1, each cell in the human body is surrounded by a plasma membrane. Most of them consist of a phospholipid bilayer separating and protecting the cell from its surroundings. Along with the lipid layer are different proteins that provide a path for the transport of specific molecules across the membrane, without these proteins the membrane would be just an impenetrable barrier [17].

The process that makes the membrane permeable, when exposed to an electric field strong enough, that leads to an electrical breakdown, allowing molecules that otherwise would not be able to pass, is called the electroporation of the membrane. The electroporation of the membrane can be reversible or irreversible both with several applications in medicine and biotechnology [17].

In order to better understand the electroporation process, it is necessary to know the constituents of the membrane, namely the lipids. The most abundant in the membrane are phospholipids, however it also consists of glycolipids and cholesterol. These three classes of lipids have a hydrophilic, polar, and more compact part, and a more elongated hydrophobic part, which are usually called the head and tail, respectively. When in aqueous solutions a lipid bilayer is spontaneously formed, the hydrophobic structure being oriented inwards, placing the polar part in contact with water and dissolved ions in the surrounding environment [17].

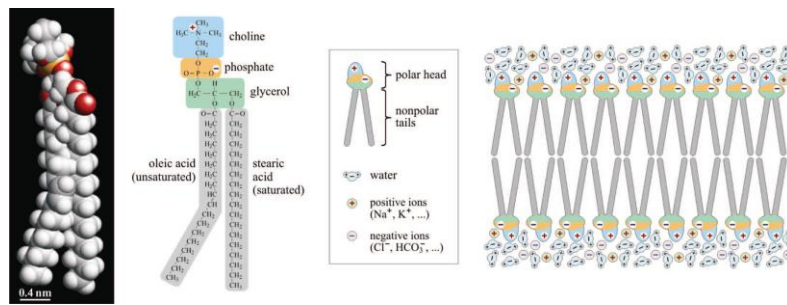


Figure 3.11. Left: space-filling model and structural formula of the SOPC (1-stearoyl-2-oleoyl-phosphatidylcholine) molecule, a typical membrane lipid. Right: a bilayer of such lipids in an aqueous electrolyte solution [17].

Due to the non-polar interior of the membrane, it is practically impermeable to polar molecules on both sides of the membrane, although water and monoatomic ions can diffuse through it in certain circumstances, such as high temperatures, surface tension or both. This phenomenon can be attributed to the formation of small aqueous pores that last only nanoseconds and are formed due to thermal and mechanical fluctuations. These pores can be formed without assigning an electric field but are undoubtedly more unstable [17].

The exposure of biological membranes to a sufficiently high external electric field can lead to an increase in their electrical conductivity and permeability, the so-called electroporation. This process will have to occur in the lipid bilayer of the membrane since the underlying mechanism is the same in all cases, therefore the lipid bilayers are the most used in investigation of membrane electroporation [17].

Two approaches can be taken, the voltage clamp and the current clamp, which consists of applying voltage or current to the membrane and simultaneously measuring the voltage that crosses the bilayer and the current that flows through it [17].

The behaviour of the lipids allows the bilayer to return spontaneously to its previous state, so if the exposure to the electric field is neither too intense nor too long, the electroporation of the layer is reversible. To date, it has not yet been possible to observe the formation of pores in the bilayer product of electroporation, they are too small for the optical microscope and the electron microscope requires too aggressive preparation for the membrane, compromising the structure of the bilayer [17].

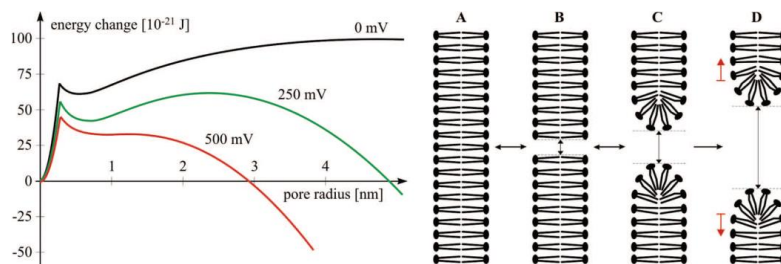


Figure 3.12. Left: change in lipid bilayer energy caused by formation of an aqueous pore, plotted as a function of the pore radius and voltage across the bilayer. Right: bilayer without pores (A), with a hydrophobic pore (B), its reversible transition into a metastable hydrophilic pore (C), and its irreversible transition into an unstable self-expanding hydrophilic pore (D; at membrane voltages above ~500 mV) [17].

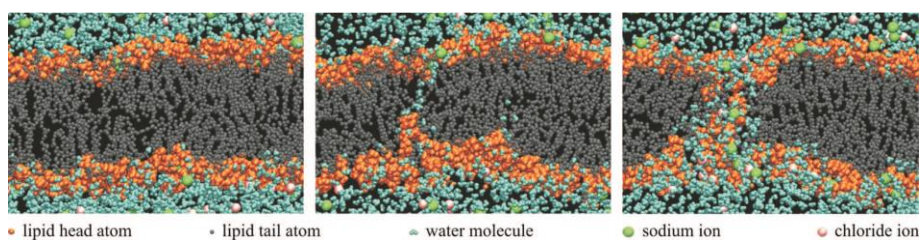


Figure 3.13. A molecular dynamics simulation of an aqueous pore forming in a lipid bilayer exposed to an electric field perpendicular to the bilayer plane. Left: the intact bilayer. Middle: water molecules penetrate the bilayer, forming a "water wire." Right: the adjacent lipids reorient with their heads toward the water molecules in the bilayer, stabilizing the aqueous pore and allowing the ions to enter [17].

As said earlier is not possible to directly observe the pores in the membrane formed by the electroporation of the lipid bilayer, but the consequences of this procedure can be determined or detected by observing larger scale manifestations, such as changes in the electrical and optical properties of the membrane, light scattering and absorption of the lipids around the pores [17].

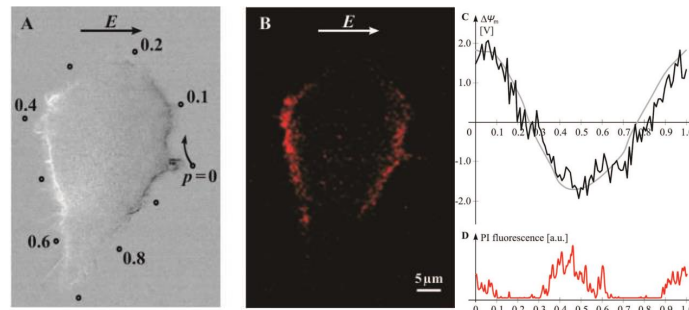


Figure 3.14. The induced transmembrane voltage (ITV) and electroporation of an irregularly shaped Chinese-hamster-ovary (CHO) cell: (A) changes in fluorescence of di-8-ANEPPS reflecting the ITV, with dark regions corresponding to membrane depolarization and bright regions corresponding to membrane hyperpolarization; (B) fluorescence of propidium iodide (PI), reflecting transport of PI across the membrane; (C) ITV along the path shown in (A) as measured (black) and as predicted by numerical computation (gray); (D) fluorescence of PI along the path shown in (A) [17].

Electroporation can be also monitored, in a dense cell suspension, by measuring the bulk electric conductivity of the suspension, which increases if a large fraction of the suspended cells is electroporated. In tissue measuring the impedance spectrum of the tissue before and after exposure to electric pulses. This approach has been successfully reported for skin and liver [17].

The most frequently used method, is also an indirect one, is imaging the transport of molecules that cannot permeate an intact membrane [17].

Reversible electroporation requires sufficiently rapid recovery so that the cell remains viable, such recovery is reflected in the transport rate decreasing more rapidly [17].

3.2.3. Electroporation & Biotechnology

When the cell is exposed to an efficient high electric field, its membrane becomes permeable, opening pores for a certain period, what allows molecules of considerable size to pass through, that otherwise could not do it. This method represents several advantages like gene electrotransfer (introducing DNA into cells) or electrochemotherapy, which enables introducing membrane-impermeant drugs to target and kill cancer cells [19][38].

3.2.3.1. Biotechnological applications

In Biotechnology, most electroporation applications are related to microbial deactivation, useful in food industry, because can kill bacteria but preserving flavour, colour and texture, as opposed to old methods like heat deactivation. Electroporation can also be used in water treatment (Figure 3.15) (whatever is fresh, sea water, waste or oilfield reinjection water) being much effective than ozone, chlorine and ultraviolet treatments [38].

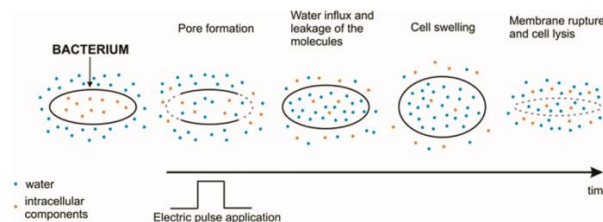


Figure 3.15. Microbial deactivation [38]

Other use for electroporation in industry, is the extraction of biomolecules from microorganisms and plants [19][39-49]. Before electroporation, the mechanisms to extract cell content were chemical extraction (alkaline lysis) and homogenization (mechanical disintegration). But both mechanisms were traumatic to the cell, once promotes whole membrane disintegration, destroying organelles and leaving residual cell husks that were difficult to remove, thus increasing the number of steps to purify the intended molecule. For extraction of bacterial DNA electroporation proved to be almost equally effective than alkaline lysis (Figure 3.16). Electroporation with short pulses also shows great results when it comes to release proteins from bacteria, yeast and cells enclosing complex structures like organelles. Other application for electroporation method is the extraction of intracellular components from vegetable cells, like sugar extraction from sugar beets or extraction of green biomass, which is the primal source of biofuel [19][39].

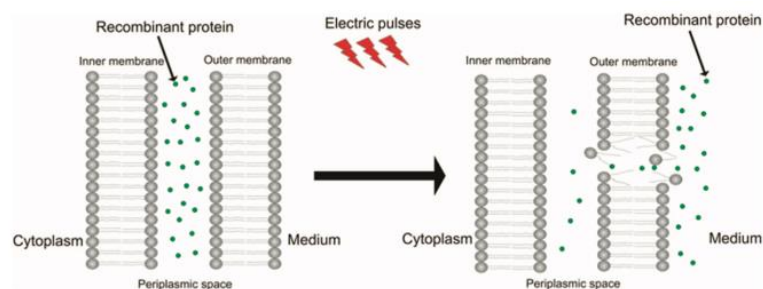


Figure 3.16. Selective release of bacteria proteins using electroporation [19].

In Vitro and in Vivo Studies

Pulsed electric fields that cause electroporation of the plasma membrane in cells are increasingly used in biotechnology and medicine, either for the extraction of biomolecules, for the transfer of genes or even for the first successful cloning of a large animal, the famous Dolly sheep [41]. These phenomena are laboratory procedures that involve experiments *in vitro* or *in vivo*. Due to ethics commissions and the stigma connected to the effects of electricity in animals and humans, *in vivo* electroporation research is more difficult to carry out. But when it comes to *in vitro* experiments, where the usual work is done with mammalian cells coming from immortalized lines, these questions do not arise [42].

Each *in vitro* application involves a specific level of electroporation, thus implementing methods for characterizing the electroporation itself. The most common measuring instruments in these procedures involve measuring the increased transport of molecules across the membrane, both to the intracellular medium and to the interstitial medium. For this, methods such as impedance and voltage measurement, changes in cell size under microscopic observation, dye assays with fluorescent or color stains of functional molecules and flow measurement of biomolecules can be performed [42].

In a nutshell, the detection of cell membrane electroporation can be done through several methods, from which one must choose the most suitable for each specific experiment, considering the available resources and conditions. Some of the main methods of detecting electroporation *in vitro* are as follows:

- Transport of non-permeant exogenous substances;
- Cell uptake of dyes: either fluorescent molecules (fluorophores) or color stains such as trypan blue which is used as a vital stain to determine cell viability as it's excluded by most living cells with intact membranes;
- Magnetic nanoparticles: Iron, manganese and gadolinium are chemical elements with paramagnetic properties and consequently have a strong effect on a local magnetic field;
- Functional molecules (Cytotoxic compounds);
- DNA and RNA: Nucleic acids can also be introduced *in vitro* and *in vivo* to cells by using electroporation (gene electrotransfer);
- Extraction of biomolecules (cell's own ions/molecules);

- Physical and chemical methods such as conductivity and impedance measurements, voltage clamp techniques, cell swelling [42].

For electroporation in *in vitro* cells, there can be used different types of conductive solutions that will influence electroporation process [43], it was showed that the effect of different compositions of electroporation buffer solutions affected cell viability. The results suggest that Mg^{2+} has an important role in electroporation, as an enzymatic co-factor leading to an enhancement of cell viability but can dramatically reduce electroporation efficiency. Thus to optimize electroporation protocols, it is of most importance to determine an electroporation-buffer solution with optimal concentration of Mg^{2+} combined with the number of pulses to apply, thus the solution can strengthen a cell ability to undergo reversible electroporation [43].

In the systematic review by Napotnik T.B. et al, the effects of electroporation using nanosecond high-voltage electrical pulses (nsEP) in eukaryotic cells *in vitro* were analyzed. They performed a statistical analysis of effects of nsEP in relation to three groups of pulse duration (A: 1–10 ns, B: 11–100 ns and C: 101–999 ns). This study confirmed that the plasma membrane is more affected with longer pulses than with short pulses, which is better observed in uptake of dye molecules after the application of single pulses [44]. More studies verified similar results and also concluded that, the choice of the electroporation detection method influences experimental results, for example, when using shorter nsEP, the smaller pores that form are more difficult to pass through the dye molecules, reducing the probability of the influx being detected [44-45][47-51]. Mi Y. et al evaluated the effects of various parameters of nanosecond pulsed electric fields combined with multi-walled carbon nanotubes on cell viability. Multi-walled carbon nanotubes have excellent electrical properties and high aspect ratios. The results show a sigmoid-type variation in cell viability with field strength, pulse width or pulse number, that is, with the growth of these variables the cell viability increases. The addition of multi-walled carbon nanotubes significantly increases the killing effect of nanosecond pulsed electric fields, which can improve the electrical safety of nanosecond pulsed electric fields for the treatment of tumors [52].

Regarding fibroblasts disorders and the effectiveness of electroporation in their treatment, an example of proliferative scarring was studied [46]. Proliferative scarring is a human disease that probably involves deregulation of fibroblast signaling and consequently delayed apoptosis, resulting in hypertrophic scars, with no effective treatment available. The advantage of pure electroporation treatment is the fact that is a chemical-free method. Intermittently delivered pulsed electric fields (IDPEF) with electrical parameter of 5-100 pulses, with a duration of 70 μ s and a frequency of 1Hz, and an electric field strength of 150 V/mm, were used for an *in vitro* study of fibroblast growth, death and regeneration of human and healthy dermal cells in culture. It was observed that the fraction of surviving fibroblasts in opposition to death cells (by irreversible plasma membrane damage) after IDPEF depended on the number of pulses applied. Thus, optimizing a PEF application protocol could be the answer to control fibroblast's density culture and this way maintaining a normal human dermal fibroblast density control in human healing [46].

Numerical modeling of local electric field distribution within electroporated tissues has played an important role in treatment planning procedures in clinical and experimental settings. In the study by Corovic S. et al, the aim was to investigate whether the increase in electric conductivity of tissues needs to be considered when modeling tissue response to the electroporation pulses and how it affects the local electric distribution within electroporated tissues. They examined electric field distribution during electroporation in linear models in which tissue conductivity is constant and non-linear models in which tissue conductivity is electric field dependent. The results demonstrate that non-linear models fit experimental data better than linear models. The findings of this study can significantly contribute to the current development of individualized patient-specific electroporation-based treatment planning (electrochemotherapy, gene electrotransfer for gene therapy and DNA vaccination, tissue ablation with irreversible electroporation and transdermal drug delivery) [53].

In the treatment of solid tumors, it's extremely important that the coverage and exposure time of the treated tumor to the electric field are within the specified range. In the study by Pintar M. et al, a model based on the inverse analysis of experimental data was applied, which provides the time course of tissue electroporation, to a complex *in vivo* example of electroporation with different types of tissue and with a long-term follow-up. The results of the simulations proved that the proposed numerical model can successfully capture the transient effects, the evolution of electric current during each pulse and the effects of pulse frequency because of electroporation on the tissue [54].

3.2.3.2. Biomedical Applications

When it comes to electroporation and medical applications, it is important to pay attention to ethics commissions and for this reason their evolution represents a slower step than industrial applications.

Neumann et al. introduced the medical application of electroporation in 1982, using pulsed electric fields to temporarily permeabilize cell membranes and provide foreign DNA into cells. Later, new clinical applications have emerged namely electrochemotherapy and gene electrotransfer. Electrochemotherapy employ electroporation of membranes and makes easier the transport of cytotoxic drugs (bleomycin and cisplatin). Gene electrotransfer uses specific electric pulses for cellular uptake of naked plasmid DNA, encoding for a specific therapeutic protein with the means of molecular directed for therapy of cancer. Nonthermal irreversible electroporation is known as a new medical application of the electroporation technology used for the ablation of solid tumors [38][55].

Gene electrotransfer (GET) and DNA Vaccination

Other use for electroporation is gene electrotransfer (further designated as GET) for applications in biotechnology, as developing recombinant cells to produce heterologous proteins, and for biomedical applications as for gene therapy and DNA Vaccination [56-57].

Transfer of genes has been tested in many ways, to reach the cells and change their biological function. This has become essentially popular for the treatment of genetic defects of the immune system. Gene electrotransfer is a non-viral method to introduce DNA molecules through electric pulses (Figure 3.18), which proved to be more effective than most biochemical methods, without having the unwanted side effects of introducing viral or chemical agents [57-58]. DNA vaccination shows also a great potential. It consists of a technique to protect an organism against disease by injecting it with genetically modified DNA and thus producing an immune response more safely when compared to the classic technique of inoculating the entire microorganism. This biomedical application has been used mainly for DNA vaccination against cancer, infectious diseases, arthritis, multiple sclerosis, inflammation after organ transplantation and also in regenerative medicine [56-59].

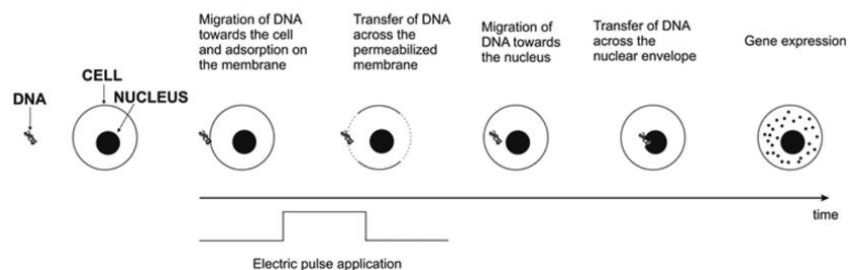


Figure 3.17. Gene electrotransfer technique [42].

As mentioned before, the first experience with GET was an *in vitro* study and reports to 1982, the year in which the guidelines for good practice were also determined. Since then, several studies have been carried out, also testing various electrical parameters. And despite its success and its extensive use, the molecular mechanism of GET has not yet been fully understood, since the process of introducing DNA is much more complex than diffusion phenomenon. The main problem is the slow

diffusion rate of DNA by ECM due to the obstacles of its components, which is why enzymes have started to be used to cause the degradation of part of the matrix and to facilitate this process. Here, it is also important to determine the injection site and the ideal electrical parameters. Several years after the first *in vitro* study, GET is now used in skin or cornea [56-59].

Transdermal administration has the potential to introduce drugs that are not suitable for intravenous or oral administration and can overcome many of the disadvantages of other routes of administration. The skin also undergoes continuous regeneration and due to its size and accessibility it represents an appropriate delivery element for drugs. The skin is composed of several layers, namely the stratum corneum, viable epidermis, dermis, and hypodermis. However, simple transdermal delivery generally implies limited flow mainly due to the impermeable outermost layer of the skin, the stratum corneum, but this barrier can be overcome through electroporation [55-56].

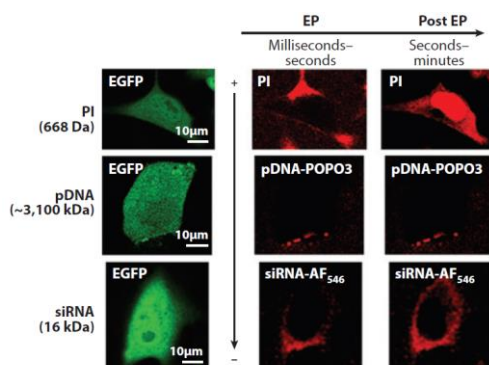


Figure 3.18. Direct microscopical observation of electrotransfer of PI, siRNA and pDNA into murine melanoma cell [42].

Example of an *in vitro* application - Electroporation-based CRISPR/Cas9 Gene Editing

CRISPR/Cas 9 is an effective gene editing technology, adapted from a naturally genome editing system in bacteria, as such, most of initial works with CRISPR (Clustered Regularly Interspaced Short Palindromic Repeats) used plasmid delivery to easy transfect cancer cell lines. Most of the cancer cell lines were adapted to laboratory proposes, lacking parts of the innate immunological response to foreign nucleic acids. Although effective in cancer lines, it was verified, however, that in other types of more complex cell lines or even in primary lines CRISPR was hard-to-transfect [60].

For these difficult cells lines, emerged the Cas9 (CRISPR associated protein 9), which is an RNA guided to the DNA of an endonucleotic enzyme, associated with the CRISPR of the immune adaptation system, constitutes the CRISPR / Cas9 [60].

Cas9 is more effective in the production of recombinant proteins such as Zinc finger nucleases and TALENS, but this system has limitations, as it makes delivery too fast in a short time frame. Several experiments have been carried out to fill these gaps, such as the use of complexes in association with CRISPR / Cas9, such as the chemically modified sgRNA (Single guide RNA) that together with the Cas9 protein form a ribonucleoprotein (RNP) prior to cellular delivery [60].

Electroporation is a promising tool, still in experimental phase, for the combined use with CRISPR / Cas9, since it can permeabilize the nuclear membrane and allow its introduction, thus increasing delivery efficiency in difficult cell lines and primary cells that are difficult to transfect by conventional chemical base methods [60].

Electrochemotherapy

The most known and accepted medical technique involving electroporation is electrochemotherapy (further designated as ECT) [38].

Chemotherapeutic drugs act on cells division, so they also can affect healthy cells and therefore healthy tissue, causing side effects. In general, the drugs used in chemotherapy have low permeability

against the membrane, which requires high doses to increase their effectiveness against the tumour, this has very aggressive side effects for the body [38][53][61].

ECT presents itself as a promising treatment since electroporation increases the permeability of the membrane, facilitating the access of drugs to the intracellular medium and increasing its effectiveness, even at lower doses. This implies a lower dose of drug and therefore less side effects.

ECT works as a local anti-tumoral treatment, in which electrical impulses are applied to the tumor after the injection of the anti-cancer drug (Figure 3.20) [38][55].

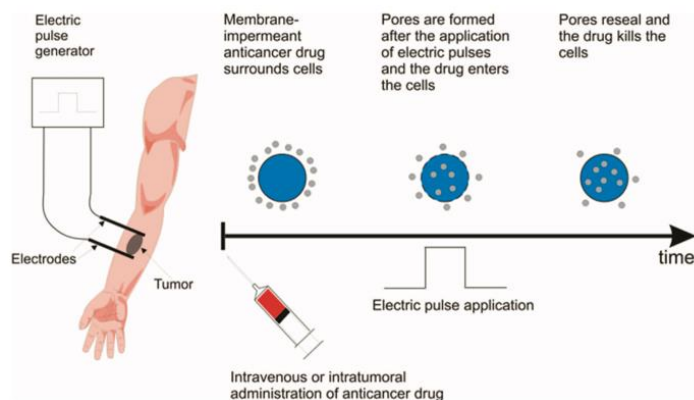


Figure 3.19. ECT steps [55].

Important factors in ECT are the selection and delivery form (intravenous or intratumoral) of the drug, the type of electrode (plate or needle) and the electrical parameters, being the standard protocol, 8 pulses of 100 μ s, in 1 Hz to 5 Hz frequency [38][53][55].

The effectiveness of this method is enhanced by 3 additional effects to ECT, the vascular block after the application of electrical impulses, which decreases the vascularization of the tumor allowing the drug to remain longer in the tumour cells; the vascular disruption, which causes the blood supply to the tumour to be reduced; and an increase in the immune response, due to the substance shedding tumor, after ECT the immune system is requested and as such antibodies are produced [61].

The first trials took place in the early 1990s, with the administration of bleomycin and the subsequent application of PEF. These trials were quite successful, what led to trials with cisplatin, which together with PEF, showed a 73.7% efficacy in the eradication of tumor nodules in patients with melanomas. ECT is a promissory treatment not only for cutaneous tumors but also to deep tumors [38][53][55][61].

Due to the effectiveness of these treatments, it was created, in 2002, the European Standard Operation Procedures for Electrochemotherapy and Electrogenethrapy (ESOPE) in order to create standard procedures and ensure patient safety [53][55][61-63].

Nonthermal tissue ablation

Finally, there is another promising medical application using irreversible electroporation that is called nonthermal tissue ablation [55].

As mentioned earlier, irreversible electroporation is the process in which PEF is applied across a cell, causing permanent permeabilization of its membrane, or its complete disruption.

This occurs due to a biophysical phenomenon where the extensive permeabilization of the membrane causes instability in intracellular medium due to ions leakage.

One of the side effects due to PEF applications is Joule heating. Medicine, however, uses the Joule heating for tissue ablation, through radiofrequency, microwaves, alternative current or direct current [55].

The main handicap of Joule heating is the cell death through inactivation of biological molecules present in the heated volume, and the destruction of blood vessels and nerves.

Irreversible electroporation can be performed to the same volume but without overheating the sample. This is a new molecularly selective tissue ablation method designed as nonthermal

irreversible electroporation (further designated as NTIRE). NTIRE makes possible the ablation of malignant tissue with minimum damage to blood vessels or nerves, with enhancement of immune system activity (that is connected to all parts of the ablate tissue) and maintains the ECM intact which facilitates the regeneration of tissue in blood vessels, nerves, liver, and small intestines [55].

All this advantages, plus the fact that NTIRE is fast and technically simple, because only requires the insertion of electrodes in a form of needles, with reduction of anesthesia time, pain and complications, using conventional imaging methods, made this technique easy to implement in the medical area to treat advanced carcinomas of liver, pancreas, lung, kidney and brain [55].

Electroporation for valorization of platelets with no therapeutic value for transfusion medicine

Platelets are one of the main components of blood, they act in response to bleeding. Platelets are also rich in bioactive factors. When responding to bleeding, platelets release molecules that trigger tissue growth and regeneration, promoting healing. Some of these factors are platelet-derived growth factor (PDGF), insulin growth factor (IGF) and transforming growth factor (TGF) [64].

Blood banks are the entities responsible, among other things, for the conservation of platelet concentrates, which are obtained by the separation of blood components. To keep platelet concentrates in a preserved condition, blood banks maintain the necessary temperature and storage conditions, however these concentrates have only 5 days of stability, or 7 days if undergoing treatment to reduce pathogens, and if they are kept between 20°C to 24°C in continuous agitation. The platelets that are no longer reliable for blood transfusions can be used for biomedical applications and in regenerative medicine [64].

In the specific case of this experiment, pulse electric fields (PEF) were applied, which promoted the electroporation of cell membranes, and the goal was to obtain the bioactive factors of platelet concentrates, that could no longer be used in transfusions but that can be extracted and used for other applications, such as therapeutic and commercial. In a first stage, the platelet concentrate was subjected to a PEF of a pulse of 5 kV/cm with 2 μ s and the release of PDFG was measured by ELISA method, which proved that the PDFG was release into the supernatant, with only one treatment with PEF. After PEF was applied, the concentrate was stored at -20°C for future use [64].

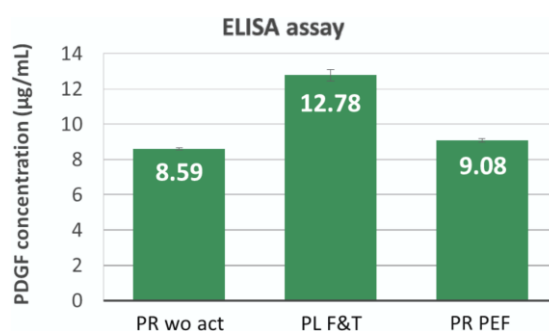


Figure 3.20. PDGF concentration (µg/mL) in different processing conditions [64].

In conclusion, the cells exposed to the PEF had a difference of 6% standard deviation in relation to the unexposed ones, which, although not quite significant, shows differences in the two values promoted by the application of PEF. It also demonstrated that, not all platelets were affected by electrical pulses and, in relation to the traditional method of freezing cells, which is an irreversible process, the PEF approach is reversible allowing the release of factors (PDFG) in a more controlled way. These results demonstrate the high potential of this technique for the transformation of platelet concentrates into biomedical applications [64].

3.3. Analytical methods

3.3.1. Trypan blue exclusion assay for cell viability and density

The trypan blue exclusion method assay is one of the earliest and simplest tests to determine cell viability of cells in suspension. Using only the trypan blue dye and an hemocytometer, like the Neubauer chamber (Figure 3.22), we can observe under the microscope that the living cells resemble like shiny pearls surrounded by a blue membrane, because the blue trypan surrounds the cell membrane but without penetrating it, this occurs because both trypan blue dye and cell membrane are negatively charged, so they repel themselves [65-66].

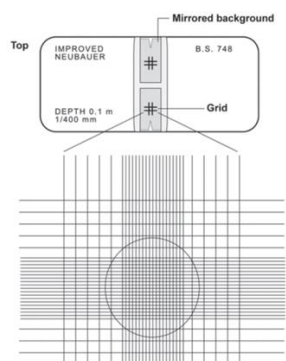


Figure 3.21. Hemocytometer – Neubauer chamber, and the area for cell counting [67].

In the other hand, the dead cells become blue, resemble like blueberries, as trypan blue can penetrate the non-viable cell, binding with intracellular proteins and renders the blue color.

This is based on the principle that living cells have their cell membrane intact and therefore impervious to dyes such as trypan blue, eosin or even propidium [65-66].

The procedure is quite simple, cells are mixed with trypan blue micro-pipetting up and down, then left to incubate for less than 3 minutes, because after this time most cells die [65-66][68].

If not otherwise, the volume of trypan blue should be equal to the volume of cells in suspension, so the dilution ratio should be 1 to 2. For example, 20µL of trypan blue and 20µL of cell suspension. The hemocytometer supports 10 to 20µL in each side. But if needed, dilution factor can also be calculated by formula 8, being the initial volume the one from the sample, and the final volume the sum of the sample volume with the blue trypan volume. The dilutions chosen are to give an eligible number of cells for hemocytometer counting [68-69].

$$f = \frac{\text{final volume}}{\text{inicial volume}} \quad (8)$$

Table 3.3. Example of different dilution factors in trypan blue exclusion method assay

Dilution factor <i>f</i>	10			5			2.5			1.25			1.11		
Total volume / Final volume (µL)	50	100	200	50	100	200	50	100	200	50	100	200	50	100	200
Cell volume / Initial volume (µL)	5	10	20	10	20	40	20	40	80	40	80	160	45	90	180
Trypan blue dye volume (µL)	45	90	180	40	80	160	30	60	120	10	20	40	5	10	20

The living cells are counted as well as dead cells (to know the number of total cells), calculating cell viability, dividing the number of living cells by the total number of cells, and multiplying by 100, as seen in formula 9. A good viability is considered above 90%.

$$\text{Cell Viability} = \frac{n \text{ living cells}}{n \text{ total cells}} \times 100 \quad (9)$$

On the other hand, we also can determine cell mortality, which is used to determine the percentage of dead cells, relating the number of dead cells with the number of total cells, multiplied by 100 (formula 10).

$$\text{Cell Mortality} = \frac{n \text{ dead cells}}{n \text{ total cells}} \times 100 \quad (10)$$

To finish this topic, it is also important to calculate the number of viable cells, which is called cell density and is expressed in formula 11, where the volume is expressed in mL, and the hemocytometer field volume is, by definition, 0,0001mL.

Cell density determination is important to know the real number of cells seeded and their expansion.

$$\text{Cell Density} = \frac{n \text{ living cells} \times \text{dilution factor} \times \text{volume}}{\text{hemocytometer field volume}} \quad (11)$$

3.3.2. FTIR spectroscopy for component analysis

Since the 20th century, infrared (IR) spectroscopy coupled with microscopy (IR microspectroscopy) has been considered a non-destructive, unlabeled, and highly sensitive and specific analytical method, with many useful applications in different fields in the biomedical area and specifically in research cancer. Fourier transform (FT) infrared (IR) spectrometers were commercially introduced in 1970 [70-71].

Fourier transform infrared (FTIR) spectroscopy is a universal analytical technique used in the evaluation of a wide range of materials, namely, to identify unknown materials that can be pure substances, mixtures, impurities, or compositions of various materials. The FTIR technique has become very useful in screening applications due to its speed of analysis, being fundamental for the analysis of pharmaceuticals, polymers and plastics, food, environment, and counterfeit materials, including medicines. Currently, the modification of biomaterials and their possible applications in medical implants or other biomedical devices is increasingly relevant and advanced FTIR technologies are useful for investigations in this area. FTIR is an inexpensive technique that can allow direct quantitative measurements of some organic substances, including adsorbed/immobilized compounds, using a standard calibration curve of known concentrations. One of the advantages of the quantitative FTIR procedure is also the accurate measurement of compounds that are difficult to quantify because they don't absorb visible UV light or require expensive analytical procedures. The appearance of new functional groups in the FTIR spectra can identify covalent modifications and, on the other side, the displacement of the spectral bands' characteristic of the material or the immobilized molecule can indicate non-covalent interactions such as Van der Waals interactions and hydrogen bonds [70].

Electromagnetic waves in a wide and continuous range of frequencies constitute an electromagnetic spectrum and are widely used in cancer research and diagnosis. In the electromagnetic spectrum, X-rays and gamma rays are characterized by the highest energy photons associated with shortest wavelength and highest frequency. On the other hand, radio waves are characterized by the lowest energy photons associated with the highest wavelength and the lowest frequency. Infrared (IR) radiation covers an interval of the electromagnetic spectrum between the red

end of the visible region ($\lambda \sim 780 \text{ nm}$, $\nu \sim 0.38 \times 10^{15} \text{ Hz}$ and $h\nu \sim 1.59 \text{ eV}$) and the beginning of the microwave region ($\lambda = 1 \text{ mm}$, $\nu = 3 \times 10^{11} \text{ Hz}$ and $h\nu = 1.24 \times 10^{-3} \text{ eV}$). The wavenumber ($\tilde{\nu}$), the wavelength (λ) and the frequency (ν) are related by the equations 12 and 13:

$$\lambda = \frac{c}{\nu} = \frac{1}{\tilde{\nu}} \quad (12)$$

$$\tilde{\nu}(\text{cm}^{-1}) = \frac{1}{\lambda(\mu\text{m})} \quad (13)$$

Where c is the speed of light in vacuum ($3 \times 10^8 \text{ m/s}$).

The fundamental vibrational modes that can be detected by mid-IR spectroscopy are represented mainly by bond stretching (symmetric and antisymmetric) and bond deformations (mainly symmetric and antisymmetric bending). For example, the Figure 3.22 shows the vibrations associated with the water molecule where the free H-O-H molecule contains the antisymmetric and symmetric stretching vibrations that occur at $\sim 3500 \text{ cm}^{-1}$ and $\sim 1650 \text{ cm}^{-1}$, respectively, and the bending deformations of the O-H group that occur at $\sim 600 \text{ cm}^{-1}$. Once the frequency of a vibration is simultaneously determined by the bond strength, the vibrational mode and reduced mass of atoms that make up chemical groups as well as the frequencies at which specific vibrations occur within the spectrum are reasonably constant for a given functional group (for example, $-\text{CH}_2$, $-\text{C}=\text{O}$, O-H) [72].

Transmittance is the fraction of incident light with a specific wavenumber that passes through a sample of matter. It consists of the unchanged passage of radiation through matter, caused by the saturation of this energy. The intensity of mid-IR radiation passing through the sample and reaching the detector (I) is compared to the intensity of infrared radiation reaching the detector without passing through the sample (I_0). The resulting percentage of transmitted radiation, % T, can be obtained by the equation 14:

$$\%T = \frac{I(\tilde{\nu})}{I_0(\tilde{\nu})} \times 100 \quad (14)$$

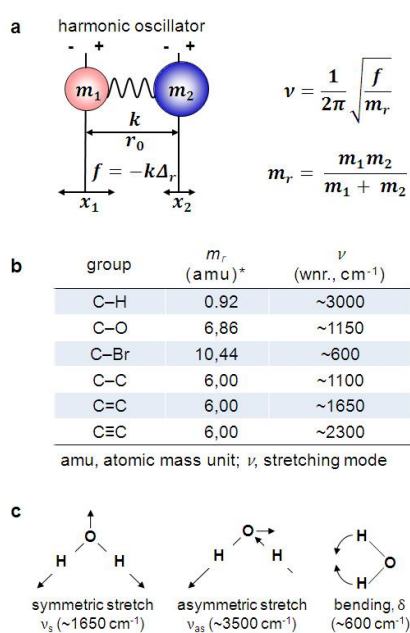


Figure 3.22. a) The harmonic oscillator models. b) Table illustrating the relationship between vibrations of some functional groups, atomic masses, and bond strength. c) Fundamental vibrational modes of a free water molecule detectable at specific frequency values of the electromagnetic spectrum [72].

Absorbance is the intrinsic ability of materials to absorb radiation at a specific frequency. The absorbance is proportional to the thickness of a sample and the concentration of the substance in it, in contrast to the transmittance that varies exponentially with the thickness and concentration. The corresponding amount of mid-IR radiation absorbed, A , by the sample is obtained by equation 15.

$$A_{(\bar{\nu})} = \log_{10} \frac{1}{T_{(\bar{\nu})}} = \log_{10} \frac{I_{(\bar{\nu})}}{I_{0(\bar{\nu})}} \quad (15)$$

The Lambert–Beer law relates the absorption of light with the properties of the material it passes through (equation 16).

$$A_{(\bar{\nu})} = a_{(\bar{\nu})}lc \quad (16)$$

Where $A_{(\bar{\nu})}$ is the absorbance, $a_{(\bar{\nu})}$ is the molar absorptivity of the substance, l is the optical path length and c is the concentration of the sample.

FTIR analysis can be performed in transmission or reflection modes. The specific FTIR analysis mode, as well as the sample preparation method, is selected based on the particular characteristics of the sample. The sample can be inspected for visible light in the transmission, while the medium infrared radiation passes through the sample, is reflected by the coating on the low-e slide and then passes through the sample again and directs to the detector. Attenuated total reflectance is a special form of FTIR reflectance where IR radiation makes several passes through the ATR crystal and with each pass a relatively thin layer of the adjacent sample is analyzed. ATR is an internal reflection technique in which the infrared beam is directed through an internal reflection element (IRE) with the highest refractive index, n_1 , for the sample with the lowest refractive index, n_2 , as shown in Figure 3.23. As the fingerprints of many organic compounds are unique, the FTIR is most used to provide qualitative identification of compounds [56].

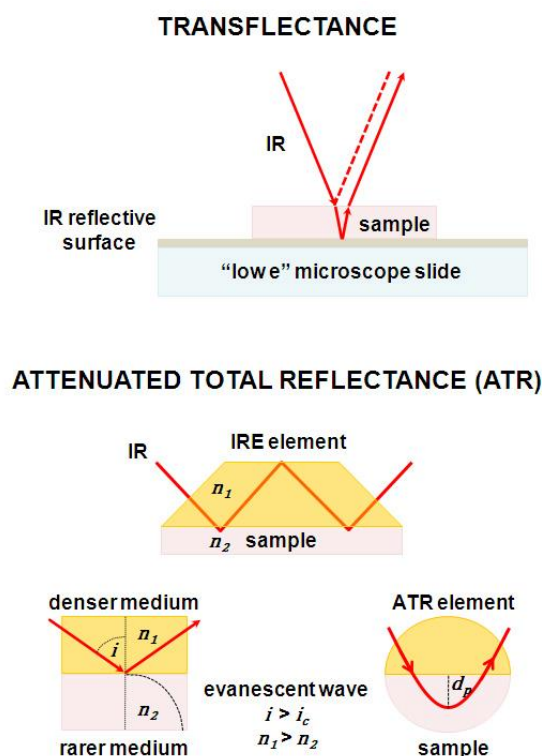


Figure 3.23. Above, the transflectance technique that couple's absorption and reflection through the sample, and below, the attenuated total reflectance (ATR) technique [72].

The main peaks are Amide I and Amide II, characterizing the spectrum of proteins and polypeptides. The amide I band which absorbs $\sim 1650 \text{ cm}^{-1}$ identifies the C=O stretching mode associated with the vibrations of a secondary amide, $-\text{C}(=\text{O})\text{N}(\text{H})-$, while the amide II band ($\sim 1550 \text{ cm}^{-1}$) refers to the combination of N-H bending and C-N stretching vibrations. The $\nu_{\text{as}}\text{CH}_3$ and $\nu_{\text{as}}\text{CH}_2$ vibrations observed at wavenumbers $\sim 2958 \text{ cm}^{-1}$ and $\sim 2920 \text{ cm}^{-1}$, together with $\nu_{\text{s}}\text{CH}_3$ and $\nu_{\text{s}}\text{CH}_2$ occurring at $\sim 2872 \text{ cm}^{-1}$ and $\sim 2852 \text{ cm}^{-1}$, respectively identify lipid molecules. The stretching vibrations $\nu_{\text{as}}\text{PO}_2$ and $\nu_{\text{s}}\text{PO}_2$ ($\sim 1240 \text{ cm}^{-1}$ and $\sim 1085 \text{ cm}^{-1}$, respectively) can mean the absorption of O-P=O bonds of the polynucleotide chains in DNA and RNA. However, the IR spectrum of a cell usually contains a high number of bands, some of which it is impossible to associate with absolute certainty for a specific group, analyzing the "fingerprint region".

In Figure 3.24, some of the most relevant functional groups and respective vibrational modes are represented, each of which is associated with a specific wavenumber or range of values as well as the common designation of the biochemical component [72].

Figure 3.25 is an example of a spectra obtained by FTIR identifying the respective bands from which it gets the structure of the analyzed compound.

Wavenumber (cm ⁻¹)	Functional group	Vibrational mode	Commonly assigned biochemical component
3500 - 2500 X-H stretching vibrations (where X is C, O, or N)			
~ 3300	N-H	$\nu(\text{N-H})$	Amide A: peptide, protein
~ 3100	N-H	$\nu(\text{N-H})$	Amide B: peptide, protein
2957	C-CH ₃	$\nu_{\text{as}}(\text{CH}_3)$	lipids
2920	$-(\text{CH}_2)_n-$	$\nu_{\text{as}}(\text{CH}_2)$	
2872	C-CH ₃	$\nu_{\text{s}}(\text{CH}_3)$	
2851	$-(\text{CH}_2)_n-$	$\nu_{\text{s}}(\text{CH}_2)$	
2000 - 1500 fundamental stretching vibrations of double bonds (e.g., C=O, C=C, C=N)			
~ 1740	$-\text{CH}_2-\text{COOR}$	$\nu(\text{C=O})$	Phospholipid esters
~ 1655	O=C-N-H	80% $\nu(\text{CO})$, 20% $\nu(\text{CN})$	Amide I peptide, protein
~ 1645	H-O-H	$\gamma(\text{HOH})$	Water
~ 1545	O=C-N-H	60% $\gamma(\text{N-H})$, 30% $\nu(\text{C-N})$, 10% $\nu(\text{C-C})$	Amide II peptide, protein
$\sim 1500 - 600$ the "fingerprinting region": many overlapped vibrations			
~ 1450	$-(\text{CH}_3)_n-$	$\delta_{\text{as}}(\text{CH}_3)$	Lipid, protein
	$-(\text{CH}_2)_n$	$\delta_{\text{as}}(\text{CH}_2)$	
~ 1395	$-(\text{CH}_3)_n-$	$\delta_{\text{s}}(\text{CH}_3)$	Lipid, protein
	$-(\text{CH}_2)_n$	$\delta_{\text{s}}(\text{CH}_2)$	
~ 1380	C-CH ₃	$\gamma_{\text{s}}(\text{CH}_3)$	Phospholipid, fatty acid, triglyceride
1400 - 1200	O=C-N-H, CH ₃	$\gamma(\text{N-H})$, $\nu(\text{C-N})$, $\gamma(\text{C=O})$, $\nu(\text{C-C})$ and $\nu(\text{CH}_3)$	Amide III peptide, protein, collagen
$\sim 1245 - 1230$	RO-PO ₂ ⁻ -OR	$\nu_{\text{as}}(\text{PO}_2^-)$	DNA, RNA, phospholipid, phosphorylated protein
~ 1170	R-COO-R'	$\nu_{\text{as}}(\text{C-O})$	Ester
~ 1160 and ~ 1120		$\nu(\text{C-O})$	RNA ribose
~ 1150	C-O, C-O-H	$\nu(\text{CO})$, $\gamma(\text{COH})$	carbohydrates
~ 1095 , ~ 1084 , ~ 1070	RO-PO ₂ ⁻ -OR	$\nu_{\text{s}}(\text{PO}_2^-)$	DNA, RNA, phospholipid, phosphorylated protein
~ 1078	C-C	$\nu(\text{CC})$	glycogen
~ 1060 , 1050 , 1015	C-O	$\nu(\text{CO})$	DNA and RNA ribose
~ 1050	C-O-P	$\nu(\text{COP})$	Phosphate ester
~ 1028	C-O-H	def(CHO)	glycogen
~ 965	PO ₃ ²⁻	$\nu(\text{PO}_3^{2-})$	DNA and RNA ribose
~ 950	P-O	$\nu(\text{PO}_3^{2-})$	Phosphorylated protein
~ 920	C-O-P	$\nu(\text{COP})$	Phosphorylated protein

ν , stretching; δ , bending; γ , wagging, twisting, and rocking; def, deformation, as, antisymmetric; s, symmetric.

Figure 3.24. Summary of the vibrational frequencies of some functional groups, associated with a wavenumber, in molecules in the mid-IR region of the electromagnetic spectrum [72].

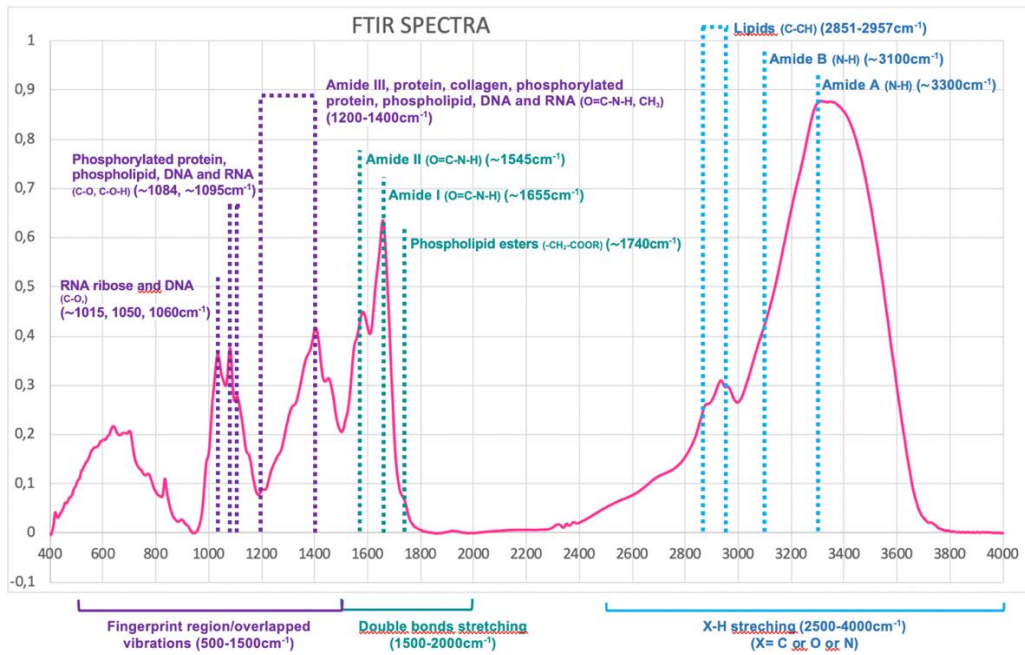


Figure 3.25. Spectra obtained by FTIR, infatizing the peaks where each type of biochemical component belongs. In the image is visible three different regions; the stretching region, where are Amide A and B and Lipids; the double bonds stretching region, where are Amide I and II and phospholipid esters; and the Fingerprint region, where are Amide III, diverse proteins like collagen and others, DNA and RNA.

[This page is intentionally left blank]

Chapter 4

4. Materials & Methodologies

4.1. Preliminary tests

With the aim of correctly design all experiments, the equipment and cell line had to be explored, to do so, a series of preliminary tests were carried out, as seen in figure 4.1.

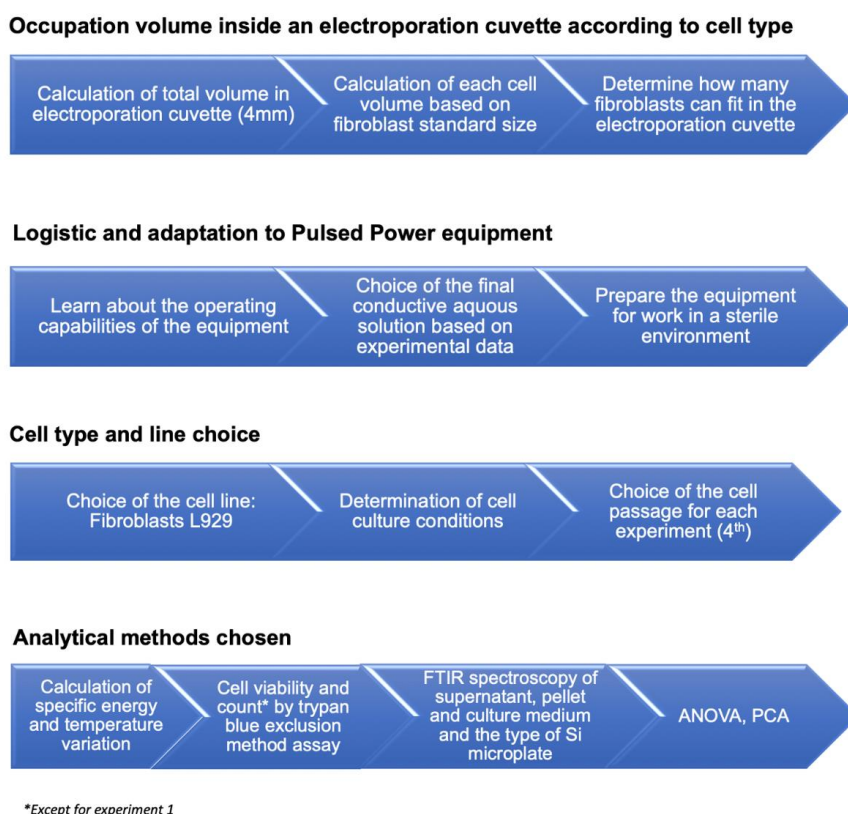


Figure 4.1. Summary scheme of all preliminary tests

4.2. Cell line and cryopreservation

The cells used in this work were L929 Fibroblasts from mouse lung, gently supplied by *Instituto Superior Técnico* (IST) Laboratories, in vials of cryopreservation with 1×10^6 of cells per mL of a solution composed by 70% of DMEM medium, 25% of FBS and 5% of DMSO, and preserved in liquid nitrogen.

The transport was carried out in a Styrofoam box for the Research & Development Laboratory in Health and Engineering of *Instituto Superior de Engenharia de Lisboa* (ISEL), where the cells were, in the first place, preserved for a short period of time in the -80°C refrigerator and then thawed, expanded and growth in a form of subculture for the Master cell bank, at ISEL. At ISEL, the cells were cryopreserved at -80°C in the same cryopreservation solution as indicated above.

4.3. Cell culture – Thaw and expansion

For cell culture and maintenance, it was used a complete culture medium composed by Dulbecco's Modified Eagle Medium (further designated as DMEM) with 4.5g/L Glucose and L-Glutamine, supplemented with 10% of GIBCO® Fetal Bovine Serum (further designated as FBS) and 1% of Streptomycin and Penicillin. To rinse and detach cells were used GIBCO® Dulbecco's Phosphate-Buffered Saline (further designated as DPBS) and GIBCO® Trypsin-EDTA (Ethylenediaminetetraacetic acid) (0.25%), phenol red, respectively. Trypan blue (0.4%) solution prepared in (0.85%) NaCl, by Lonza, was used to dye cells.

All the proceedings involving cell culture were carried out with different solutions, the complete medium, DPBS, and Trypsin-EDTA, which were stored primarily on the refrigerator 4°C and then slightly heated to 37°C in the *BINDER IP 20 incubator*, to avoid thermal shocks in the cells.

All procedures where cells could be exposed to air were conducted inside a laminar flow cabinet (vertical flow) from Faster brand and the model *BHG 2006* (Figure 4.1). Cell centrifugations were conducted in a Hettich Universal 32 model centrifuge equipped to support falcon tubes of 15mL. Optical microscopy observations of T-flasks and culture plates were made with an inverted phase microscope *Zeiss Axiovert 40 CFL* (Figure 4.2). Cell viability and cell density determination were conducted with an ordinary optical microscope Olympus BX41, using a hemocytometer – improved Neubauer chamber from *Hirschmann-Laborgeräte* (Figure 4.3) – with trypan blue dye.



Figure 4.2. Left: Laminar vertical flow cabinet. Right: Work inside the laminar flow cabinet, using the automatic motorized pipette to remove culture medium.

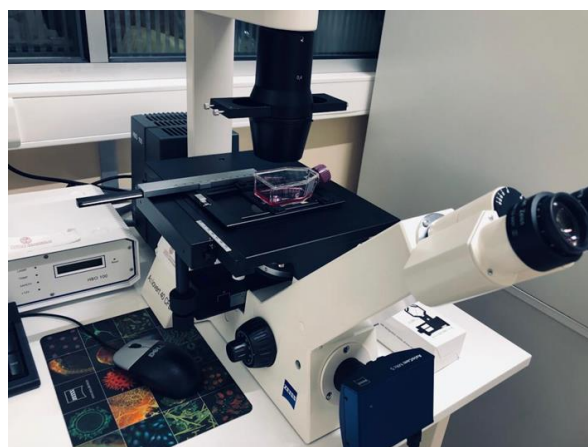


Figure 4.3. Cell culture in T-flask observed by the inverted phase microscope *Zeiss Axiovert 40 CFL*.

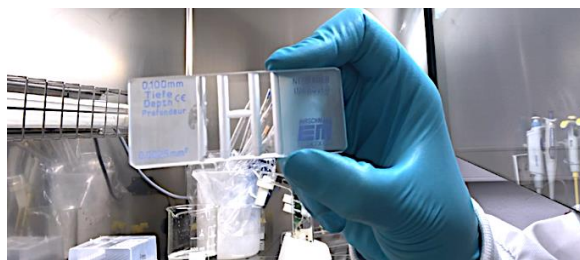


Figure 4.4. Hemocytometer (before assembly) improved Neubauer chamber from *Hirschmann-Laborgeräte*.

For initiate the cell culture from cryopreserved vials, cells were thawed in a MICROM SB80 warm bath at 37°C, where the cryogenic vial was dive in for a short time, until almost all sample was liquid. The sample was then transported for the laminar flow cabinet and quickly transfer for a 15mL falcon tube with 4mL of complete culture medium and subsequently centrifuged at 1400RPM for 9 minutes. The supernatant was discarded, and the pellet resuspended in 1mL of complete culture medium. Cell density and viability were determined using the hemocytometer, so it could be determined the number of cells to seed in T25 Nunc flasks (25cm²) (Figure 4.4), knowing in advance that the number of cells recommended for sowing is between 2500 to 5000 per cm², which represents 100,000 cells sown in 4 to 5mL of complete medium. Cells were subsequently grown and preserved in a CO₂ incubator by BINDER model CB150, at 37°C and 5% CO₂, so it can maintain the pH and temperature in optimum levels, and the medium of culture changed every 48 hours until they reach between 80% to 90% of confluence.



Figure 4.5. Two different T25-Flasks (25cm² of adhesion surface) with Nunclon Delta treated surface for cell culture.

After cells reach the desired confluence, the old medium was discarded, and the cells were rinsed with DPBS to remove typical FBS proteins. Thereafter, 1.25mL of trypsin-EDTA (0.5mL trypsin-EDTA per 10cm²) was added and the T25 flasks were returned to the CO₂ incubator at 37°C for no more than 3 minutes. After this, it was observed under the microscope that the cells were already completely detached from the flasks. It was subsequently added to each T25 flask 2.5mL (twice the volume) of complete medium to the trypsin (to inhibit its protein degradation action and cell death), then, cells were transferred to a 15mL falcon tube and centrifuge at 1700RPM for 10 minutes. The supernatant was discarded, and the pellet resuspended in 1mL of complete medium.

Cell density and viability were performed using a hemocytometer under a microscope, with cells stained with trypan blue. For this procedure, it was used a dilution factor of 10, that is, 180µL of solution containing the pellet and 20µL of trypan blue dye. The stained cells were left to rest in the hemocytometer for 2 minutes, so that the trypan blue could have time to act. After this time, the hemocytometer was taken to the microscope and the stained cells counted.

The cells were sown once more, using several T25 flasks, thus expanding the culture, so that, in the end, it could be a master cell bank and a working cell bank, in which the cells for this work were taken.

4.4. PEF experiments

These experiments aim to study, on the one hand, the viability of the sample before and after different PEF applications, and in the other hand, the influence of cell density in the electric field and the possibility to repeat PEF applications in the same sample.

The Pulsed Electric Fields (PEF) applications were made using the *EPULSUS-LPM1B-10* equipment (i.e. 10 kV/400A/3kW lab equipment) (Figure 4.5), technology developed by *Energy Pulse Systems*, in sterilized electroporation cuvettes from *VWR* with a capacity of 0.8 to 1mL with 4mm gap between electrodes (Figure 4.6).



Figure 4.6. EPULSUS-LPM 1B-10 equipment inside culture room for PEF applications.



Figure 4.7. Electroporation cuvette from VWR with a capacity of 0.8 to 1mL.

Once more, all procedures where cells could be exposed to air were conducted inside the laminar flow cabinet already described. DPBS was used not only to rinse cells before enzymatic detachment but also to resuspend cells during the PEF application, functioning as a conductive medium. To detach the cells, it was used Trypsin-EDTA. To stained cells for viability, before and after PEF, trypan blue dye was used. To inhibit Trypsin action and to put cells in culture, after PEF application, it was used complete medium DMEM with 4.5g/L Glucose and L-Glutamine, supplemented with 10% FBS and 1% Streptomycin and Penicillin.

For all PEF experiments, Fibroblasts L929 cells in culture at the 4th passage were used. For these experiments, cells were rinsed with DPBS and detached enzymatically with trypsin and EDTA solution for no more than 3 minutes. After this, double of the volume in complete medium was added to the cells resuspended in trypsin and then taken to centrifuge at 1700 RPM for 9 minutes. If not otherwise stated, cells were counted and apportioned, in the desired cell quantity, into Eppendorf tubes with 800-1000 μ L of DPBS (depending on the experiment) and maintained in low temperature of 4°C in the refrigerator 15 minutes before starting PEF application and then transferred to a box of ice inside the laminar flow cabinet, in order to lower cell metabolism so that they could resist longer outside the CO₂ incubator.

In general, all PEF experiments were conducted in triplicates and in specific cases using triplicates of the triplicates. A positive and a negative control were performed, except in the first experiment. The

negative control group was conducted as the operation groups except that was not submitted to PEF and the positive control was based on completed cell lysis through three cycles of freezing (at -80°C) and thawing (in the warm bath).

After PEF, cells in DPBS returned to the Eppendorf tubes and maintained at 4°C in the box of ice, where part of the volume of the solution was used to determine cell density and viability, other part of the volume were used for seeding into a 24-well adherent Nunc® plate (Figure 4.7) with complete medium that was subsequently placed in a CO₂ incubator. For this, seeding calculations were made, to obtain the desired number of cells. The remaining volume was centrifuged for 1700 RPM for 15 minutes, where the supernatant and the pellet were separately taken for FTIR analysis on Si microplates of 96-well or 384-well (Figure 4.8) after the plates have been dehydrated in the desiccator. The FTIR equipment used was VERTEX 70 spectrometer from Bruker (Germany) equipped with an HTS-XT module, also from Bruker (Figure 4.9). The FTIR equipment is connected to a computer and the data acquisition is obtained by OPUS 6.5 software, from Bruker. The resulting spectra was converted by Unscrambler X software and the data analyzed in Excel Microsoft software.

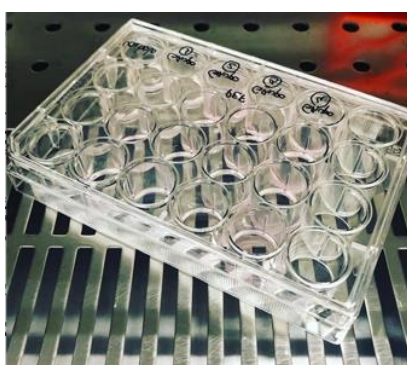


Figure 4.8. 24-well adherent Nunc culture plate.

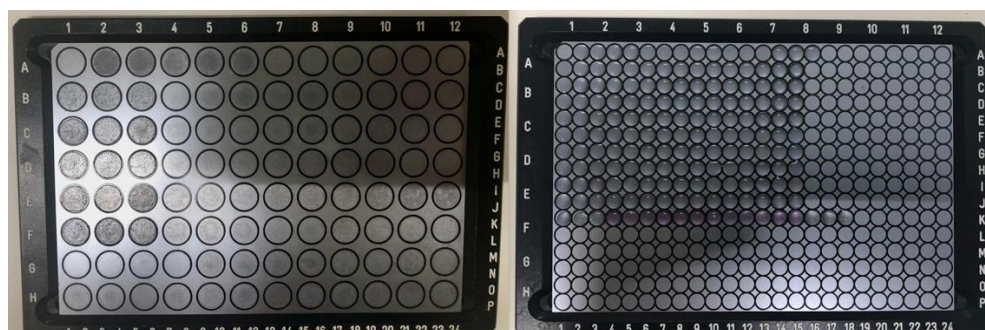


Figure 4.9. Si microplates of 96-well (left) and 384-well (right) for FTIR analysis.



Figure 4.10. FTIR equipment: VERTEX 70 spectrometer from Bruker equipped with an HTS-XT module, also from Bruker, connected to a computer for data acquisition obtained by OPUS software, from Bruker.

4.4.1. Experiment 1 - Effect of PEF variations

This experiment aims to evaluate which are the best electrical parameters for PEF applications in fibroblasts.

The total number of cells required was $1,500 \times 10^3$ resuspended in 15mL of DPBS. The number of sterilized Eppendorf tubes for the assay was defined by triplicates of five groups A, B, C, D, E, this is, 15 Eppendorf tubes in total, properly labeled (A1, A2, A3, B1, B2, B3, C1, C2, C3, D1, D2, D3, E1, E2, E3). Each Eppendorf tube contains 100,000 cells per 1mL of DPBS.

The Eppendorf tubes were stored in low temperature, at 4°C, in the refrigerator, 15min before starting the PEF application, and then transferred to a Styrofoam box with ice inside the laminar flow cabinet, where the tubes remained for the entire experiment, so cells could have a lower metabolic status and thus optimizing their chances of survival.

PEF application protocol

It was taken, from each Eppendorf tubes, 1000µL of solution with 100,000 fibroblasts resuspended, and placed inside the electroporation cuvette and then transported to the PEF application equipment. Each group used its own cuvette, new and sterilized. After this, the solution of cells returned to the Eppendorf tubes from which they were taken and remain on ice, repeating the process for the remaining Eppendorf tubes of the same group, using the same energy field in each triplicate group, and in the case of the negative control group (group A), the same procedure was performed but only with PEF application simulation.

The following PEF parameters were used for each group, using the PEF equipment display (Figure 4.10) to set different conditions, and using a digital oscilloscope, from Lecroy model WaveAce 224 - 200MHz (Figure 4.11), to control the waveform:

- Group A, not exposed to PEF (negative control group);
- Group B, exposed to a field of 10kV/cm (4kV in 0.4cm) and 20 Pulses of 5µs with $f=1\text{Hz}$;
- Group C, exposed to a field of 10kV/cm (4kV in 0.4cm) and 2 Pulses of 5µs with $f=1\text{Hz}$;
- Group D, exposed to a field of 15kV/cm (6kV in 0.4cm) and 1 Pulse of 5µs with $f=1\text{Hz}$;
- Group E, exposed to a field of 10kV/cm (4kV in 0.4cm) and 10 Pulse of 5µs with $f=1\text{Hz}$.



Figure 4.11. PEF equipment display to set the electrical parameters.

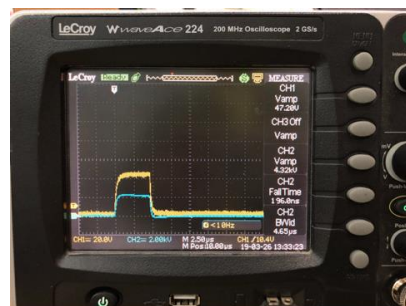


Figure 4.12. Digital oscilloscope, from Lecroy model WaveAce 224 - 200MHz, to show graphically varying signals and control the waveform of each pulse.

Analysis protocol after PEF application

- 1) The cells of each Eppendorf tube were gently resuspended with a micropipette, subsequently 40 μ L of the solution, containing approximately 4,000 cells (alive and dead cells), was taken and mixed with 10 μ L of trypan blue dye in a dilution factor of 1.25. With a micropipette, the stained solution was placed in a Neubauer chamber where it rests for 2 minutes (so that the trypan blue assay could be effective) and taken to the optical microscope Olympus BX41, where cells were counted, and their viability calculated.
- 2) 77.20 μ L of the remaining solution, containing approximately 7,720 cells (4,000 cells per cm² in wells of 1.93cm²), were taken from each cuvette and seeded into a 24-well adherent Nunc® plate (Figure 4.12) with 422.8 μ L of complete medium and placed in culture in the CO₂ incubator, to reassess at 48 and 72h.
- 3) The remaining cuvette volume, corresponding approximately to 882.80 μ L, was placed into the Eppendorf tubes and taken to centrifuge at 1700RPM for 15min, where the supernatant (DPBS) and the pellet were separately taken for FTIR analysis. 25 μ L of supernatant was plated in each well of the Si 96-well FTIR plate (Figure 4.13), and the pellet from the triplicates of group A, B, C, D and E were resuspended together, centrifuged at 1700RPM for 15min and plated in a volume of 25 μ L for well with each well containing approximately 264,840 cells (Figure 4.9). The Si plates of 96-well were dehydrated in the desiccator for a minimum of 2.5h and read in the FTIR equipment already described.
- 4) The resulting spectra was converted and analyzed by Unscrambler X and Excel software.
- 5) The remaining Eppendorf tubes were stored at -20°C for future analysis.
- 6) The cells in culture were observed in the inverted phase microscope Zeiss Axiovert 40 CFL at 48h and then again at 72h, and a sample of their medium was centrifuged, 1700RPM for 15min, and the supernatant taken to FTIR analysis. At 72h, each well was subjected to enzymatic detachment. To do so, each well medium was aspirated with a micropipette and put aside for further FTIR analysis. Subsequently, the cells were rinsed with DPBS to obliterate traces of FBS proteins. The washing DPBS was discarded, and 96.5 μ L of trypsin-EDTA (0.5 ml trypsin/10 cm²) was added to the cells, and the culture plate taken to the CO₂ incubator for no longer than 3min. After this time the culture plate was observed under the inverted phase microscope to confirm that cells were already loose. 193 μ L were added to the trypsin and this solution with cells aspirated and taken to centrifuge, 1400RPM for 9min. Subsequently the cells were resuspended in 1000 μ L of DPBS and their viability and density calculated in a trypan blue exclusion assay. Cell pellets were plated separately in a 96-well microplate such as the reserved medium. The microplate was dehydrated for 2.5h, read in the FTIR equipment, the spectra obtained in OPUS, converted in Unscrambler X and analyzed in Excel software.

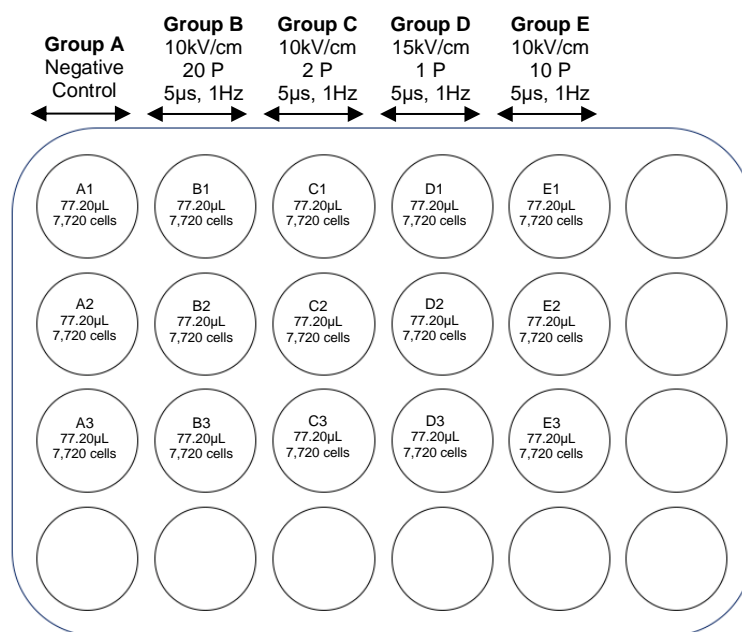


Figure 4.13. Schematic image of the sown cells in a Nunc® 24-well adherent culture plate.

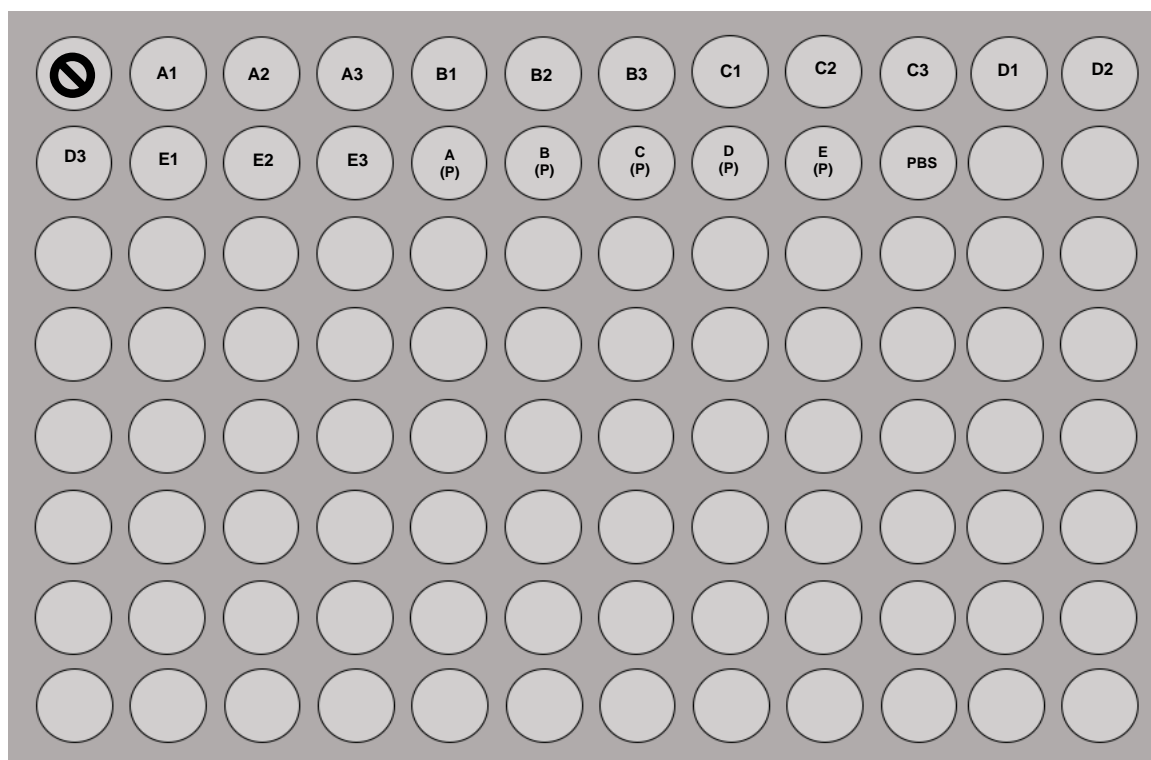


Figure 4.14. Schematic image of the Si 96-well microplate for FTIR analysis in experiment 1, immediately after PEF. A1 to E3 are the samples of DPBS without the cells. From A(P) to E(P) there are samples of cells pellet. PBS is pure DPBS without contacting cells, for control of single DPBS signal versus DPBS that contacted with cells.

4.4.2. Experiment 2 - Effect of cell density

The objective of this experiment was to change the cell density per group but always using the same electrical parameters for the entire experiment, i.e. 10kV/cm (4kV in 0.4cm) and 5 Pulses of 5 μ s with $f=1$ Hz, in order to evaluate how can cell density affect the electrical field.

For all groups the total number of required cells was 9.5×10^6 , distributed in different quantities for 25 Eppendorf tubes properly labeled (A1, A2, A3, A-, A+, B1, B2, B3, B-, B+, C1, C2, C3, C-, C+, D1, D2, D3, D-, D+, E1, E2, E3, E-, E+) with 800 μ L of DPBS in each Eppendorf tube. The cells were kept at 4°C, 15min before starting PEF application.

PEF application protocol

800 μ L of solution of DPBS with fibroblasts, was taken from each Eppendorf tube and placed inside the cuvette correspondent to its group, and then transported to the equipment for PEF application. After this, the cells returned to the Eppendorf tubes from which they were taken and remain in ice, repeating this process three times, using DPBS to wash the cuvette before using the same energy field in each triplicate group, and in the case of the negative control group, exactly the same procedure was performed but only with PEF application simulation. The positive control, with the specific objective of promoting cell lysis, was not exposed to PEF but instead subjected to three successive cycles of freezing and thawing.

Five conditions were defined for the groups submitted to pulsed electric fields:

- Group A, containing 1×10^6 cells (with the triplicates A1, A2, A3, a negative control A- and a positive control A+);
- Group B, containing 500,000 cells (with the triplicates B1, B2, B3, a negative control B- and a positive control B+);
- Group C, containing 250,000 (with the triplicates C1, C2, C3, a negative control C- and a positive control C+);
- Group D, containing 100,000 cells (with the triplicates D1, D2, D3, a negative control B D- and a positive control D+);
- Group E, containing 50,000 with the triplicates E1, E2, E3, a negative control E- and a positive control E+).

Analysis protocol after PEF application

- 1) The volume of solution containing the cells from each cuvette was taken according to the belonging group, since the dilution factor must be adapted to the concentration of cells:
 - 20 μ L from group A (mixed with 80 μ L of trypan blue dye, dilution factor 5);
 - 40 μ L from group B (mixed with 60 μ L of trypan blue dye, dilution factor 2.5);
 - 80 μ L from group C (mixed with 20 μ L of trypan blue dye, dilution factor 1.25);
 - 90 μ L from group D (mixed with 10 μ L of trypan blue dye, dilution factor 1.11);
 - 90 μ L from group E (mixed with 10 μ L of trypan blue dye, dilution factor 1.11).The mixed solutions were taken into Neubauer chambers, and the viability calculus proceeded the same way as the previous experiment. The total number of living cells after the assay was also calculated.
- 2) To cell culture, the sown was according to the total number of living cells on each Eppendorf tubes, in order to have 7720 cells per well (4,000 cells per cm^2 in wells of 1.93cm^2), the following volumes were extracted from each Eppendorf:
 - 7.35 μ L from Eppendorf tube A1;
 - 7.72 μ L from Eppendorf tube A2;
 - 8.58 μ L from Eppendorf tube A3;
 - 6.43 μ L from Eppendorf tube A-;
 - 77.20 μ L from Eppendorf tube A+;

- 25.73 μ L from Eppendorf tube B1;
- 16.25 μ L from Eppendorf tube B2;
- 25.73 μ L from Eppendorf tube B3;
- 12.87 μ L from Eppendorf tube B-;
- 308.80 μ L from Eppendorf tube B+;
- 44.11 μ L from Eppendorf tube C1;
- 56.15 μ L from Eppendorf tube C2;
- 51.47 μ L from Eppendorf tube C3;
- 25.73 μ L from Eppendorf tube C-;
- 617.60 μ L from Eppendorf tube C+;
- 173.70 μ L from Eppendorf tube D1;
- 231.60 μ L from Eppendorf tube D2;
- 694.80 μ L from Eppendorf tube D3;
- 63.16 μ L from Eppendorf tube D-;
- 694.80 μ L from Eppendorf tube D+;
- 694.80 μ L from Eppendorf tube E1;
- 694.80 μ L from Eppendorf tube E2;
- 694.80 μ L from Eppendorf tube E3;
- 138.96 μ L from Eppendorf tube E-;
- 694.80 μ L from Eppendorf tube E+.

These cell solutions were transferred to new and sterilized Eppendorf tubes and taken to centrifuge at 1400RPM for 9min, the supernatants discarded, and the pellets resuspended in 500 μ L of complete medium, and then taken to two 24-well adherent plates (Figure 4.14) and placed in culture in the CO₂ incubator.

- 3) The original Eppendorf tubes and their remaining solutions were centrifuged at 1700RPM for 15min, to separate the supernatant and the pellet, so, they can be analyzed separately. The supernatants (DPBS) were plated, in triplicates, in a 384-well FTIR microplate, being the volume of each well 5 μ L (Figure 4.15). The pellets were plated in triplicates, as well. The plates of 384-well were dehydrated in the desiccator for a minimum of 3h and read in the FTIR equipment.
- 4) The resulting spectra obtained in OPUS format was converted and analyzed by the Unscrambler X and Excel software.
- 5) The remaining Eppendorf tubes were stored at -20°C, for future work.
- 6) The cells in culture were observed in the inverted phase microscope Zeiss Axiovert 40 CFL at 72h and the medium aspired with a micropipette, centrifuged, 1700RPM for 15min, and the supernatant transferred to Eppendorf tubes to be plated in the 384-well microplate and analyzed by FTIR. The cells in culture medium were released with trypsin (as described in experiment 1), taken to centrifuge, 1400RPM for 9min and, subsequently, resuspended in 1000 μ L of DPBS for the viability assay in a trypan blue exclusion assay (also described before), with the same dilution factor per group as in step 1, and after this, centrifuge, 1700RPM for 15min, and the pellet of each Eppendorf tube plated in the 384-well microplate, making triplicates of each sample. The microplate was dehydrated for 3h, read in the FTIR equipment, the spectra obtained in OPUS, converted in Unscrambler X and analyzed in Excel software.

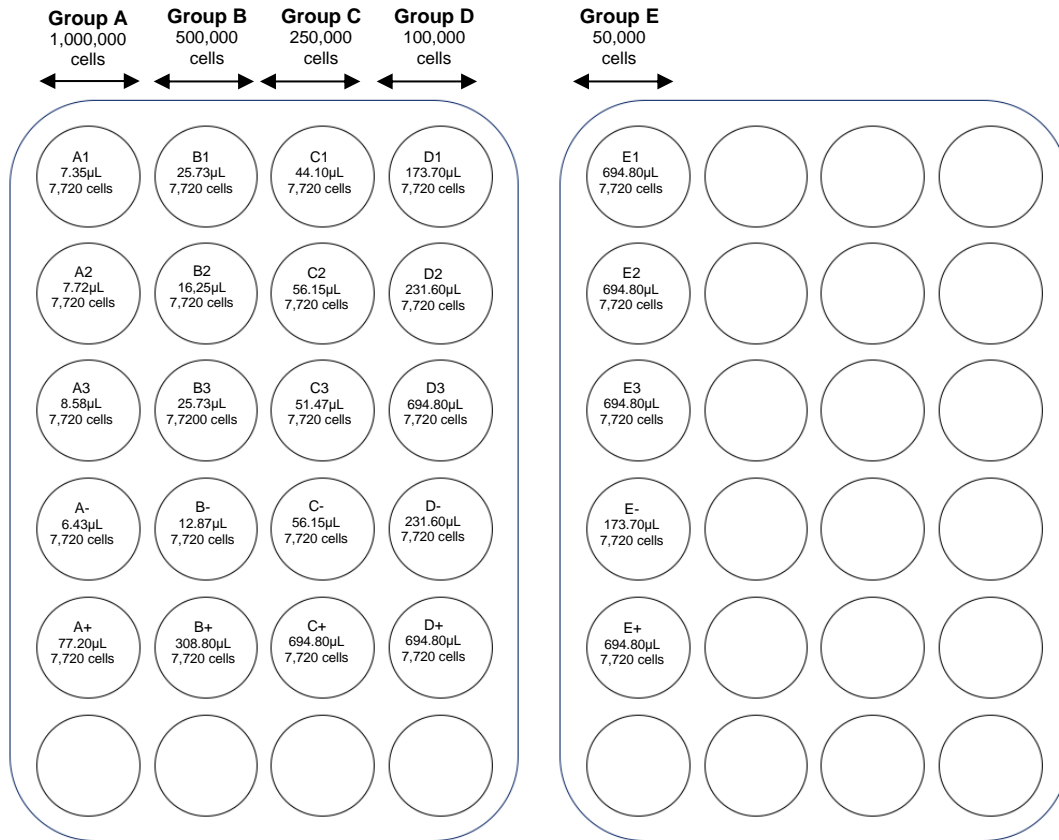


Figure 4.15. Schematic image of the sown cells in the two Nunc® 24-well adherent culture plate, in experiment 2.

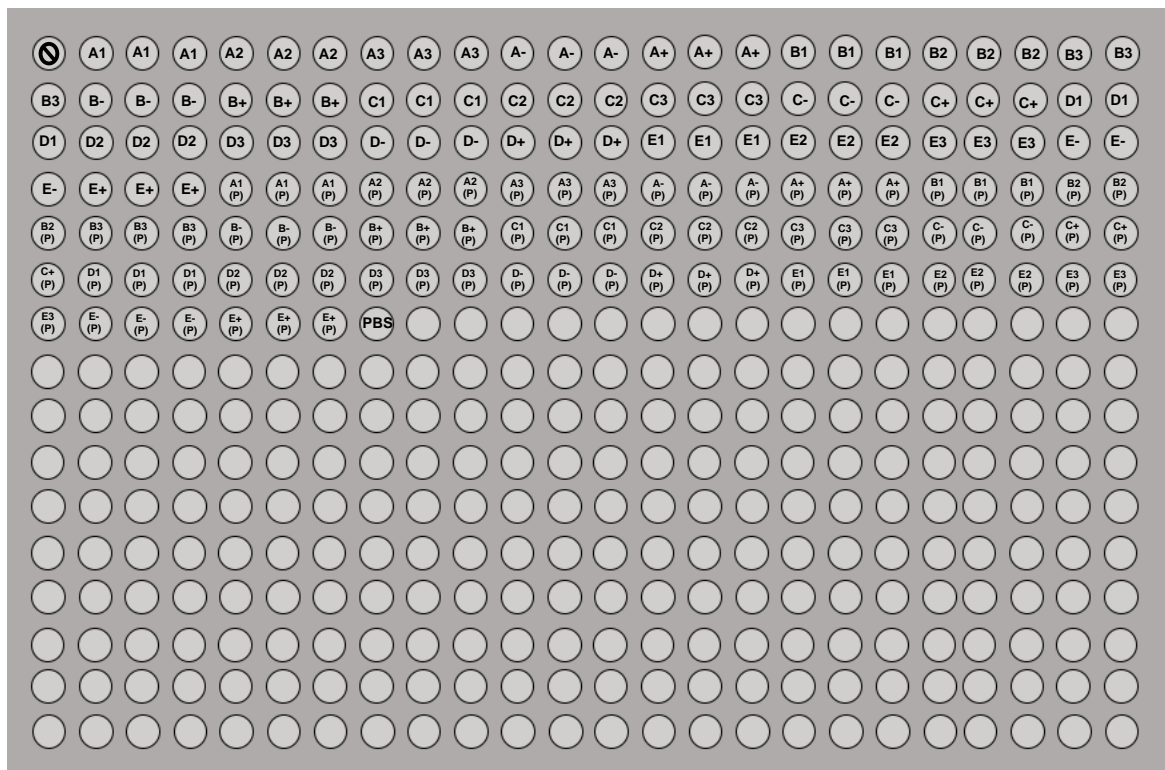


Figure 4.16. Schematic image of the Si 384-well microplate for FTIR analysis in experiment 2, immediately after PEF. A1 to E3 are the samples of DPBS without the cells. A1(P) to E+(P) are the samples of cell pellet. PBS is the DPBS pure with no cell contact for spectra comparison with the supernatant experimental groups.

4.4.3. Experiment 3 - Effect of repeated PEF

The main goal of this experiment was to study the resistance capacity of cells when exposed to repeated PEF applications. To do so, PEF applications were repeated 3 times, with intervals of 48 hours between each application, repeating the same procedure each time. These repeated applications were called first assay (T=0h), second assay (T=48h) and third assay (T=96h).

The electrical parameters remain unchanged in the three assays. Cells were subjected to an electrical field of 10kV/cm (4kV in 0.4cm) and 5 Pulses of 5 μ s with $f=1$ Hz.

4.4.3.1. First Assay (t=0h)

For all groups the total number of cells required was 12×10^6 , distributed over 12 Eppendorf tubes, properly labeled (A1, A2, A3, A-, B1, B2, B3, B-, C1, C2, C3, C-), thus each Eppendorf tubes from group A containing 1.5×10^6 cells, group B 1×10^6 cells and group C 500,000 cells in 800 μ L of DPBS. As previously done, cells were stored in low temperature 4 $^{\circ}$, in the refrigerator, 15min before starting and then transferred to the ice box inside the laminar flow cabinet.

PEF application protocol

It was taken, from the Eppendorf tubes, 800 μ L of solution (with the number of fibroblasts corresponding to each group) and placed inside the electroporation cuvette and then transported to the equipment for PEF application, after this, the cells returned to the Eppendorf tubes from which they were taken and remain in ice, repeating the process three times, using the same energy field in each triplicate group, and in the particular case of the positive control group, exactly the same procedure was performed but only with PEF application simulation.

The chosen electrical parameters were 10 kV/cm (4 kV in 0.4cm) and 5 Pulses of 5 μ s with $f=1$ Hz. Three conditions were defined, according to the number of cells, for the groups that were submitted to pulsed electric fields:

- Group A containing $1,5 \times 10^6$ cells (with the triplicates A1, A2, A3 and the negative control A-);
- Group B containing 1×10^6 cells (with the triplicates B1, B2, B3 and the negative control B-);
- Group C containing 500,000 cells (with the triplicates C1, C2, C3 and the negative control C-).

Analysis protocol after PEF application

- 1) The volume of solution containing the cells from each cuvette were taken according to the belonging group and the dilution factor had to be adapted to the concentration of cells, so 10 μ L were taken from group A, 20 μ L from group B, 40 μ L from group C. The samples were mixed with trypan blue dye, 90 μ L for group A, 80 μ L for group B and 60 μ L for group C.- Stained cells solutions were placed in Neubauer chambers, where they rested for 2min and then observed in the optical microscope. Cell density and cell viability were calculated.
- 2) The volume of solution containing the cells from each Eppendorf tube was taken to seed according to the correspondent group, with the objective of having similar cells quantity per group, for the second assay. So, for group A, in order to have 1,500,000 cells for per well after 48h it had to be seeded 28,500 cells per well (7,500 cells per cm^2 in wells of 3.8cm^2), to have 1,000,000 cells in group B 19,000 cells were sown (5,000 cells per cm^2 in wells of 3.8cm^2), and for group C 9,500 cells had to be seeded (2,500 cells per cm^2 in wells of 3.8cm^2) in order to have 500,000 cells for the second assay. Then were taken the following volumes, from each Eppendorf tubes:
 - 25.91 μ L from Eppendorf tube A1;
 - 16.76 μ L from Eppendorf tube A2;
 - 23.75 μ L from Eppendorf tube A3;
 - 15.83 μ L from Eppendorf tube A-;
 - 27.14 μ L from Eppendorf tube B1;

- 25.33 μ L from Eppendorf tube B2;
- 17.27 μ L from Eppendorf tube B3;
- 15.83 μ L from Eppendorf tube B-;
- 54.28 μ L from Eppendorf tube C1;
- 47.50 μ L from Eppendorf tube C2;
- 31.67 μ L from Eppendorf tube C3;
- 22.35 μ L from Eppendorf tube C-.

The taken volumes were seeded in a 12-well Nunc adherent plate (Figure 4.16) with 2mL of complete medium and placed in culture in the CO₂ incubator.

- 3) The remaining cells solutions were taken to centrifuge, where the supernatant and the pellet were separately taken for FTIR analysis. 5 μ L of supernatant was plated in each well of the 384-well FTIR microplate, doing, once more triplicates of each sample and doing the same procedure for the pellets (described in experiments 1 and 2). The plates of 384-well were dehydrated in the desiccator for a minimum of 3h and read in the FTIR equipment and the analysis processed as described in the other two experiments.
- 4) The resulting spectra was converted and analyzed by Unscrambler X and Excel software.
- 5) The remaining samples were properly stored at -20°C.
- 6) The culture plate was subjected to microscope observation at 48h, in the same moment where the Second Assay took place.

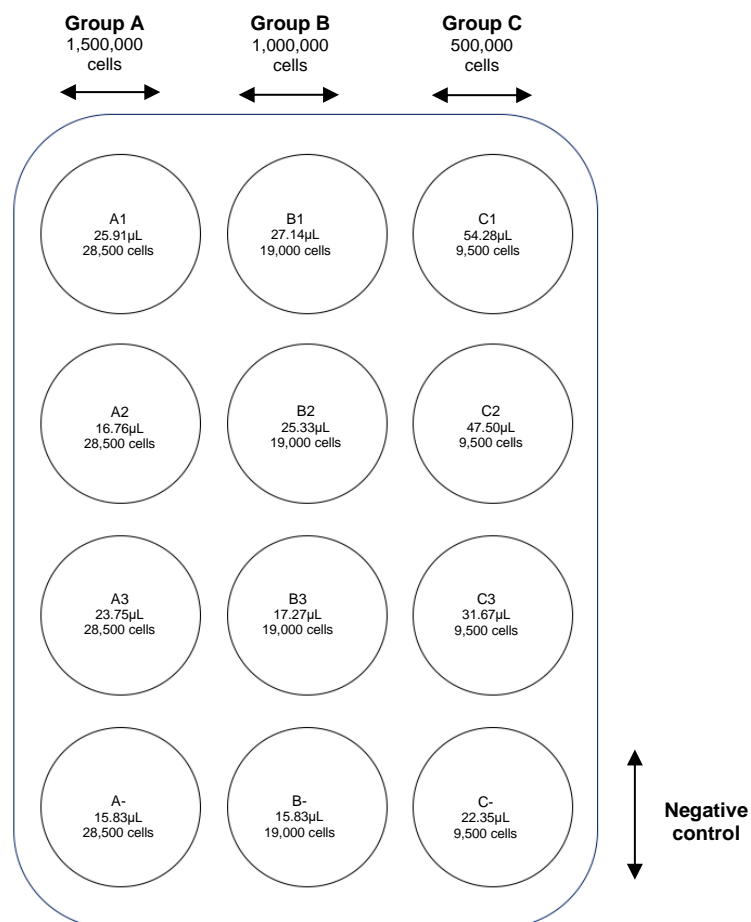


Figure 4.17. Schematic image of the sown cells in a Nunc® 12-well adherent culture plate, in 1st assay in experiment 3.

4.4.3.2. Second Assay (t=48h)

All cell groups exposed once to PEF, in the previous assay, were seeded in culture in the 12-well adherent plate, inside the CO₂ incubator for 48h. After this time, cells in culture were taken from the incubator and transported to the laminar flow cabinet. The culture medium was removed and stored for FTIR analysis, and the cells rinsed with DPBS to remove residues of FBS proteins. Thereafter, 192.5µL of trypsin (0.5mL trypsin/10 cm²) was added to each well and the culture plate returned to the CO₂ incubator at 37°C for 3min (in adherent plates it is more difficult to release the cells than in T-flasks). After this time, it was observed under the microscope that the cells were already completely loose and in suspension. The plate was returned to the flow cabinet, where twice the volume in complete medium (385µL) was added to the trypsin in each well, passing the cells to the respective Eppendorf tubes already labeled as A1, A2, A3, A-, B1, B2, B3, B-, C1, C2, C3, C-, for centrifugation at 1700 RPM for 10min. The supernatant was discarded, and the pellet resuspended in 1000µL of DPBS.

10µL of solution from Eppendorf tubes from Group A was taken and mixed with 90µL of trypan blue for counting under a microscope in a Neubauer chamber. 20µL were taken from group B and mixed with 80µL of trypan blue and 40µL of solution from group C were taken and mixed with 60µL of trypan blue. The objective of counting the cells before the PEF application is to study the metabolic status and proliferation between PEF applications. After counting, DPBS were added to Eppendorf tubes, in order to have a final volume of 800µL in each Eppendorf (that is the ideal volume to be electroporated), 310µL of DPBS was added to all Eppendorf tubes from group A, 320µL to group B and 340µL to group C.

Pulsed electric fields application protocol

The electrical parameters of 10 kV/cm (4 kV in 0.4cm) and 5 Pulses of 5 µs with $f=1\text{Hz}$ were maintained. The three groups have grown and proliferated besides the PEF application. So, it was used the number of cells that was in each Eppendorf tube:

- Eppendorf A1 containing 800,000 viable cells;
- Eppendorf A2 containing 600,000 viable cells;
- Eppendorf A3 containing 900,000 viable cells;
- Eppendorf A- containing 1,100,000 viable cells;
- Eppendorf B1 containing 300,000 viable cells;
- Eppendorf B2 containing 100,000 viable cells;
- Eppendorf B3 containing 550,000 viable cells;
- Eppendorf B- containing 750,000 viable cells;
- Eppendorf C1 containing 125,000 viable cells;
- Eppendorf C2 containing 125,000 viable cells;
- Eppendorf C3 containing 100,000 viable cells;
- Eppendorf C- containing 400,000 viable cells.

The cells were stored in low temperature 4°C (in the refrigerator and then on ice) 15 minutes before starting.

It was taken, from the Eppendorf tubes, 800µL of solution (with the number of fibroblasts corresponding to each Eppendorf tube) and placed inside the cuvette and then transported to the equipment for PEF application, after this, the cells returned to the Eppendorf tube from which they were taken and remain in ice, repeating the process for the other group cells, using the same energy field in each triplicate, and in the particular case of the negative control group, exactly the same procedure was performed but only with PEF application simulation.

Analysis protocol after PEF application

- 1) The volume of solution containing the cells from each cuvette were taken according to the belonging group, and the dilution factor remained the same as in the first assay, so 10µL

were taken from group A and mixed with 90 μL of trypan blue dye, 20 μL were taken from group B and mixed with 80 μL of trypan blue, 40 μL were taken from group C and mixed with 60 μL of trypan blue. The mixed solutions were placed in hemocytometers, left to rest for 2 minutes and cell count and viability calculation were performed.

- 2) The volume of solution containing the cells from each Eppendorf tube was taken to be sown according to the correspondent group and, exactly as in the first assay, with the objective of seeding 28,500 (7,500 cells per cm^2 in wells of 3.8cm^2), for group A, 19,000 cells (5,000 cells per cm^2 in wells of 3.8cm^2) for group B and 9,500 cells (2,500 cells per cm^2 in wells of 3.8cm^2) for group C. As such, there were taken the following volumes, from each Eppendorf tubes:

- 95.00 μL from Eppendorf tube A1;
- 71.25 μL from Eppendorf tube A2;
- 71.25 μL from Eppendorf tube A3;
- 21.92 μL from Eppendorf tube A-;
- 95.00 μL from Eppendorf tube B1;
- 380.00 μL from Eppendorf tube B2;
- 63.33 μL from Eppendorf tube B3;
- 21.11 μL from Eppendorf tube B-;
- 95.00 μL from Eppendorf tube C1;
- 190.00 μL from Eppendorf tube C2;
- 126.67 μL from Eppendorf tube C3;
- 20.00 μL from Eppendorf tube C-.

The taken volumes were sown in a 12-well Nunc adherent plate (Figure 4.17) with 2mL of complete medium and placed in culture in the CO_2 incubator.

- 3) The remaining volumes of each Eppendorf tube were taken to centrifuge, 1700 RPM for 15min, where the supernatant and the pellet were separately taken for FTIR analysis using a 384-well FTIR plate as described in the first assay, plus the culture medium already collected and centrifuged and that represents the study of the medium at 48h of cells in culture. Once more triplicates of each sample were performed, for more accuracy (Figure 4.18). The 384-well microplate was dehydrated in the desiccator for a minimum of 3h30 and read in the FTIR equipment from Bruker.
- 4) The resulting spectra was converted and analyzed by unscramble and Excel software.
- 5) The remaining Eppendorf tubes were stored at -20°C .

4.4.3.3. Third Assay (t=96h)

The cell groups that had already undergone PEF exposure twice plus the cell negative control group and were seeded in the 12-well adherent plate and placed in the CO₂ incubator for culture, during another 48h, total time of 96h after the 1st assay. At the end of this time, the culture medium was collected, centrifuged and reserved for FTIR analysis, and the cells were resuspended in exactly the same way as in the previous assay (in volume of 1000µL of DPBS) with their density and viability calculated, once more, through the trypan blue exclusion method assay, described before, and respecting the same dilution factors. Like before, more DPBS was added to each Eppendorf tube to fill the required volume of 800µL. In the end, twelve Eppendorf tubes remained and labeled as A1, A2, A3, A-, B1, B2, B3, B-, C1, C2, C3, C-.

Pulsed electric fields application protocol

The electrical parameters of 10 kV/cm (4 kV in 0.4cm) and 5 Pulses of 5 µs with $f=1\text{Hz}$ were maintained and the application protocol performed exactly as described in the 1st and 2nd assays of experiment 3. Each Eppendorf tube had the following number of viable cells, before PEF application:

- Eppendorf A1 containing 150,000 viable cells;
- Eppendorf A2 containing 200,000 viable cells;
- Eppendorf A3 containing 100,000 viable cells;
- Eppendorf A- containing 250,000 viable cells;
- Eppendorf B1 containing 50,000 viable cells;
- Eppendorf B2 containing 75,000 viable cells;
- Eppendorf B3 containing 50,000 viable cells;
- Eppendorf B- containing 200,000 viable cells;
- Eppendorf C1 containing 25,000 viable cells;
- Eppendorf C2 containing 37,500 viable cells;
- Eppendorf C3 containing 12,500 viable cells;
- Eppendorf C- containing 212,500 viable cells.

Just like before, the cells were stored in low temperature at 4°C, 15min before starting, and then transferred to a Styrofoam box with ice, where they remained in the labeled Eppendorf tubes until PEF applications.

It was taken, from the Eppendorf tubes, 800µL of solution (with the number of fibroblasts corresponding to each group) and placed inside the cuvette and then transported to the equipment for PEF application, after this, the cells returned to the Eppendorf tubes from which they were taken and remain in ice, repeating the process for the remaining Eppendorf tubes of each group, using the same energy field in each triplicate group, and in the particular case of the negative control group, exactly the same procedure was performed but only with PEF application simulation.

Analysis protocol after PEF application

- 1) Cell density and viability were performed, like before, using the trypan blue exclusion assay, with the same dilution factors corresponding for each group, thus the following number of cells:
 - Eppendorf A1 containing 80,000 viable cells,
 - Eppendorf A2 containing 160,000 viable cells;
 - Eppendorf A3 containing 80,000 viable cells;
 - Eppendorf A- containing 240,000 viable cells;
 - Eppendorf B1 containing 40,000 viable cells;
 - Eppendorf B2 containing 80,000 viable cells;
 - Eppendorf B3 containing 40,000 viable cells;
 - Eppendorf B- containing 160,000 viable cells;
 - Eppendorf C1 containing 20,000 viable cells;

- Eppendorf C2 containing 30,500 viable cells;
 - Eppendorf C3 containing 0 viable cells (outlier);
 - Eppendorf C- containing 200,000 viable cells.
- 2) The volume of solution containing the cells from each Eppendorf tubes was taken to seed according to the correspondent group exactly as in the first and second assays, with the objective of seeding 28,500 (7,500 cells per cm² in wells of 3.8cm²), for group A, 19,000 cells (5,000 cells per cm² in wells of 3.8cm²) for group B and 9,500 cells (2,500 cells per cm² in wells of 3.8cm²) for group C. Since this was the last assay and the only objective of seeding was to study the culture medium at 144h of the 1st assay.
- Knowing that already 10μL of total volume were taken from Group A, 20μL from Group B and 40μL were from Group C, for cell counting and viability, all the Eppendorf tubes were taken to centrifuged for 1700 RPM for 9min. Subsequently, the supernatants were reserved for a longer centrifugation (to lose cells that could still be in it) and for FTIR analysis, plating like described in the previous assay in the 384-well microplate. Cell pellets were resuspended in 800μL of complete medium where the following volumes were taken from each Eppendorf to the 12-well culture plate:
- 285.00μL from Eppendorf tube A1;
 - 142.50μL from Eppendorf tube A2;
 - 285.00μL from Eppendorf tube A3;
 - 95.00μL from Eppendorf tube A-;
 - 380.00μL from Eppendorf tube B1;
 - 190.00μL from Eppendorf tube B2;
 - 380.00μL from Eppendorf tube B3;
 - 95.00μL from Eppendorf tube B-;
 - 380.00μL from Eppendorf tube C1;
 - 380.00μL from Eppendorf tube C2;
 - 380.00μL from Eppendorf tube C3 (this was an outlier in this assay, so it was assumed the same volume as the other two Eppendorf tubes from its group);
 - 38.00μL from Eppendorf tube C-.
- The cells were seeded in the 12-well Nunc adherent plate (Figure 4.19) filling each well with complete medium until reach 2mL of volume and placed in culture in the CO₂ incubator for reevaluation after 48h.
- Cells were resuspended and 3x5μL were taken from each Eppendorf tube to the 384-well microplate.
- The remaining Eppendorf tubes volume were centrifuged, 1700RPM for 9min, where the supernatants were discarded, and the pellet taken for FTIR analysis. In the final 384-well microplate there were the supernatant and pellet from 3rd assay and the culture medium of 2nd assay, plated in triplicates of 5μL per well. The plate of 384-well was dehydrated in the desiccator for a minimum of 3,5h and read in the FTIR equipment from Bruker.
- 3) The resulting spectra was converted and analyzed by unscramble and Excel software.
 - 4) The remaining Eppendorf tubes were stored at -20°C.
 - 5) 48h after the cells of the 3rd assay were maintained in culture, microscope observation was performed, the culture medium taken to FTIR analysis (once more in the 384-well microplate), data was collected, and the culture was discarded.

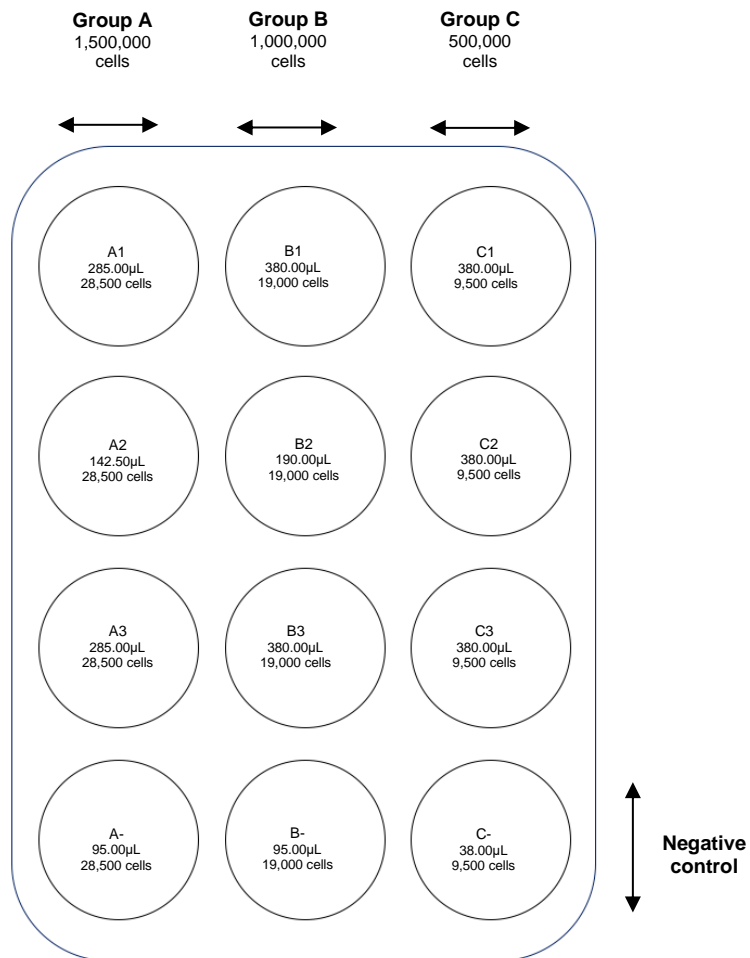


Figure 4.20. Schematic image of the sown cells in a Nunc® 12-well adherent culture plate, in the 3rd assay of experiment 3.

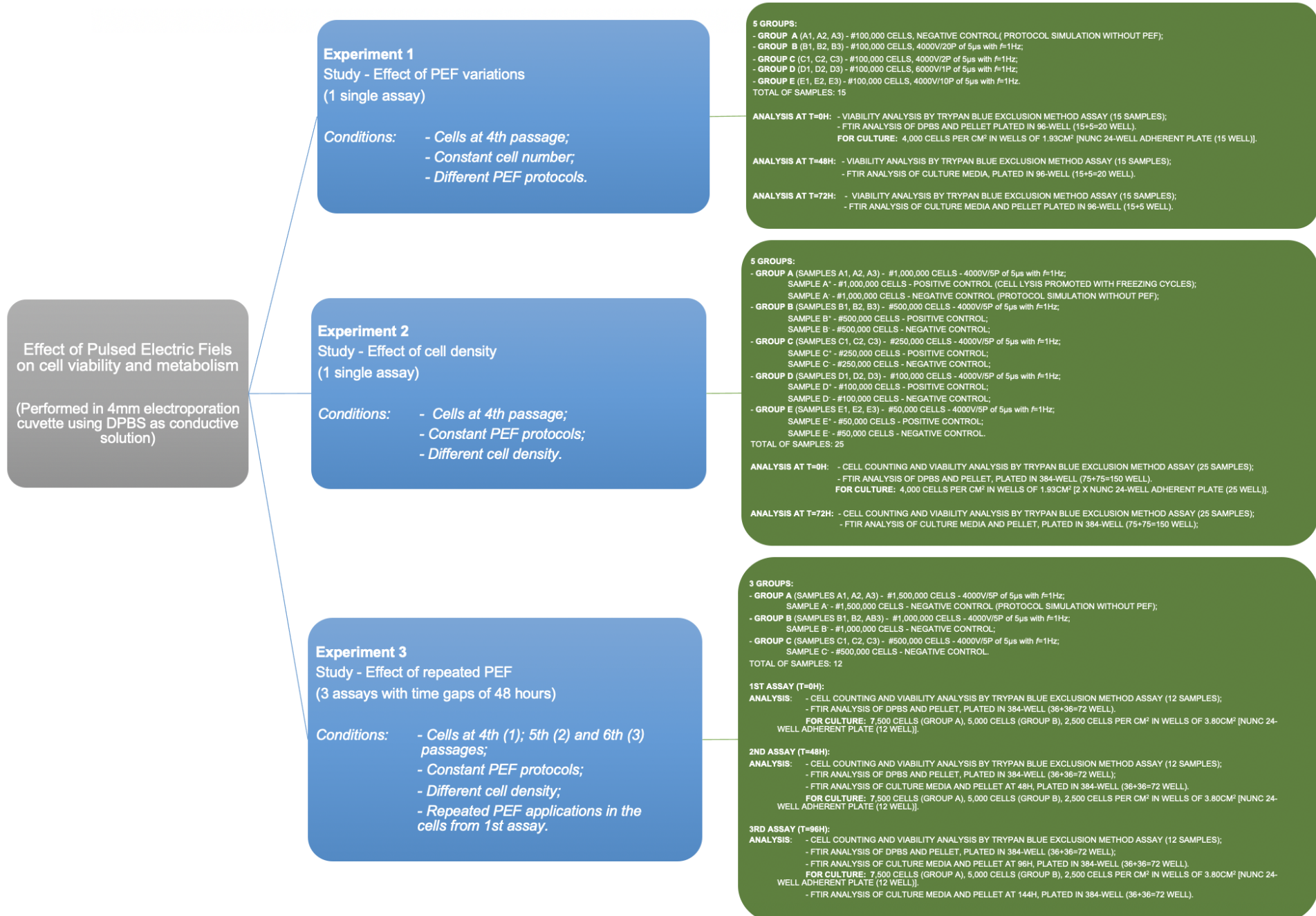


Figure 4.21. Summary scheme of all experiences.

5. Results & Discussion

5.1. Preliminary tests

Occupation volume inside an electroporation cuvette according to cell type

A series of preliminary tests took place between April and May of 2019, in the R&D Lab. in Health & Engineering at ISEL, to choose the appropriate equipment for the experiments and made it available by the company EPS. The equipment chosen was EPULSUS-LPM1B-10 (i.e. pulse generator for +10kV/400A/3kW) and the way to electroporate was through VWR electroporation cuvettes, with a capacity of 1mL and with aluminum electrodes and a gap of 4mm between them, which have a lower field strength and so recommended to work with mammalian cells.

Still in relation to the cuvettes, some calculations were carried out, to be able to understand the ideal volume of solution and cells to be electroporated, this was called correlation between the size of fibroblasts and the useful volume of the cuvette. For this it was used the useful area of the cuvette and the size in a fibroblast, as you can see in the following calculation:

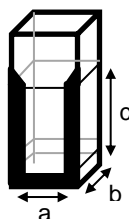


Figure 5.1. Schematic image of a cuvette used in the electroporation test.

In Figure 5.1, it's possible to see the type of cuvette used in the electroporation tests performed in the present work, where a is the distance between electrodes accepted to electroporate animal cells (4mm), b is the length of the cuvette (10mm) and c is the height up to which the sample to be analyzed is inserted (20mm).

The useful volume of the cuvette is calculated as follows:

$$V = a \times b \times c = 4 \times 10 \times 20 = 800 \text{ mm}^3 = 800 \text{ }\mu\text{L} \quad (17)$$

Where $V = 800 \text{ }\mu\text{L}$ is the volume that is required to perform electroporation.

The size of the fibroblast is 10 to 15 μm . The volume of the fibroblast is calculated as follows:

$$V(\text{ball/fibroblast}) = \frac{4\pi r^3}{3} \quad (18)$$

Where r is the radius of the fibroblast, which can vary between 5 and 7.5.

If the cell has 10 μm :

$$V(\text{ball/fibroblast}) = \frac{4\pi 5^3}{3} = 523.6 \text{ }\mu\text{m}^3 \quad (19)$$

$$\begin{aligned} 1 \text{ cell} &\rightarrow 523.6 \text{ }\mu\text{m}^3 \\ x \text{ cells} &\rightarrow 800 \times 10^9 \text{ }\mu\text{m}^3 \end{aligned}$$

$$x = \frac{800 \times 10^9}{523.6} = 1,527,883,881 \text{ cells/cuvette} \quad (20)$$

If the cell has 15 μm :

$$V(\text{ball/fibroblast}) = \frac{4\pi 7.5^3}{3} = 1767.1 \mu\text{m}^3 \quad (21)$$

$$\begin{aligned} 1 \text{ cell} &\rightarrow 1767.1 \mu\text{m}^3 \\ x \text{ cells} &\rightarrow 800 \times 10^9 \mu\text{m}^3 \end{aligned}$$

$$x = \frac{800 \times 10^9}{1767.1} = 452,719,144 \text{ cells/cuvette} \quad (22)$$

So, it was inferred that a 4mm gap electroporation cuvette supports between 452,719,144 to 1,527,883,881 cells, the last number representing 100% of the total volume.

Logistic and adaptation to Pulsed Power equipment

During the preparation period, the logistic of the equipment and its installation, inside the culture room, was studied, not only to maintain the culture room environment sterile but also to organize experiments schedules according to equipment availability.

In order to work correctly with the EPULSUS-LPM1B-10 equipment, Engineers from Energy Pulse Systems gave a small lecture showing the right way to handle the equipment and with the software developed by the company itself.

The conductivity of different solutions and media was also studied to choose the appropriate conductive solution in which the cells would be resuspended and electroporated. The solution chosen was DPBS, since its conductivity is similar to water - 5.5 mS/cm - which would be considered acceptable for this work in question, with the advantage of not having Calcium or Magnesium ions, which tend to adhere to the cuvette electrodes or interfere with the electroporation of the plasma membrane, being the DPBS a buffer solution of pH 7.4 and its composition pure H₂O of molecular weight 18.02, Na₂HPO₄·12H₂O of molecular weight 358.14, KH₂PO₄ of molecular weight 136.09, NaCl of molecular weight 58.44 and KCl of molecular weight 74.551.

Cell type and line choice

The chosen cells were immortalized lines of L929 fibroblasts, kindly provided by the laboratories of *Instituto Superior Técnico* and later expanded to the Master cell bank, in the R&D Lab. in Health & Engineering at ISEL. The choice of fibroblasts lies in the fact that they are the most representative cells of the connective tissue and fibroblast lines and strains are more resistant and easier to work with in comparison with other cell types.

L929 fibroblasts behavior was observed during the primary culture and then again in the subcultures, and a curve of growth was charted (Figure 5.2), showing a very proliferative and resistant cell strain, with its full potential at 4th and 5th passages, respectively.

This cell culture started from cryopreservation vials with 1 million cells each, which were seeded in T-25 flasks (25cm²), with more medium being added as the culture expanded. Major advantages of using T-25 culture flasks, in laboratory, lies on the one hand in the fact that there is less chance of contamination, since each flask has a smaller amount of cells, being each flask with cells in culture isolated from the others, and on the other hand there is an enormous advantage in reducing the waste of culture media, since they use less media (approximately 5mL) and still have good cell expansion.

When culture flasks are used, regardless of the volume that they can support, it is necessary to pay attention to the type of treatment that is done on the adherent surface. The flasks with Nunclon

Delta treatment were the most effective that the R&D Lab. in Health & Engineering ISEL laboratory provided. Another particularity is the type of lids in each T-flask, since there are lids with filters that allow the circulation of CO₂ inside the CO₂ incubator and others that are completely sealed, the technician must be careful to loosen the lid slightly when placing the flask of culture inside the CO₂ incubator.

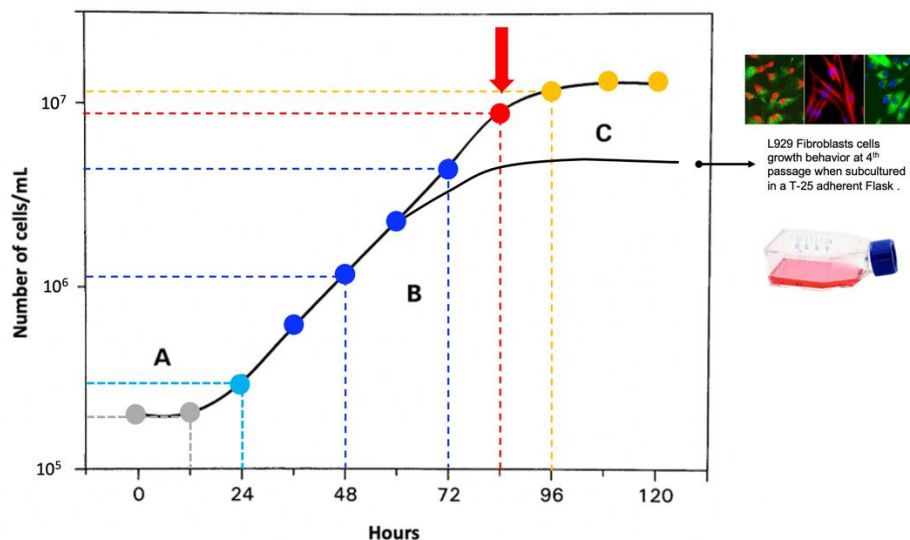


Figure 5.2. Growth expansion curves. The top curve is the normal curve of adherent cells compared with the growth expansion curve for fibroblasts L929 (bottom curve), when starting with a seeding of 1×10^5 in a T-25 flask (25cm^2). In the first 12 hours it can be seen the lag phase (A), and then a logarithmic phase of exponential growth that starts after 12 hours culture and stops at 96 hours, giving rise to the stationary phase (C). In a T-25 flask with L929 cells, at 48h they were already 10 times more than the initial number, at 72h they reached approximately 2,5 to 4 million with a confluence of 85% -98% (lack of adherent surface and space) at 96 hours they reached approximately 4.5 million.

Analytical methods chosen

Also, the analytical methods for processing the samples were defined, according to the intended studied and availability. The chosen methods were the analysis of the sample heating, after PEF application, which values were given by the digital oscilloscope and the Energy Pulsed System software; the cell viability and number of cells lysed given by trypan blue exclusion method assay, using a hemocytometer observed under a microscope; analysis by FTIR spectroscopy and consequently the statistical analysis by PCA (Principal Component Analysis) and *Anova* single factor.

To understand typical spectra obtained by FTIR spectroscopy, it was necessary to determine the different peaks obtained with different solutions. To do so, DPBS, deactivated FBS, and two different brands of media that were available in the laboratory, both with and without FBS were analyzed (Figure 5.3). These spectra would give an idea of the typical bands and would thus make easier to compare with the components extracted from an electroporated cell, with a particular attention for DPBS spectrum, once this was the chosen conductive media for PEF application (Figure 5.4).

Also, the use of different microplates used for spectra acquisition affected the spectra signal, being the 96-well microplate with $25\mu\text{L}$ well capacity (2.4mL of total volume) the one with the higher signal, while the 384-well microplate with $5\mu\text{L}$ well capacity (1.92mL of total volume) had approximately half of the spectra signal (Figures 5.5 and 5.6) when compared with the first one. Regarding FTIR spectroscopy reading types, a 96-well microplate takes approximately 1.9 min to read each well, being the total reading time of a complete microplate between 180 to 190 minutes, while the 384-well microplate takes approximately 1.1 min to read each well, being the total reading time between 6h40m to 8h00.

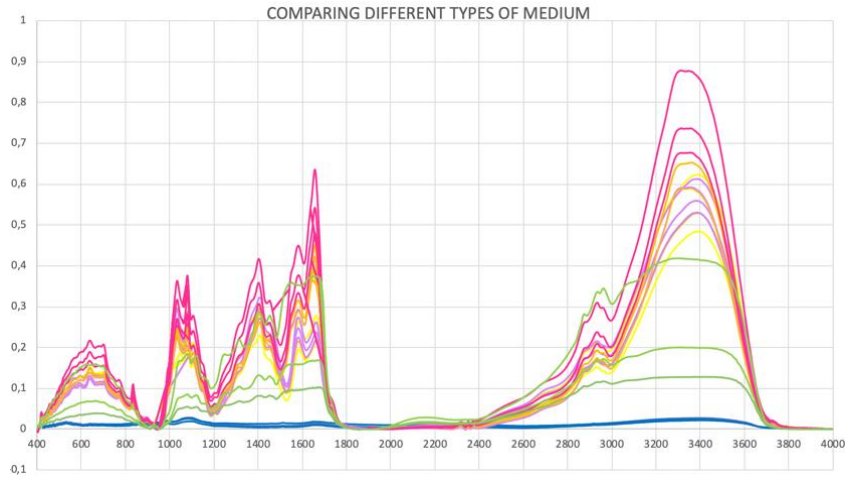


Figure 5.3. Comparing spectra from different types of media analyzed in a 96 well plate. Blue spectra: DPBS by Lonza; Green spectra FBS inactivated; Yellow spectra: Lonza DMEM; Purple spectra: Sigma DMEM; Orange spectra: Lonza DMEM with FBS; Pink spectra: Sigma DMEM with FBS.

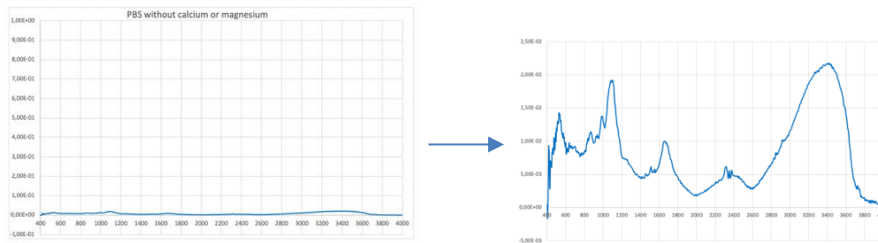


Figure 5.4. Spectra analysis (DPBS) in a 96-well plate.

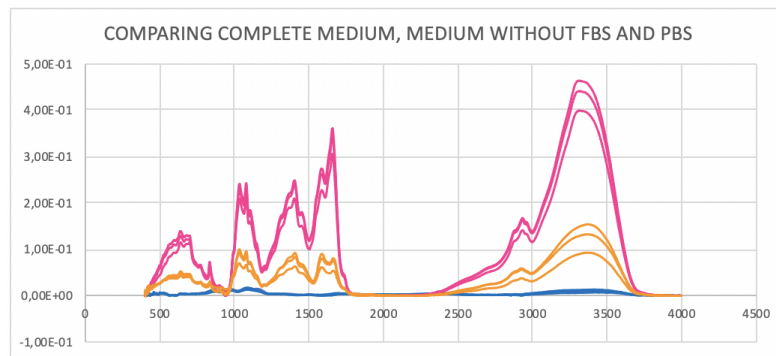


Figure 5.5. Comparing different types of medium with spectra analysis in a 384-well plate. Blue spectra: DPBS by Lonza; Green spectra FBS inactivated; Yellow spectra: Lonza DMEM; Purple spectra: Sigma DMEM; Orange spectra: Lonza DMEM with FBS; Pink spectra: Sigma DMEM with FBS.

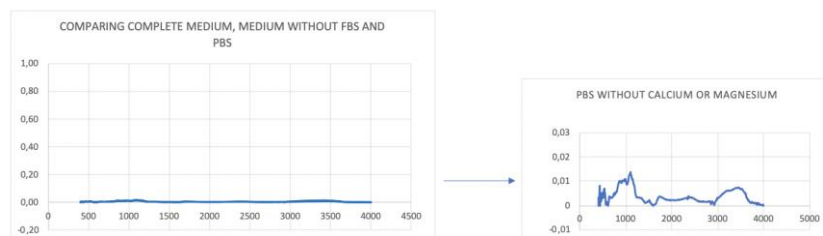


Figure 5.6. Spectra of supernatant (DPBS) in a 384-well plate.

The electroporation experiments were carried out between November 2019 and January 2020 and are described below.

5.2. Experiment 1 – Effect of PEF Variations

5.2.1. Overview

To be able to understand the dynamics of fibroblasts with the chosen Pulsed Power equipment, the cells were subjected to various preparatory tests with different PEF applications.

In these tests, the main goal was to understand how much energy it could be given to the fibroblast cells, thus defining a voltage, a frequency, the pulse period, and the number of pulses. So, this way, it could be studied the current variations and the temperature increase in the sample.

From the preparatory tests the definition of four electrical conditions arose, working with electric fields in the order of 10 to 15kV/cm (see formulas in chapter 3).

This experiment started from a well-defined number of cells, 100,000 cells for a pre-defined 1mL volume of DPBS. The number of cells was chosen based on their availability, and to give an acceptable FTIR signal. Then the electrical parameters were stipulated and varied according to the group, these groups being only four plus the control group, labeled as group A (negative control group), group B, group C, group D, group E, but always represented in triplicates (A1, A2, A3, B1, B2, B3, C1, C2, C3, D1, D2, D3, E1, E2, E3).

In this experiment, the cells were stored in low temperature 4°C, 15min before starting, so they can lower their metabolic status and doing so, resist more time outside the CO₂ incubator and to other procedures where cells could be exposed.

For analysis methods, it was used a trypan blue exclusion method assay to determine cell viability, and FTIR spectroscopy to determine released components in the electroporation solution (DPBS) and in the culture medium after cells were submitted to PEF application and placed in culture. So, there were obtained spectra from t=0h, t=48h and t=72h.

5.2.2. Variations in electrical parameters and temperature increase

To define and control the PEF parameters, a digital oscilloscope connected to a PC was used with a software - Picoscope6. Although the PEF parameters can also be defined directly in the pulsed power equipment and the current variations observed in it, the use of the oscilloscope and Picoscope6, allows better control of the PEF parameters, calculating in real time the current variations, as well as the specific energy and temperature increase, in addition to having the advantage of observing the pulse with its specific rectangular shape (Figure 5.7).

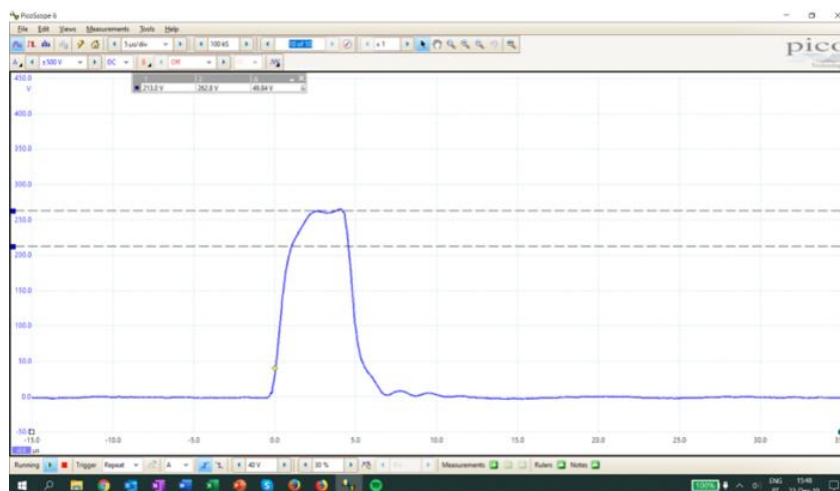


Figure 5.7. Image obtained by Picoscope6, representing the real pulse applied. The controlled pulse represents a well-defined area, almost a rectangle, that shows an application time of 5 μ s with a controlled Voltage and Current.

Predefined E or electric field for each group:

- Group A = Control Group = 0 kV/cm
- Groups B, C and E

$$E = \frac{U}{d} = \frac{4000}{0.4} = 10 \text{ kV/cm}$$

- Group D

$$E = \frac{U}{d} = \frac{6000}{0.4} = 15 \text{ kV/cm}$$

Parameters to be defined

- W = Pulse Energy (J)*
- Wt = Total Energy (J)*
- Ws =Specific Energy (kJ/mL or kJ/kg)*
- ΔT = Temperature increase (C°)*

*Using formulas (3), (5), (6) and (7) from Chapter 3

In table 5.1. it can be seen the different electrical parameters chosen for this first experiment, being maintained as constant conditions for all groups (except the negative control group A), the frequency (f) of 1Hz and the pulse time (t_{on}) of 5 μ s, only varying the Voltage (U or V) and the number of pulses (P) and thereby influencing the current (I) and the electric field (E).

Thus, group B is exposed to an electric field of 10kV/cm, that is, a voltage of 4000V divided by the gap of 0.4cm between electrodes. This electric field is maintained in groups C and E, varying only the number of pulses, which in group B are 20 pulses, in group C are 2 pulses and in group E are 10 pulses. Group D is the only one exposed to an electric field of 15kV/cm, that is, it is subjected to a voltage of 6000V but only in a single pulse. These values are important to determine the energy per pulse (W), the total energy (Wt), the specific energy (Ws) and one of the most important values when working with biological samples and electrical current, which is the increase of temperature in each sample (Δt). To calculate the latter, formulas (3), (5) and (6) from Chapter 3 were used.

Table 5.1. Electrical parameters and calculations for Groups A, B, C, D and E

GROUP	PULSES (P)	CURRENT (A)	VOLTAGE (V)	T _{ON} (μS)	FREQUENCY (Hz)	ENERGY FIELD (KV/CM)	W (J)	WT (J)	WS (KJ/KG)	ΔT (C°)	ΔT (C°) Average	
A	A1	0	0	0	0	0	0	0	0	0	0	
	A2	0	0	0	0	0	0	0	0	0		
	A3	0	0	0	0	0	0	0	0	0		
B	B1	20	210	4000	5	1	10	4.2	84	105.0	25.1	26.7
	B2	20	230	4000	5	1	10	4.6	92	115.0	27.5	
	B3	20	230	4000	5	1	10	4.6	92	115.0	27.5	
C	C1	2	240	4000	5	1	10	4.8	9.6	12.0	2.9	2.8
	C2	2	230	4000	5	1	10	4.6	9.2	11.5	2.8	
	C3	2	230	4000	5	1	10	4.6	9.2	11.5	2.8	
D	D1	1	345	6000	5	1	15	10.4	10.4	13.0	3.1	3.1
	D2	1	345	6000	5	1	15	10.4	10.4	13.0	3.1	
	D3	1	345	6000	5	1	15	10.4	10.4	13.0	3.1	
E	E1	10	230	4000	5	1	10	4.6	46	57.5	13.8	13.8
	E2	10	230	4000	5	1	10	4.6	46	57.5	13.8	
	E3	10	230	4000	5	1	10	4.6	46	57.5	13.8	

Analyzing table 5.1, it can be seen that the specific energy (Ws) is largely conditioned, not only by the current or voltage, but above all by the number of pulses that occur. Thus, increasing the temperature with each pulse that is given. This is explained by group C and group D, where the electric field is considerably different, but the number of pulses are close, with group C having an electric field 5kV/cm lower when compared to the electric field of group D, but as it has two pulses and group D only has a single impulse, the temperature increase is 2.8°C for group C and 3.1°C for group D, that is, they differ only by 0.3°C.

In turn, the remaining two groups, group B and group E, whose electric field is the same but the pulses are 20 for group B and 10 for group E, have a difference in specific energy which is 57, 5kJ/kg in group E and 111.7kJ/kg for group B, i.e. practically twice the specific energy, which will also be reflected in the increase temperature average, which is 26.7°C for group B and 13.8°C for group E.

5.2.3. Cells microscope observation and cell viability

Each group of cells were observed under a microscope, before and after exposure to pulsed electric fields and after being in culture for 48 hours and 72 hours. Confluence (?)

This observation was first conducted directly in the 24-well culture plate (Figures 5.8 and 5.9).

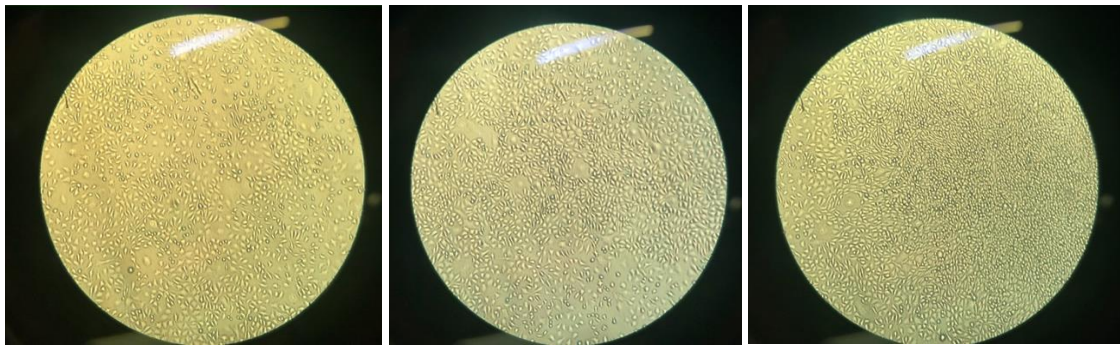


Figure 5.8. Cells image obtained by the inverted phase microscope, of group A, or negative control group, 72h after experiment 1. Left: well A1 with confluence over 98%. Middle: well A3 with confluence over 99%. Right: well A2 overconfluent.

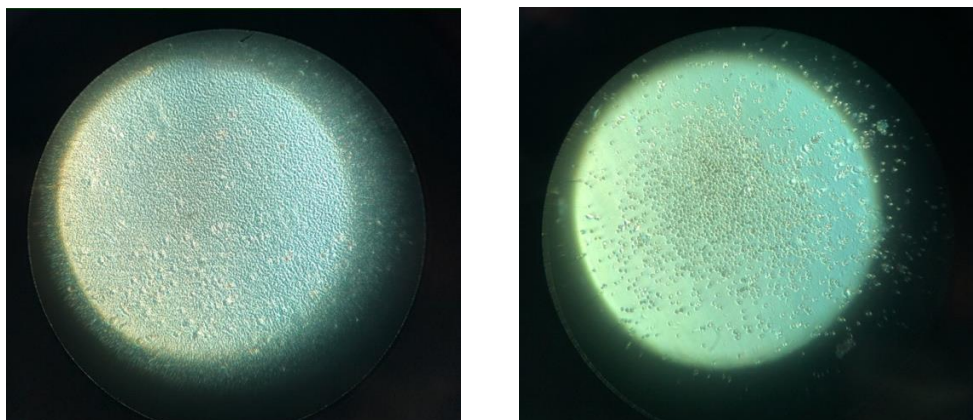


Figure 5.9. Cells image obtained by the inverted phase microscope, immediately after PEF application ($t=0h$). Left: Group D (D1) where is observed an increase of ECM density, making it almost gelatinous to the eye, this shows the result of exposure to a higher energy field (15kV/cm) where almost 90% of cells are non-viable by plasma membrane lysis. Right: Group B (B2) where there was a change in cell size, making it smaller, due to reversible electroporation where there was a loss of intracellular water. This last process was reversible, and the cells start recovering their shape at 48h.

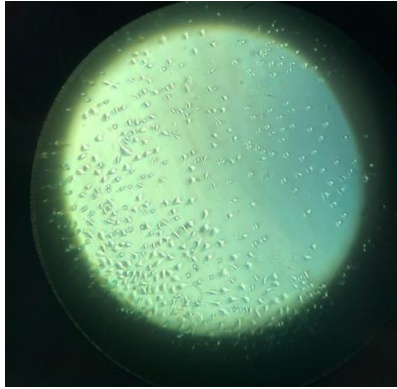


Figure 5.10. Cells image obtained by the inverted phase microscope, 48h after PEF application, well B2 from group B, recovered cell shape, being an example of reversible electroporation, where cells open pores in their membranes and in the one hand can release some components to extracellular environment turning themselves shrunken or in the other hand can let the passage of some components into the intracellular medium turning themselves turgid, but in both phenomena, the recovery of membrane is possible.

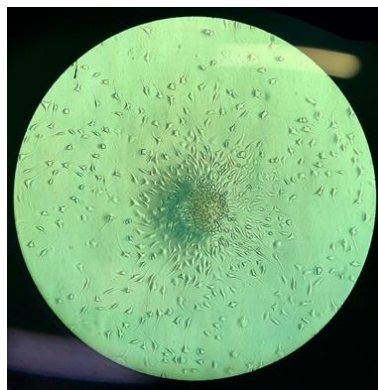


Figure 5.11. Cells image obtained by the inverted phase microscope, at 72h where is visible a migration of almost all cells of group B (B2) to a unique spot, placing themselves on top of each other.

The remaining observations were carried out on the hemocytometer - Neubauer chamber – proceeding to a simple blue trypan exclusion method assay using a DF of 1.25, explained by the low number of cells in each group. Trypan blue is a dye that surrounds the cell membrane of living cells (assuming distinct blue circles) and penetrates dead cells (observing blueberry-like blue spheres), as can be seen in Figure 5.12.

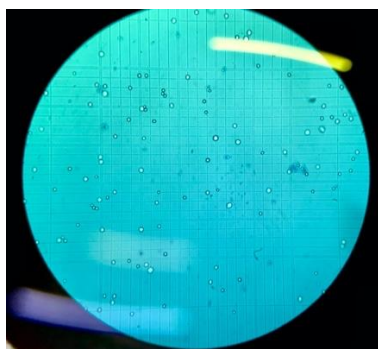


Figure 5.12. Cells image obtained by an optical microscope, to perform a blue trypan exclusion method assay. It can be seen, the hemocytometer geometrical lines with the counting squares, and living cells correspondent to blue circles and dead cells corresponding to dark blue dots.

This type of observation under the microscope is used to calculate cellular density and to cellular viability assays and in this case, it is very important to have an idea of the number of cells that survive after PEF exposure. To determine cell viability, which defines the percentage of living cells, it was used formula 9 from chapter 3, the results can be seen in table 5.2.

Table 5.2. Cell viability immediately after PEF application, and after cells re-cultures after 48hours and 72 hours (light blue: control group).

Experimental Groups		Variable PEF Parameters			Non-variable PEF Parameters		Blue Trypan exclusion method assay					
		Electric Field (kV/cm)	Voltage (V)	Number of Pulses (P)	t _{on} (μs)	Frequency (Hz)	Cellular Viability (%)					
							After PEF application t=0h		After PEF application t=48h		After PEF application t=72h	
A	A₁	∅	∅	∅	∅	∅	91.2	Average	92.3	Average	98.4	Average
	A₂						99.8	95.4	100.0	96.8	100.0	99.2
	A₃						95.0		98.0		99.3	
B	B₁	10	4000	20	5	1	22.0	Average	25.0	Average	56.3	Average
	B₂						12.7	14.2	33.3	25.6	63.4	51.2
	B₃						7.8		21.4		33.9	
C	C₁	10	4000	2	5	1	92.8	Average	94.0	Average	99.0	Average
	C₂						95.0	94.3	96.1	95.8	98.8	99.2
	C₃						95.0		97.4		99.8	
D	D₁	15	6000	1	5	1	8.5	Average	12.1	Average	53.3	Average
	D₂						10.1	9.9	22.0	18.7	54.1	46.9
	D₃						11.1		21.9		33.3	
E	E₁	10	4000	10	5	1	89.2	Average	91.9	Average	94.9	Average
	E₂						78.3	80.8	79.1	82.7	93.0	92.6
	E₃						75.0		77.0		89.8	

As shown in table 5.2. group A, or the negative control group not exposed to electrical fields (represented in light blue) has an average viability of 95.4% at t=0h, assuming that the initial viability was between 99% and 100%, this can be explained due to the procedure where group A was transferred from the Eppendorf to the cuvette, being outside the flow cabinet and inside the PP machine for the same time as the other groups, since it was exposed to a simulation without application of electricity. As such, it was expected that some cells could die. However, group A viability presents a recovery during the 72h in culture.

Looking at the table, it can be seen the poor viability with low recovery of group B as in group D, group B was the group with most Pulses application and group D the one with higher electrical field exposure. Therefore, the most promising groups, in terms of viability is group C and E, presenting differences in their viability between 6.6% to 13.5%, with a final viability above 90% for both groups. In the particular case of group C, the recovery immediately after PEF application is above 94%, and the final average viability is the same as in the negative control group.

5.2.4. FTIR spectroscopy

FTIR spectroscopy analysis was performed immediately after PEF application (t=0h), of the supernatant of the conductive solution (DPBS) used for cells electroporation and the corresponding pellet. The comparative spectrum of DPBS before and after electroporation is shown in Figure 5.13.

The FTIR spectra of DPBS presents peaks between 0 to 0.025 of absorbance. Spectrum from group A (negative control group) has the lowest and consistent peaks as well as group C, with a lower signal. The higher signals are from group B, group D and group E.

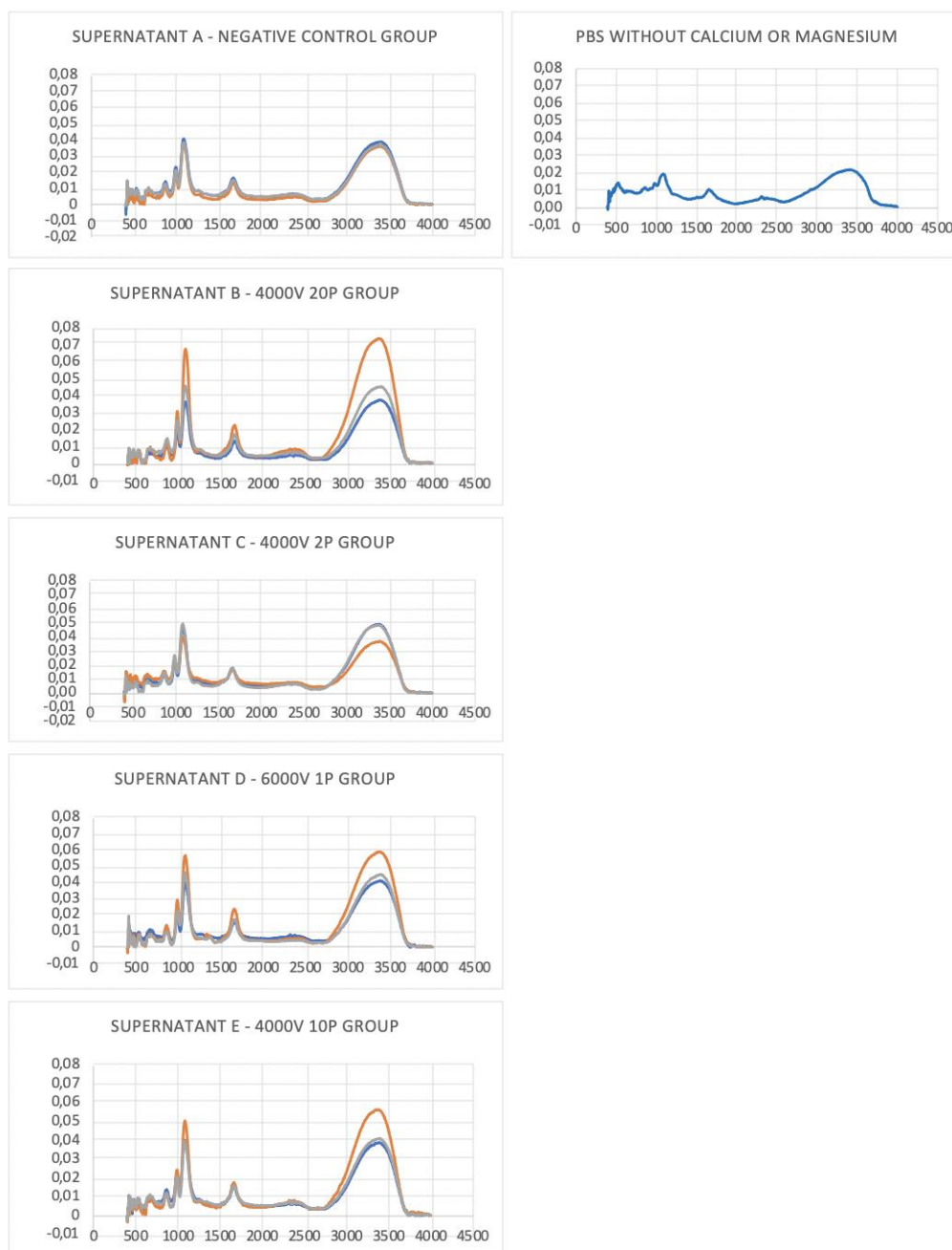


Figure 5.13. Left: Spectra of supernatant (DPBS) of different groups, with different electrical parameters, immediately after PEF application, only group A is the control group without any PEF application. Right: Typical spectra of DPBS. All spectra were submitted to atmospheric compensation and baseline correction.

After 48 hours ($t=48h$) and 72 hours ($t=72h$), the medium where the cells were in culture was gently removed and analyzed by FTIR spectroscopy, and their spectra compared with the complete medium spectrum (medium that were never in contact with cells). The results can be seen in Figure 5.14. The spectra of experiment 1 at 48h, when compared with the original and not consumed medium shows lower peaks than the spectrum of the original medium. This can be explained by the consumption of nutrients present in the medium, that are most needed to the cell in their first 48h of culture (Figure 5.14). On the contrary, the spectra relative to 72hrs of culture presents higher absorbance values, especially from cultures with higher cell's viability, most probably due to compounds secretion or some cell lysis. (Figure 5.14).

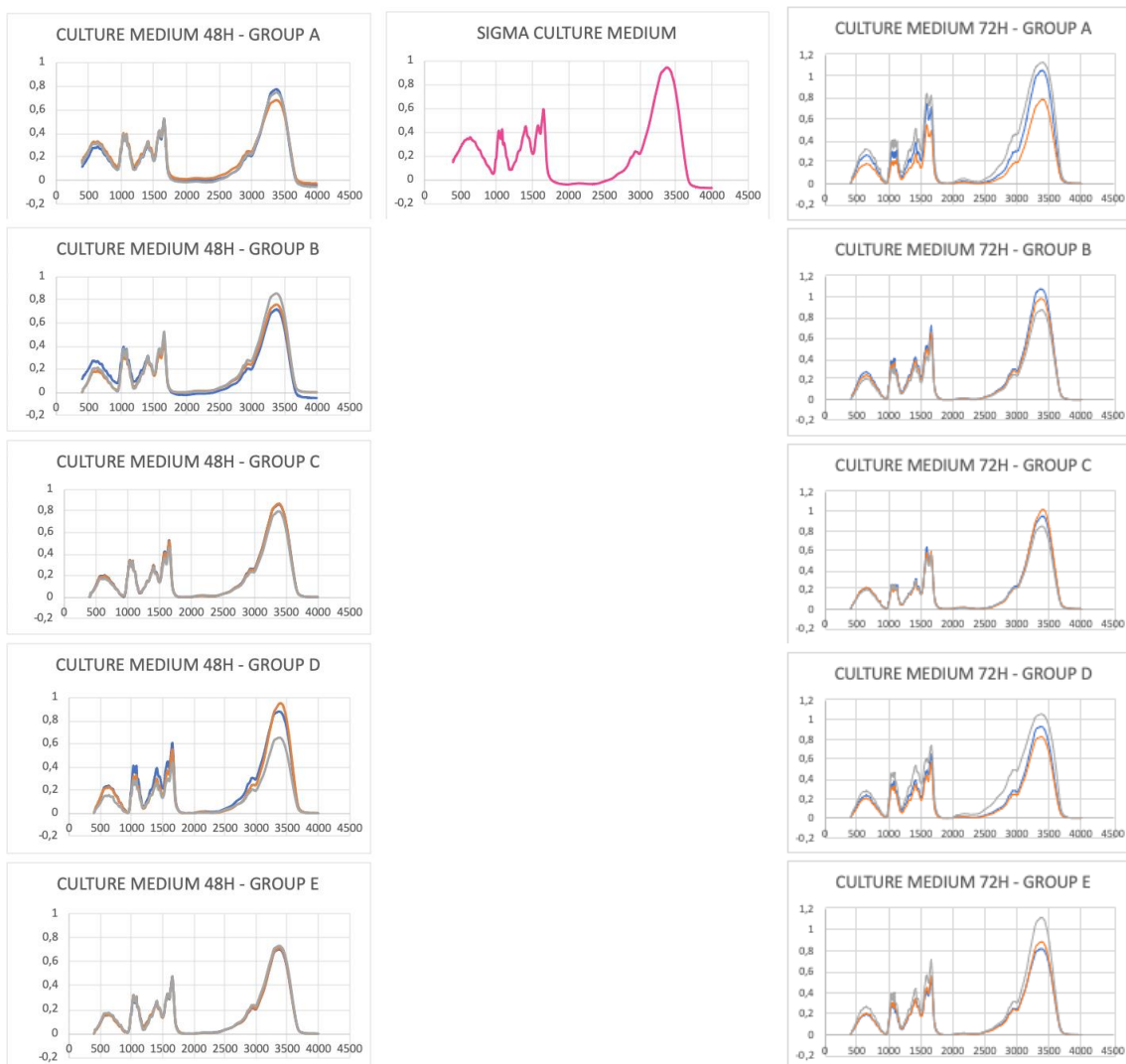


Figure 5.14. Left: Spectra analysis of the culture medium of the cells 48 hours after PEF application. Middle: Spectrum of DMEM. Right: Spectra analysis of the culture medium of the cells 72 hours after PEF application. All spectra were submitted to atmospheric compensation and baseline correction.

The FTIR spectra of the medium after the PEF assay points mostly to the vibrations of molecular bonds of DPBS, where differences between spectra are due to some cell's lysis and release compounds from the cells.

For simplicity of analysis, it was considered the sum of absorbances at all wavenumbers. Pure DPBS, resulted in a spectrum with a total absorbance of 44, where samples submitted to 6kV presented a sum of absorbances between 42 to 52, resulting in an average of the triplicates of 47, higher than the control, as represented in Figure 5.16. Indeed, the meaning of sum of absorbance of the negative control experiment (i.e. conducted without PEF) was significantly different ($p=0.00967$ based on ANOVA) in relation to the meaning of experiments conducted with PEF. It was not observed significant differences between the mean values of the different PEF assays. This is probably due to the high dilution degree of compounds liberated from cells to the medium.

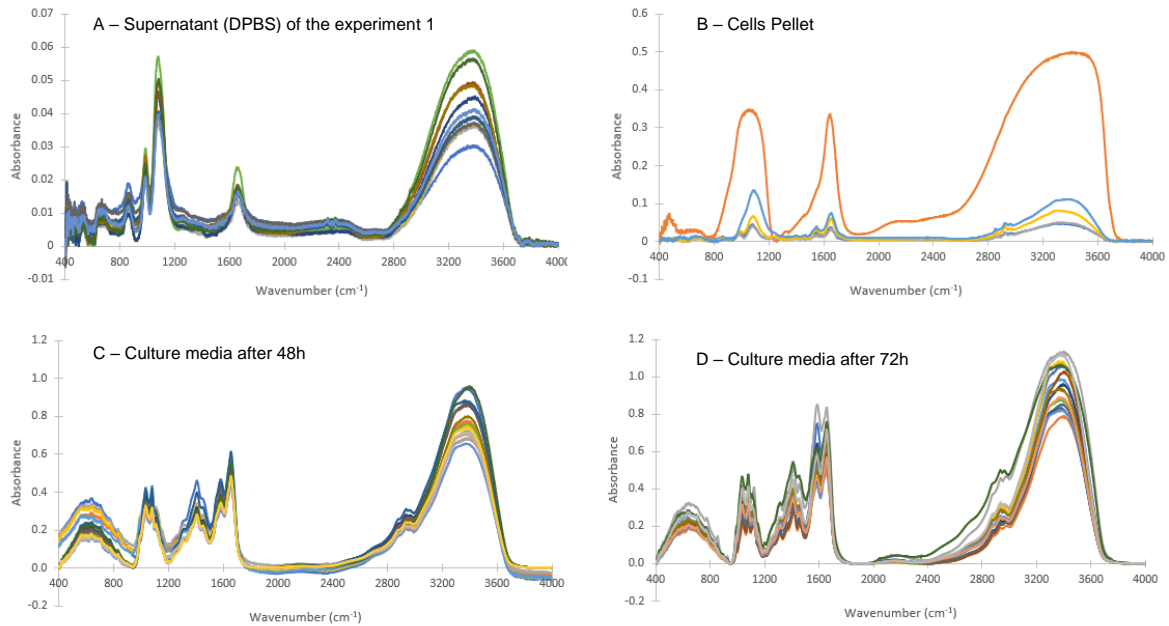


Figure 5.15. IR spectra of supernatant (A) and cell pellet (B) of the assay after PEF, respectively, and the spectra of culture media after plating cells after the PEF experiment and grown for 48 h (C) or 72h (D).

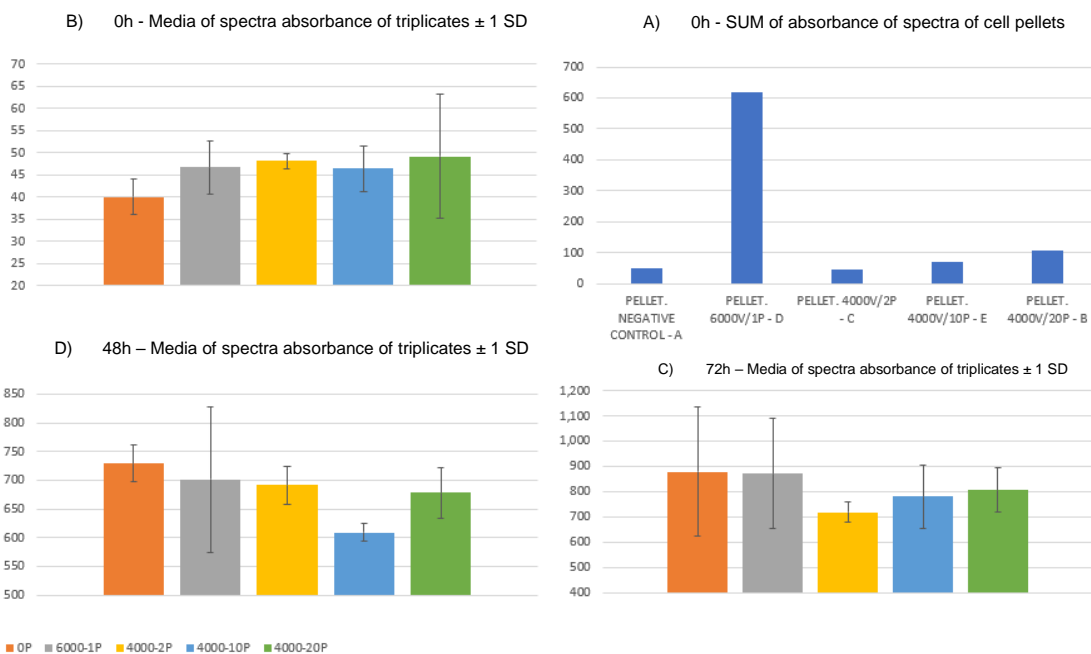


Figure 5.16. Average and corresponding standard deviation of the sum of absorbances of whole IR spectra of triplicated PEF assays, concerning the supernatant (A) and the cell pellet (B) of the assay immediately after PEF, respectively, and the IR spectra of culture media from, and the spectra of culture media after plating cells after the PEF experiment, and grown for 48h (C) or 72h (D). The spectra relative to cell pellet was not conducted in triplicate.

The spectra of the cell pellet obtained in the negative control, i.e. not submitted to PEF, reflects the cells composition and not the DPBS, as the spectra points to amide I and II bands not observed in the DPBS spectra. The 13-fold higher sum of absorbances observed with the 6 kV/cm field in relation to the negative control reflects most probably the whole cell lysis, where the increase absorbance observed with 4000 kV/cm field with 10 and 20 pulses, 1.4 and 2.2 fold-higher in relation to negative control probably reflects a small percentage of cell lysis in relation to the negative control. Interestingly, the assay with 4000 kV/cm field with 2 pulses, presented 0.92 of the sums of absorbance in relation to the negative control, indicating a lower influence of PEF on cells lysis.

The PCA score-plot of spectra of the supernatant of the assay after PEF is represented in Figure 5.17. The sample from pure PBS is localized apart of the assay samples with cells (blue square in Figure 5.17A). The scores of the triplicate samples of the negative control are near each other (red circles in top graph of Figure 5.17), pointing to a replicated assay. Triplicate samples submitted to PEF are slightly grouped in relation to other assays, pointing out that different PEF conditions resulted always in a different impact of cells metabolism or cell lysis. The high dispersion between triplicated assays is according with the high standard deviation represented in Figure 5.15A.

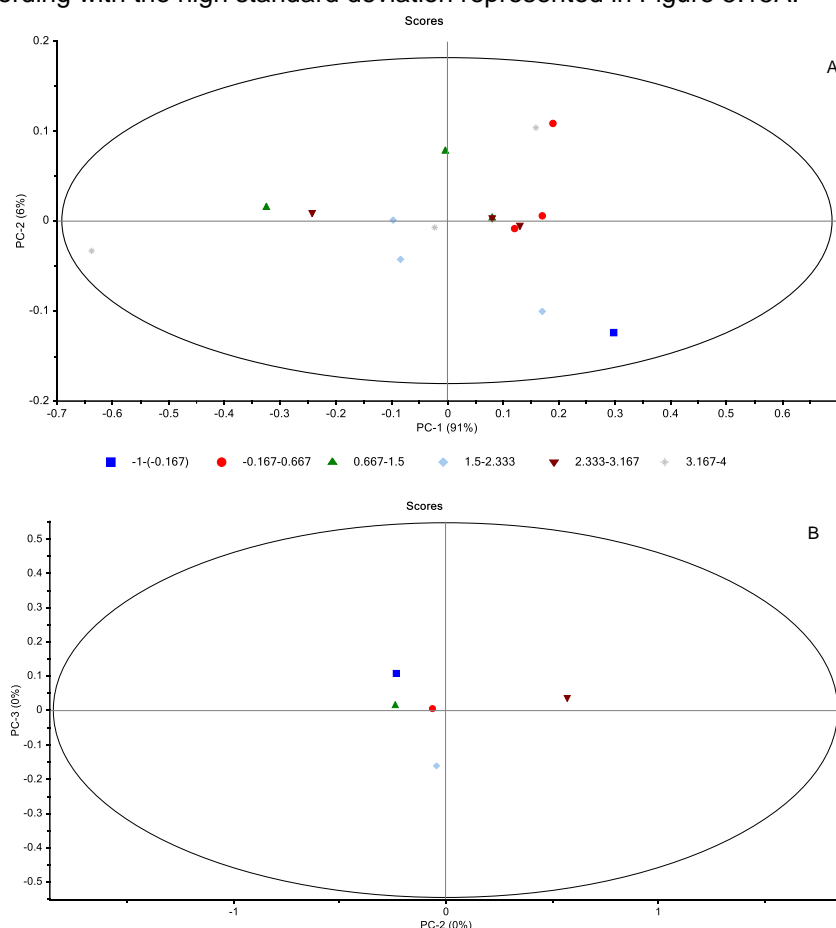


Figure 5.17. PCA of baseline corrected spectra of supernatant (A) and cell pellet of PEF assays (B). The Hotelling's ellipse at 5% is represented. Graph A, symbols correspond to: blue square, pure PBS; red circle, negative control, i.e. without PEF; green triangle, 6000KV/cm; light blue lozenge, 4000 KV/cm 2P; brown inverted triangle, 4000 KV/cm 10P; grey lozenge, 4000 KV/cm 20P. Graph B, symbols correspond to: blue square, negative control; red circle, 6000KV/cm ; green triangle, 4000 KV/cm 2P; light blue lozenge, 4000 KV/cm 10P; brown inverted triangle, 4000 KV/cm 20P.

The PCA score-plot of cell pellets of the PEF assay shows the negative control (blue square) far away from the samples submitted to PEF (other symbols in graph below of Figure 5.17), indicating the PEF effect on cells metabolism or cell lysis.

Cells after PEF were plated in microplates with 24 wells. The FTIR spectra of the culture medium from the plated cells after 48h and 72h are represented in Figure 5.15C and D, being observed a high variability in the sum of absorbances of triplicated assays as represented in Figure 5.16C and D. After 48h and 72h, it was not observed a significant difference in mean terms of the sum of absorbance of the spectra between cultures submitted to PEF and the negative control.

The PCA of the culture media at 48h and 72h are represented in Figure. 5.18, that highlights the spectra of pure media completely separated from the remaining samples, pointing that the spectra acquired the impact of the cell's metabolism on the culture media. After 48h of culture, replica experiments are more together than at 72h, as expected, most due to cells senescence due to cells confluence occurring for long periods of culture. Interestingly, at 48h the samples with the highest

variability among triplicates were from experiments conducted at 6000kv/cm and 4000 kV/cm with 20P, reflecting most probably that these conditions were the ones with the highest impact on cells viability and metabolism.

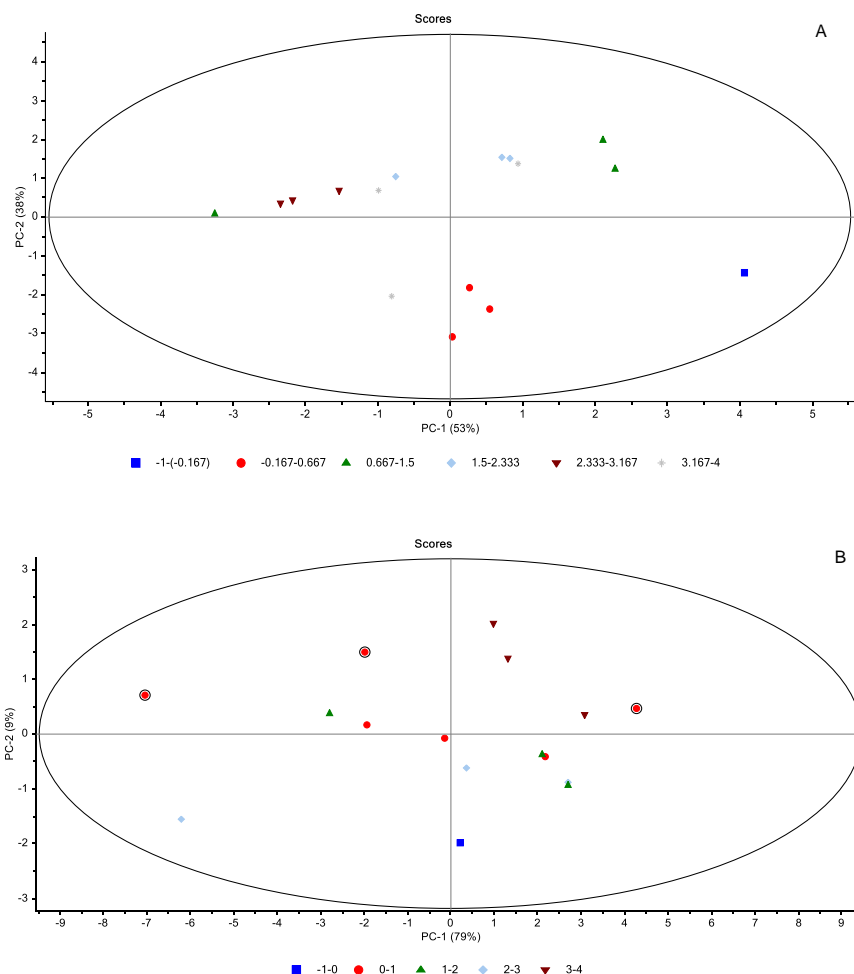


Figure 5.18 - PCA of baseline corrected spectra of culture media of cells plated and grown for 48h (Top) and 72h (Bottom). The Hotelling's ellipse at 5% is represented. Symbols correspond to: blue square, DMEM media; red circle, negative control, i.e. without PEF; green triangle, 6000KV/cm; light blue lozenge, 4000 KV/cm 2P; brown inverted triangle, 4000 KV/cm 10P; grey lozenge, 4000 KV/cm 20P. Graph B, symbols correspond to: blue square, negative control; red circle, 6000KV/cm ; green triangle, 4000 KV/cm 2P; light blue lozenge, 4000 KV/cm 10P; brown inverted triangle, 4000 KV/cm 20P.

In resume, it was observed that all PEF conditions evaluated had an impact on cells metabolism, resulting even in some cases in whole cell lysis (in case of the 6000 kV/cm field), or even impairing the cells viability and metabolism with high impact on cells proliferation when plated as observed under 4000 kV/cm with 2pulses.

5.2.5. Conclusions on experiment 1

The main objective of this experiment was to determine the effects of varying electrical parameters in a biological sample, through an in vitro experiment.

From here, other parameters would be calculated, such as specific energy and temperature increase in the sample, with a starting point for new experiments.

The results of the calculations obtained are in table 5.1. will condition the choice of non-variable electrical parameters for experiment 2, since group B - 4000V and 20P - has a temperature increase of 27.5°C, which can be considered too high for a biological sample, and group E - 4000V and 10P -

has a temperature increase of 13.7°C, but less cell viability. In turn, group C has good cell viability and low temperature increase, but the spectra obtained by FTIR analysis are weak, both in the analysis of the supernatant after PEF, and of the culture medium after 48H and 72H.

Another issue of this first experiment was the ideal number of cells per cuvette to electroporate, but at the same time ensuring that a FTIR spectra with a high signal to noise ratio would be obtained. To obtain an acceptable spectrum, the ideal minimum number for plating a 96-well FTIR plate would be in the order of 249,000 cells in 20 to 25uL per well. And for that same reason we chose 100,000 cells per cuvette, each group having tripled, after removing the cells needed to count and see the cell viability and the cells needed to culture, the contents of the 3 cuvettes would be added arriving thus to a pellet of 249,000. However, considering that the maximum number of fibroblast cells that the cuvette supports - between 452,719,144 and 1,527,883,881 - it was realized that only 0.007% to 0.02% of its useful volume would be used, which would conditionate the behavior of the electroporated cells and the very way they would react to the current. For that same reason, it was decided to carry out Experiment 2, to define the ideal number of cells per cuvette.

5.3. Experiment 2 – Effect of cell density

Starting from the results of the previous experiment, where according to viability, temperature increase and FTIR spectra, the most promising groups were group C and E, that only differ in the number of pulses, it was decided to choose an intermediate pulse value, between 2 and 10, choosing this way 5 pulses. Thus, a new experiment was conducted, this time to optimize the ideal quantity of fibroblasts to electroporate.

5.3.1. Overview

For this experiment, cells at 4th passage, the following parameters were chosen, $t_{on}=5\mu s$, $f=1\text{Hz}$, $U=4\text{kV}$, $P=5$, $E=10\text{kV/cm}$, as they represent an intermediate energy field for mammalian cells with little chance of overheating the cellular material or short-circuiting as previously observed.

The goals of the experiment were to study the influence of cell concentration on the oscillation of the electric current between the electrodes and, as said before, to define the ideal number of fibroblasts per cuvette, proving this way that cell density and cell volume can be extremely important in electroporation process, especially when talking about health applications.

For this, current (in A) and the temperature (in C°) were registered. Triplicates of experiments were conducted, including negative controls (i.e. live cells submitted to the same protocol with exception to PEF) and positive controls (i.e. cells killed by three successive freezing and thawing process).

Cell viability of each triplicate was determined as well as the FTIR spectroscopic analysis of the supernatant and cell pellet, immediately after the PEF experiment, and of the media culture after 72h of PEF. FTIR spectroscopic analysis was conducted in 384 wells-microplate, as it allows to save sample and also allows to plate triplicates from each sample.

5.3.2. Variations in electrical current and temperature increase for different cell density

To study how cell concentration, from the 5 groups, affects the current flow between the electrodes and to make a relation between cell density, current and temperature increase, variations in current and voltage were observed at each pulse, with a total of 5 pulses. These groups maintained the electrical parameters, and varied cell concentration, as such, Group A with 1,000,000 cells/800 μL , Group B with 500,000 cells/800 μL , Group C with 250,000 cells/800 μL , Group D with 100,000/800 μL and Group E with 50,000/800 μL . Temperature increase was also calculated in each sample.

As can be seen in group A, represented in table 5.3, which represents the cuvette of 1,000,000 cells in the conductive solution - DPBS - it can be observed that the current (A) is variable in each pulse, reaching 269A in pulse number 5. For the increase in temperature is also variable and increasing with each pulse, reaching a maximum of 8°C of increase. For sample A₁, the average temperature is 4.34°C, for sample A₂, average temperature 4.38°C, and for sample A₃ average temperature is 4.72°C. The total average temperature for group A is 4.48°C.

In its turn, group B, which represents the cuvette with 500,000 cells per 800 μL of DPBS, also presents current variations, increasing, reaching 286A in pulse number 5. Like the current, the temperature increase is also higher than in group A, reaching 8.6°C on the last pulse. Group B is represented in table 5.4, and the average temperature increase for sample B₁ is 4.58°C, for sample B₂ is 4.72°C, and for sample B₃ is 4.66°C. The total average temperature increase for group B is 4.65°C.

Group C represents the cuvette with 250,000 cells per 800 μL of DPBS, here we can observe more current fluctuations in each pulse and a maximum value of 8.8°C in the temperature rise. Group C temperature average is presented in table 5.5, sample C₁ temperature increase is 4.46°C, sample C₂ is 5.10°C, and sample C₃ is 4.82°C. Group C total average temperature increase is 4.79°C.

Table 5.3. Group A (1,000,000 cells/800 μ L PBS)

Group	Pulses (P)	Current (A)	Voltage (V)	t_{on} (μ s)	Frequency (Hz)	Energy Field (kV/cm)	W (J)	Wt (J)	Ws (kJ/kg)	ΔT (C°)	ΔT (C°) average
A ₁	1°	12	4000	5	1	10 KV/cm	0.2	0.2	0.3	0.1	4.3
	2°	250	4000	5	1	10 KV/cm	5.0	10.0	12.5	3.0	
	3°	253	4000	5	1	10 KV/cm	5.1	15.2	19.0	4.5	
	4°	256	4000	5	1	10 KV/cm	5.1	20.5	25.6	6.1	
	5°	268	4000	5	1	10 KV/cm	5.4	26.8	33.5	8.0	
A ₂	1°	12	4000	5	1	10 KV/cm	0.2	0.2	0.3	0.1	4.4
	2°	255	4000	5	1	10 KV/cm	5.1	10.2	12.8	3.1	
	3°	255	4000	5	1	10 KV/cm	5.1	15.3	19.1	4.6	
	4°	262	4000	5	1	10 KV/cm	5.2	21.0	26.2	6.3	
	5°	262	4000	5	1	10 KV/cm	5.2	26.2	32.8	7.8	
A ₃	1°	258	4000	5	1	10 KV/cm	5.2	5.2	6.5	1.5	4.7
	2°	258	4000	5	1	10 KV/cm	5.2	10.3	12.9	3.1	
	3°	259	4000	5	1	10 KV/cm	5.2	15.5	19.4	4.6	
	4°	268	4000	5	1	10 KV/cm	5.4	21.4	26.8	6.4	
	5°	269	4000	5	1	10 KV/cm	5.4	26.9	33.6	8.0	

Table 5.4. Group B (500,000 cells/800 μ L PBS)

Group	Pulses (P)	Current (A)	Voltage (V)	t_{on} (μ s)	Frequency (Hz)	Energy Field (kV/cm)	W (J)	Wt (J)	Ws (kJ/kg)	ΔT (C°)	ΔT (C°) average
B ₁	1°	12	4000	5	1	10 KV/cm	0.2	0.2	0.3	0.1	4.6
	2°	266	4000	5	1	10 KV/cm	5.3	10.6	13.3	3.2	
	3°	268	4000	5	1	10 KV/cm	5.4	16.1	20.1	4.8	
	4°	269	4000	5	1	10 KV/cm	5.4	21.5	26.9	6.4	
	5°	280	4000	5	1	10 KV/cm	5.6	28.0	35.0	8.4	
B ₂	1°	12	4000	5	1	10 KV/cm	0.2	0.2	0.3	0.1	4.7
	2°	266	4000	5	1	10 KV/cm	5.3	10.6	13.3	3.2	
	3°	275	4000	5	1	10 KV/cm	5.5	16.5	20.6	4.9	
	4°	282	4000	5	1	10 KV/cm	5.6	22.6	28.2	6.8	
	5°	286	4000	5	1	10 KV/cm	5.7	28.6	35.8	8.6	
B ₃	1°	11	4000	5	1	10 KV/cm	0.2	0.2	0.3	0.1	4.7
	2°	268	4000	5	1	10 KV/cm	5.4	10.7	13.4	3.2	
	3°	271	4000	5	1	10 KV/cm	5.4	16.3	20.3	4.9	
	4°	278	4000	5	1	10 KV/cm	5.6	22.2	27.8	6.7	
	5°	280	4000	5	1	10 KV/cm	5.6	28	35	8.4	

Table 5.5. Group C (250,000 cells/800 μ L PBS)

Group	Pulses (P)	Current (A)	Voltage (V)	t_{on} (μ s)	Frequency (Hz)	Energy Field (kV/cm)	W (J)	Wt (J)	Ws (kJ/kg)	ΔT (C°)	ΔT (C°) average
C ₁	1°	12	4000	5	1	10 KV/cm	0.2	0.2	0.3	0.1	4.5
	2°	255	4000	5	1	10 KV/cm	5.1	10.2	12.8	3.1	
	3°	256	4000	5	1	10 KV/cm	5.1	15.4	19.2	4.6	
	4°	265	4000	5	1	10 KV/cm	5.3	21.2	26.5	6.3	
	5°	273	4000	5	1	10 KV/cm	5.5	27.3	34.1	8.2	
C ₂	1°	275	4000	5	1	10 KV/cm	5.5	5.5	6.9	1.6	5.1
	2°	275	4000	5	1	10 KV/cm	5.5	11.0	13.8	3.3	
	3°	280	4000	5	1	10 KV/cm	5.6	16.8	21.0	5.1	
	4°	288	4000	5	1	10 KV/cm	5.8	23.0	28.8	6.9	
	5°	288	4000	5	1	10 KV/cm	5.8	28.8	36.0	8.6	
C ₃	1°	13	4000	5	1	10 KV/cm	0.3	0.3	0.3	0.1	4.8
	2°	276	4000	5	1	10 KV/cm	5.5	11.0	13.8	3.3	
	3°	285	4000	5	1	10 KV/cm	5.7	17.1	21.4	5.1	
	4°	286	4000	5	1	10 KV/cm	5.7	22.9	28.6	6.8	
	5°	293	4000	5	1	10 KV/cm	5.9	29.3	36.6	8.8	

Table 5.6 presents the cuvette with 100,000 cells per 800 μ L of DPBS, here it can be seen significant increases in current, when comparable with the other groups, which can go up to 293A, with a maximum temperature increase in the order of 8.8 $^{\circ}$ C. For sample D₁ the average temperature increase is 4.62 $^{\circ}$ C, for sample D₂, average temperature increase is 5.14 $^{\circ}$ C and for sample D₃ temperature increase is 4.72 $^{\circ}$ C. Total average for temperature increase, in group D, is 4.83 $^{\circ}$ C.

Table 5.6. Group D (100,000 cells/800 μ L PBS)

Group	Pulses (P)	Current (A)	Voltage (V)	t_{on} (μ s)	Frequency (Hz)	Energy Field (kV/cm)	W (J)	Wt (J)	Ws (kJ/kg)	ΔT ($^{\circ}$ C)	ΔT ($^{\circ}$ C) average
D ₁	1 $^{\circ}$	12	4000	5	1	10 KV/cm	0.2	0.2	0.3	0.1	4.6
	2 $^{\circ}$	267	4000	5	1	10 KV/cm	5.3	10.7	13.4	3.2	
	3 $^{\circ}$	274	4000	5	1	10 KV/cm	5.5	16.4	20.6	4.9	
	4 $^{\circ}$	277	4000	5	1	10 KV/cm	5.5	22.2	27.7	6.6	
	5 $^{\circ}$	278	4000	5	1	10 KV/cm	5.6	27.8	34.8	8.3	
D ₂	1 $^{\circ}$	280	4000	5	1	10 KV/cm	5.6	5.6	7.0	1.7	5.1
	2 $^{\circ}$	280	4000	5	1	10 KV/cm	5.6	11.2	14.0	3.4	
	3 $^{\circ}$	281	4000	5	1	10 KV/cm	5.6	16.9	21.1	5.0	
	4 $^{\circ}$	283	4000	5	1	10 KV/cm	5.7	22.6	28.3	6.8	
	5 $^{\circ}$	293	4000	5	1	10 KV/cm	5.9	29.3	36.6	8.8	
D ₃	1 $^{\circ}$	11	4000	5	1	10 KV/cm	0.2	0.2	0.3	0.1	4.7
	2 $^{\circ}$	278	4000	5	1	10 KV/cm	5.6	11.1	13.9	3.3	
	3 $^{\circ}$	277	4000	5	1	10 KV/cm	5.5	16.6	20.8	5.0	
	4 $^{\circ}$	282	4000	5	1	10 KV/cm	5.6	22.6	28.2	6.7	
	5 $^{\circ}$	284	4000	5	1	10 KV/cm	5.7	28.4	35.5	8.5	

Finally, table 5.7, which is representative of the cuvette with the lowest number of cells, only 50,000 per 800 μ L of DPBS, here is where greater current oscillations occur, with a maximum value of 429A, which results in a maximum temperature increase of 12.8. Average temperature increase for sample E₁ is 4.36 $^{\circ}$ C, for sample E₂ is 4.88 $^{\circ}$ C, and sample E₃ is 5.64 $^{\circ}$ C. Total average temperature increase, for group E, is 4.96 $^{\circ}$ C.

Table 5.7. Group E (50,000 cells/800 μ L PBS)

Group	Pulses (P)	Current (A)	Voltage (V)	t_{on} (μ s)	Frequency (Hz)	Energy Field (kV/cm)	W (J)	Wt (J)	Ws (kJ/kg)	ΔT ($^{\circ}$ C)	ΔT ($^{\circ}$ C) average
E ₁	1 $^{\circ}$	12	4000	5	1	10 KV/cm	0.2	0.2	0.3	0.1	4.4
	2 $^{\circ}$	250	4000	5	1	10 KV/cm	5.0	10.0	12.5	3.0	
	3 $^{\circ}$	256	4000	5	1	10 KV/cm	5.1	15.4	19.2	4.6	
	4 $^{\circ}$	259	4000	5	1	10 KV/cm	5.2	20.7	25.9	6.2	
	5 $^{\circ}$	265	4000	5	1	10 KV/cm	5.3	26.5	33.1	7.9	
E ₂	1 $^{\circ}$	11	4000	5	1	10 KV/cm	0.2	0.2	0.3	0.1	4.9
	2 $^{\circ}$	277	4000	5	1	10 KV/cm	5.5	11.1	13.9	3.3	
	3 $^{\circ}$	286	4000	5	1	10 KV/cm	5.7	17.2	21.5	5.1	
	4 $^{\circ}$	293	4000	5	1	10 KV/cm	5.9	23.4	29.3	7.0	
	5 $^{\circ}$	298	4000	5	1	10 KV/cm	6.0	29.8	37.3	8.9	
E ₃	1 $^{\circ}$	12	4000	5	1	10 KV/cm	0.2	0.2	0.3	0.1	5.6
	2 $^{\circ}$	276	4000	5	1	10 KV/cm	5.5	11.0	13.8	3.3	
	3 $^{\circ}$	287	4000	5	1	10 KV/cm	5.7	17.2	21.5	5.2	
	4 $^{\circ}$	286	4000	5	1	10 KV/cm	5.7	22.9	28.6	6.8	
	5 $^{\circ}$	429	4000	5	1	10 KV/cm	8.6	42.9	53.6	12.8	

It can be inferred, through this analysis, that there is a relationship between the number of cells that are electroporated, the current oscillations and the temperature increase, and, by maintaining a constant voltage, a greater number of cells will lead to a decrease current flow, which results in less heating of the sample. The heating within these values is not, itself, significant, since the cells of this work (*in vitro*) are kept at 4 $^{\circ}$ C (to lower their metabolism), but even if they were exposed to room temperature, they would hardly reach total temperature values above those necessary to cause protein denaturation or destabilization of the cell membrane, that is, exceeding 40 $^{\circ}$ C.

5.3.3. Cells counting and cell viability

The number of cells available to start experiment 2 was:

$$\text{Initial Cell Density} = \frac{120 \times 10 \times 1}{0,0001} = 12,000,000 \text{ cells/1mL}$$

The necessary volume of this suspension for each group is present in Table 5.8 according to described in Chapter 3, page 26. This table also includes the results of cells counting and cells viability immediately after PEF and after 72hs of PEF of culture conducted in a 12-well adherent plate and placed in culture.

Table 5.8. Cell counting by a trypan blue exclusion assay, immediately after PEF and 72h after (negative control: light blue; positive control: light pink).

Trypan Blue exclusion method assay (Hemocytometer – Neubauer chamber – counting)														
Experimental Groups		Dilution			Before PEF	After PEF application (t=0h)				72h after PEF application (t _{culture} =72h)				
		DF	Cellular volume (μL)	Trypan Blue volume (μL)	Total number of viable cells	Total number of cells (in 800μL)	Number of viable cells (in 800μL)	Number of dead cells (in 800μL)	Number of completed lysed cells (in 800μL)	Total number of cells (in 1000μL)	Number of viable cells (in 1000μL)	Number of dead cells (in 1000μL)	Culture Viability (average) %	
A	A1	5	20	80	1x10 ⁶	1,160,000	840,000	320,000	0	200,000	175,000	25,000	87.50	
	A2					1,040,000	800,000	240,000	0	175,000	175,000	0		
	A3					920,000	720,000	200,000	80,000	225,000	175,000	50,000		
	A-					1,080,000	960,000	120,000	0	250,000	225,000	25,000		90.00
	A+					240,000	80,000	160,000	760,000	175,000	125,000	50,000		71.43
B	B1	2.50	40	60	5x10 ⁵	440,000	240,000	200,000	60,000	237,500	187,500	50,000	86.54	
	B2					460,000	380,500	79,500	40,000	187,500	175,000	125,000		
	B3					340,000	240,000	100,000	160,000	225,000	200,000	25,000		
	B-					560,000	480,000	80,000	0	212,500	212,500	0		100.00
	B+					80,000	20,000	60,000	420,000	62,500	50,000	12,500		80.00
C	C1	1.25	80	20	2.5x10 ⁵	230,000	140,000	90,000	20,000	181,250	156,250	25,000	83.16	
	C2					170,000	110,000	60,000	80,000	200,000	156,250	43,750		
	C3					220,000	120,000	100,000	30,000	212,500	181,250	31,250		
	C-					250,000	240,000	10,000	0	225,000	212,500	125,000		94.44
	C+					20,000	10,000	10,000	230,000	18,750	12,500	6,250		66.67
D	D1	1.11	90	10	1x10 ⁵	53,280	35,520	17,76	46,720	194,250	160,950	33,300	77.78	
	D2					71,040	26,640	44,400	28,960	194,250	149,985	44,265		
	D3					53,280	8,880	44,400	46,720	210,900	155,400	55,500		
	D-					106,560	97,680	8,880	0	216,450	216,450	0		100.00
	D+					17,760	8,880	8,880	82,240	5,500	0	5,500		0
E	E1	1.11	90	10	5x10 ⁴	8,880	8,880	0	41,120	105,450	88,800	16,650	70.97	
	E2					17,760	8,880	8,880	32,240	122,100	72,150	50,950		
	E3					26,640	8,880	17,760	23,360	116,550	83,250	33,300		
	E-					44,400	44,400	0	6,000	210,900	205,350	5,550		97.37
	E+					17,760	8,880	8,880	32,240	11,100	5,550	5,550		50.00

The average viability for group A was 79%, with a percentage of lysed cells inferior to 8%. Group B has an average viability of 57% and presents the percentage of lysed cells as in group C of 17% - but this last group with a lower average viability of 49%. Group D and E have the lowest viability of 23% and 18%, respectively, with high impact on cell lysis with percentages of 40% and 65%, which are similar to the positive control samples of each group.

Positive control samples were performed exposing cells to successive cycles of freezing and thawing, and the viability of these samples for all groups were inferior to 17% and the lysed cells percentages were between 65% and 92%.

The negative control samples were submitted to all PEF procedures except to PEF itself. The viability for these samples is above 85% with no plasma lysis.

It was observed that, after 72h in culture, the cells exposed to PEF had a good recovery, being the viability above 71%, which could mean that the chosen PEF parameters were acceptable to maintain cell viability and allow cell proliferation. From all conditions evaluated, group A and B were the most promising groups in terms of cells viability after 72h in culture. For analysis of cells immediately after PEF application, it can be verified that the groups with 1,000,000 cells and 500,000 cells are the ones with more impact results when it comes to cell average and cell viability after PEF. For analysis of cells 72h after being in culture, it is also clear that group A and B are the ones with better results.

Table 5.9 and Fig. 5.22, resumes the cells counts and cells viability of each group in relation to the negative control, immediately after PEF and 72hrs after, highlighting the previous observation that the groups with the higher cells' concentrations imply immediately after PEF the highest cell viability while minimizing the cells lysis. After 72 hrs of PEF, cells were able to recuperate and grown, with the highest recover observed for the experiments with the highest cell's densities.

Table 5.9. Statistic data for cell counting and cells viability, showing Average and Standard Deviation for each group of experiment 2 in terms of percentage values in relation to the negative control (i.e. conducted without PEF).

Cells used in the assay	Average cells (n=3) after PEF	Standard deviation (n=3) of cells after PEF	Cells after freeze-thaw	Average cells viability (n=3) after PEF	Standard deviation of cells viability (n=3) after PEF	Cells viability after freeze-thawed
Results immediately after the PEF assay in relation to the assay without PEF (%)						
1 000 000	96	11	22	85	3	38
500 000	74	11	14	81	16	29
250 000	83	13	8	63	5	52
100 000	56	10	17	44	27	55
50 000	40	20	40	61	35	50
Results after 72hrs of cells culture after PEF in relation to the assay without PEF (%)						
1 000 000	80	10	70	98	12	79
500 000	102	12	29	87	7	80
250 000	88	7	8	88	5	71
100 000	92	4	3	78	5	0
50 000	54	4	5	74	13	51

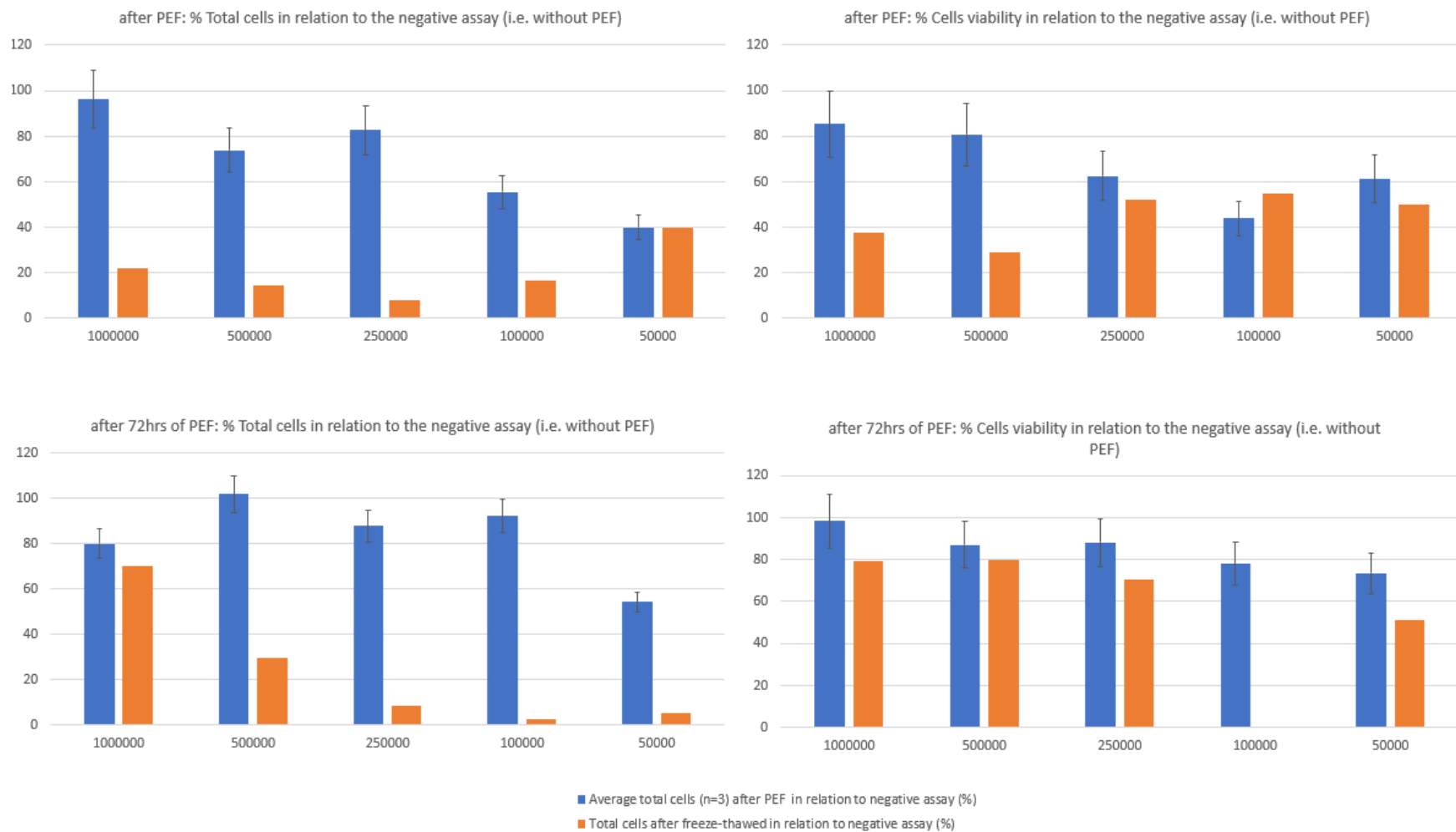


Figure 5.19. Average number of cells and cells viability of assays conducted with different cells density in relation to the assay without PEF. Data are due to assays immediately after PEF or after 72hrs of culture after PEF. The error bars are the average value of standard deviation of all assays.

5.3.4. FTIR Spectroscopy

The objective of using the FTIR analysis, for this experiment, was to understand if there were electroporation phenomena, with selective release of components for the supernatant, or for the cellular medium, varying according to the number of cells subjected to the pulsed electric fields. This analysis was done in two moments with two different solutions, DPBS or supernatant of electroporated cells, immediately after the application of PEF, and the culture media of cells exposed to PEF, after 72h.

For a simple analysis, there were chosen the DPBS in $t=0h$ and the culture media in $t=72h$, from group A, with 1,000,000 cells, and group E, with 50,000 cells, that represent the extreme groups and thus the differences in absorbance values are more visible. DPBS spectra from group A and E and the comparative spectrum of DPBS without electroporation effects are shown in Figure 5.19. There is a clear difference between the two groups, being the group with 1,000,000 cells, the one with higher absorbances. It can also be seen that cells exposed to PEF and cells from the positive control have similar absorbance values.

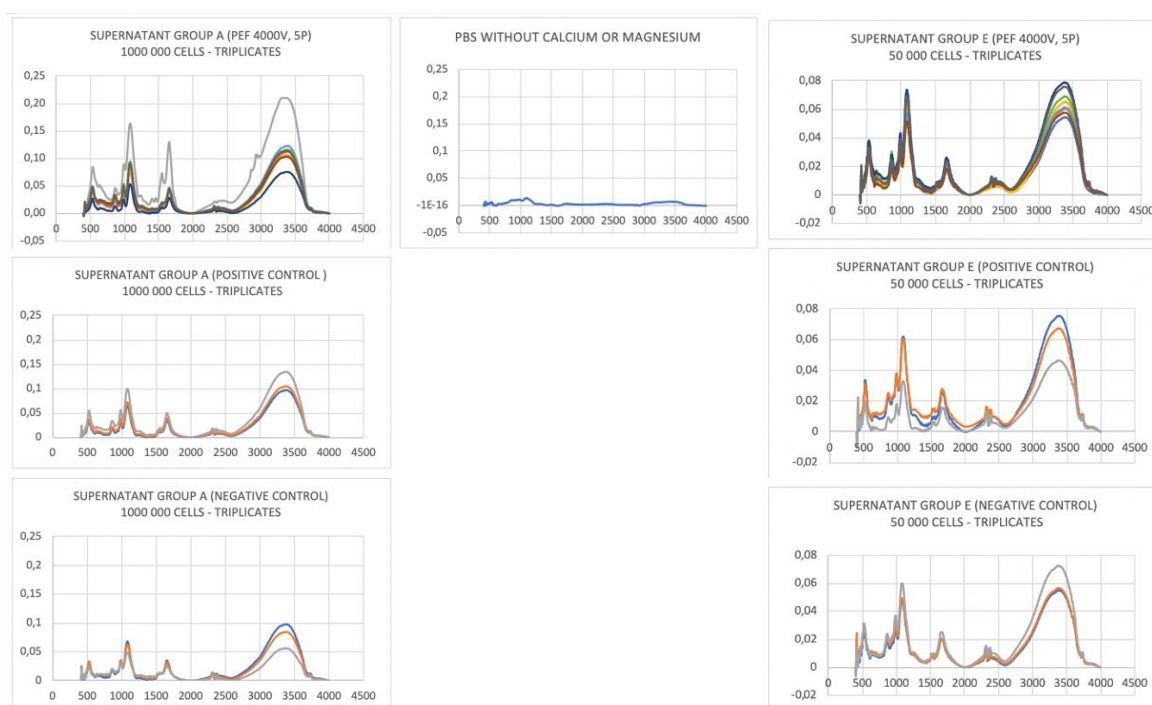


Figure 5.20. Left: Spectra of supernatant (PBS) of the 1,000,000 cells group, immediately after PEF application, and the corresponding positive and negative control. Middle: Spectrum of a typical spectra of PBS. Right: Spectra of supernatant (PBS) of the 50,000 cells group, immediately after PEF application and the corresponding positive and negative control.

The comparative spectrum of cell culture medium, at 72h after PEF application, with and without electroporation effects are shown in Figure 5.20. These are interesting spectra, for example, in general, there are not much difference in spectra from 72hrs culture, between the negative control and the samples submitted to PEF in group E. However, there is a small difference between the negative control and group A.

Figure 5.21.A represents the spectra of DPBS of the assay immediately after the PEF experiment, being visible the amide I and II peaks, probably due to cell disruption, in assays conducted with cells concentrations equal to 250,000 cells or higher. This can be verified by the bar charts on the right, representing the sum of the absorbances. It can be seen in figure 5.21, that cells exposed to PEF have significant metabolic changes in relation to the negative control and the positive control when 1,000,000 are used in the test (B).

On the other hand, when it comes to the analysis of the culture medium at 72h, it can be observed that there are discrepancies between PEF and non-PEF, with approximate values in the group with 1,000,000 cells (C).

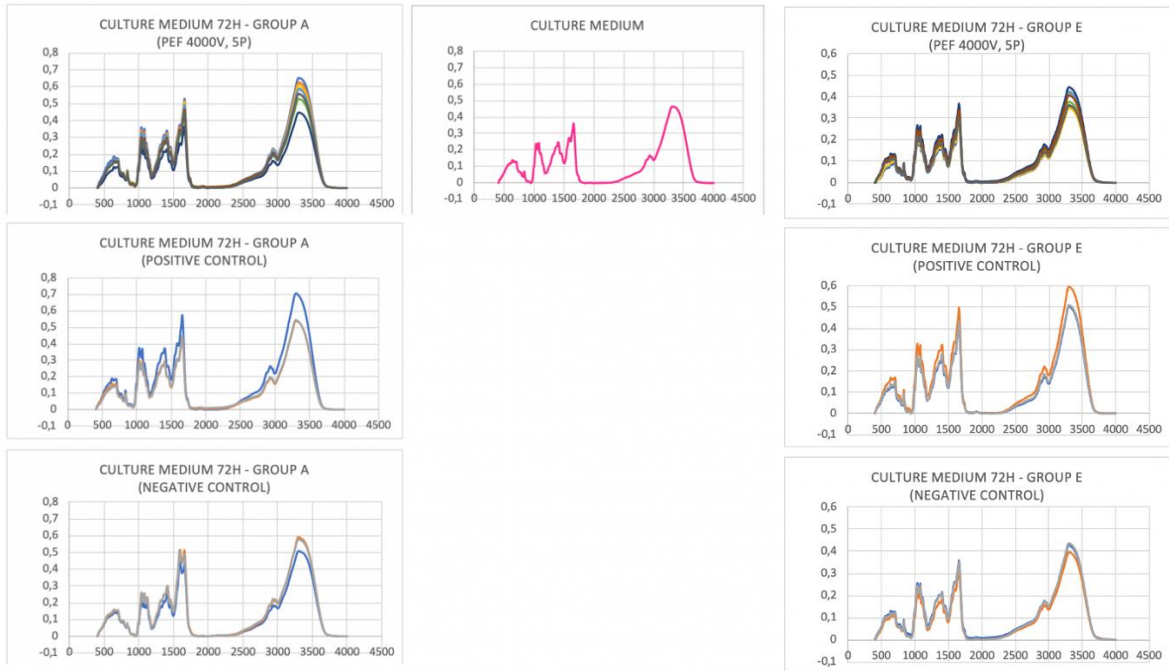


Figure 5.21. Left: Spectra of culture medium of 1000,000 cells, 72H after PEF application, and the corresponding positive and negative control. Middle: Spectrum of non-consumed culture medium. Right: Spectra of culture medium of 50,000 cells, 72H after PEF application, and the corresponding positive and negative control.

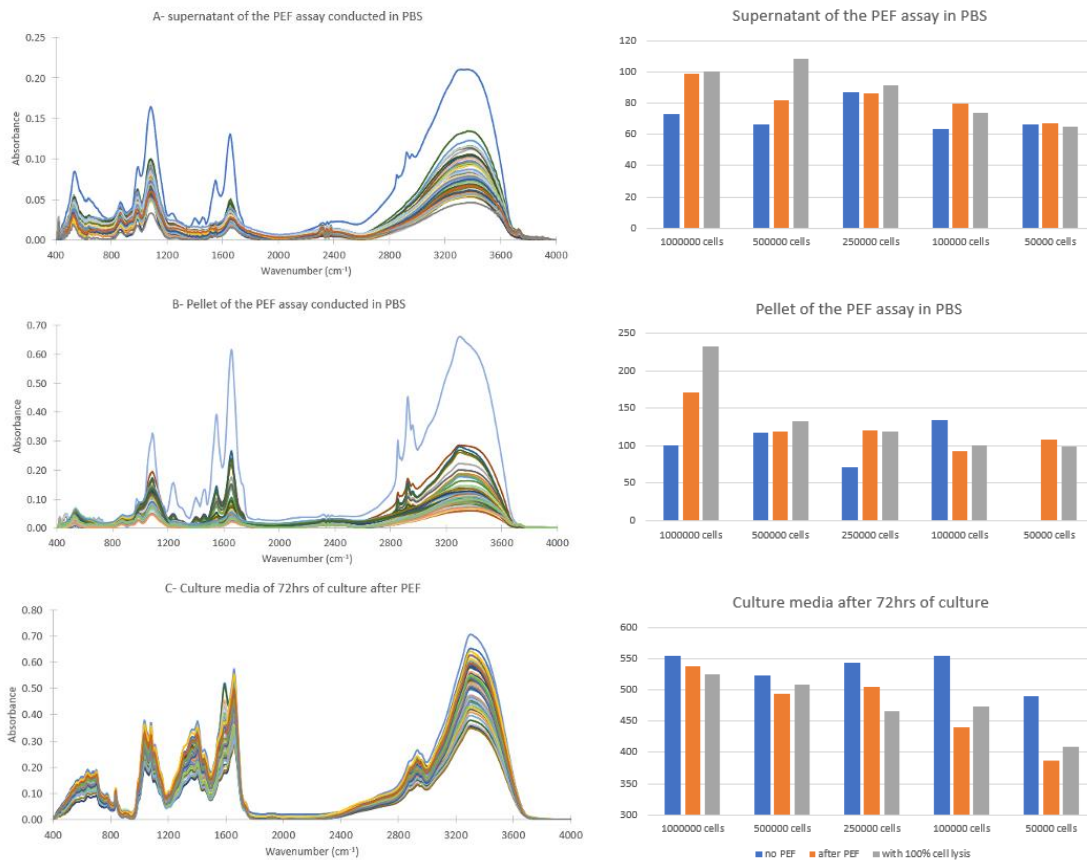


Figure 5.22. Left: IR spectra of supernatant (A) and cell pellet (B) of the assay after PEF, respectively, and the spectra of culture media after plating cells after the PEF experiment and grown for 72h (C). Right: Average of the sum of absorbances of whole spectra of triplicated PEF assays, concerning the supernatant (A) and the cell pellet (B) of the assay immediately after PEF, respectively, and the IR spectra of culture media from after plating cells from the PEF experiment, and grown for 72h (C).

Table 5.10 shows ANOVA single value analysis, for spectra absorbance of supernatant and pellet immediately after PEF and culture medium after 72hrs. It is noticed that p-value is more significant for the conditions without PEF vs with PEF and without PEF vs Cells disruption by freezing cycles, less significant is the condition with PEF vs Cells disruption by freezing cycles, given an indication that the PEF application had similar effects to disruption of plasma membrane as by freezing cycles.

Regarding the supernatant, it is significant for group B (500,000 cells), as p-value is inferior to 5% for all conditions, which means the supernatant of 500,000 is quite different from the other groups. The pellet indicates cell metabolism, and here the p-value is inferior to 5% for group A (1,000,000 cells). Culture media after 72h have non-significant values for group A (1,000,000 cells) and group B (500,000 cells), that means that, for these two groups, cells recover as the control group.

Table 5.10. Average and standard deviation of the sum of absorbances of whole IR spectra of triplicated PEF assays, concerning the supernatant and the cell pellet of the assay immediately after PEF, and from culture media grown for 72h.

	Cells used in PEF assay	A Without PEF		B With PEF		C Cells disruption by freeze/thawing		p-value of ANOVA (if <0.1) ^{*3}		
								B vs A	B vs C	A vs C
		average	SD	average	SD	Average	SD			
Supernatant	1,000,000	73	15	99 ^{*1}	17	100	24	ns	ns	ns
	500,000	66	4	82	7	109	9	0.005	0.0003	0.002
	250,000	87	8	86	21	91	7	ns	ns	Ns
	100,000	64	3	80	13	74	12	0.058	ns	ns
	50,000	66	19	67	9	65	10	0.008	ns	Ns
pellet	1,000,000	100	19	172	46	234	7	0.029	0.049	0.0003
	500,000	118	41	120	13	132 ^{*1}	6	ns	ns	ns
	250,000	71	2	120	29	119	13	0.20	ns	0.0032
	100,000	134	25	93	8	100	8	0.0023	ns	0.082
	50,000	^{*2}		109	29	99	5	-	ns	-
After 72hrs of culture	1,000,000	555	86	538	57	525	44	ns	ns	ns
	500,000	523	28	494	35	509	12	ns	ns	Ns
	250,000	543	35	505	19	466	53	0.033	0.075	0.10
	100,000	555	56	441	28	474	48	0.0007	ns	ns
	50,000	490	57	388	42	410	31	0.0069	ns	0.099

*1 – one of the FTIR spectra was considered an outline and was not considered.

*2 – this experiment was not conducted

*3 - ns- considered not significant at p>0.1

PCA of normalized second derivative spectra of supernatant or cell pellet immediately after PEF (Fig. 5.23) pointed clusters of samples according to if cells were submitted or not to PEF or freeze-thawing cycles and according to the number of cells. Since PCA was based on normalized second derivative spectra, i.e. the spectra do not depend of concentrations of metabolites or quantities of cells debris but from the sample biochemical composition, it could be inferred that cells metabolism was affected by cell density. From the PCA of spectra of culture media after 72h of PEF, it was observed that samples from cultures started from cells previously submitted to freeze-thawing are clustered together and apart from cells not submitted to this process, indicating the high effect of freeze-thawing in cells in relation to PEF (Fig. 5.24). Furthermore, the number of cells in the PEF assay also affects the cells metabolism even after 72hrs of culture, as samples in the PCA score plot are also clustered according to the number of cells at the PEF assay.

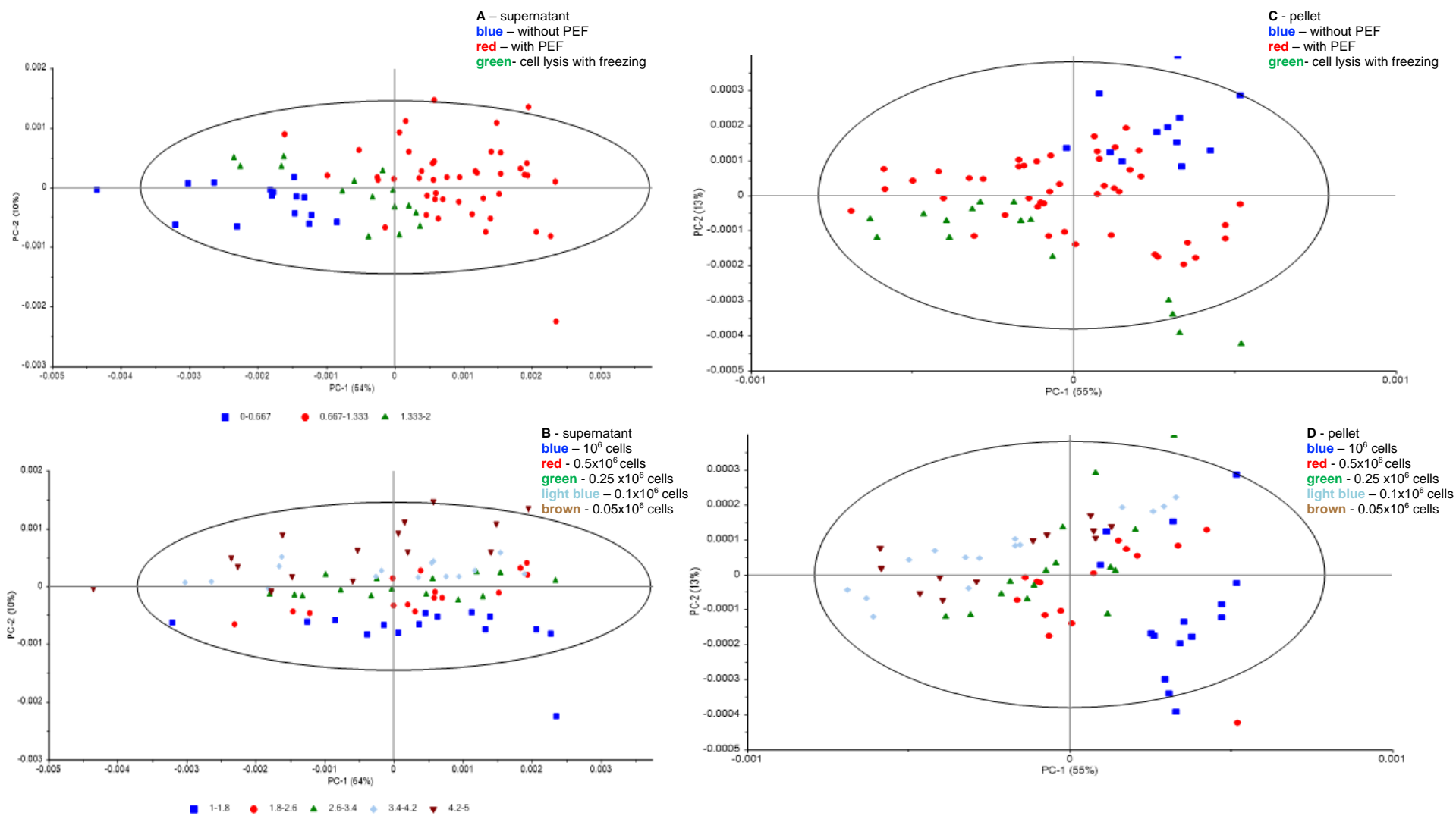


Figure. 5.23. PCA of normalized second derivative spectra of supernatant (A, B) and cell pellet (C, D) immediate after PEF . The Hotelling's ellipse at 5% is represented.

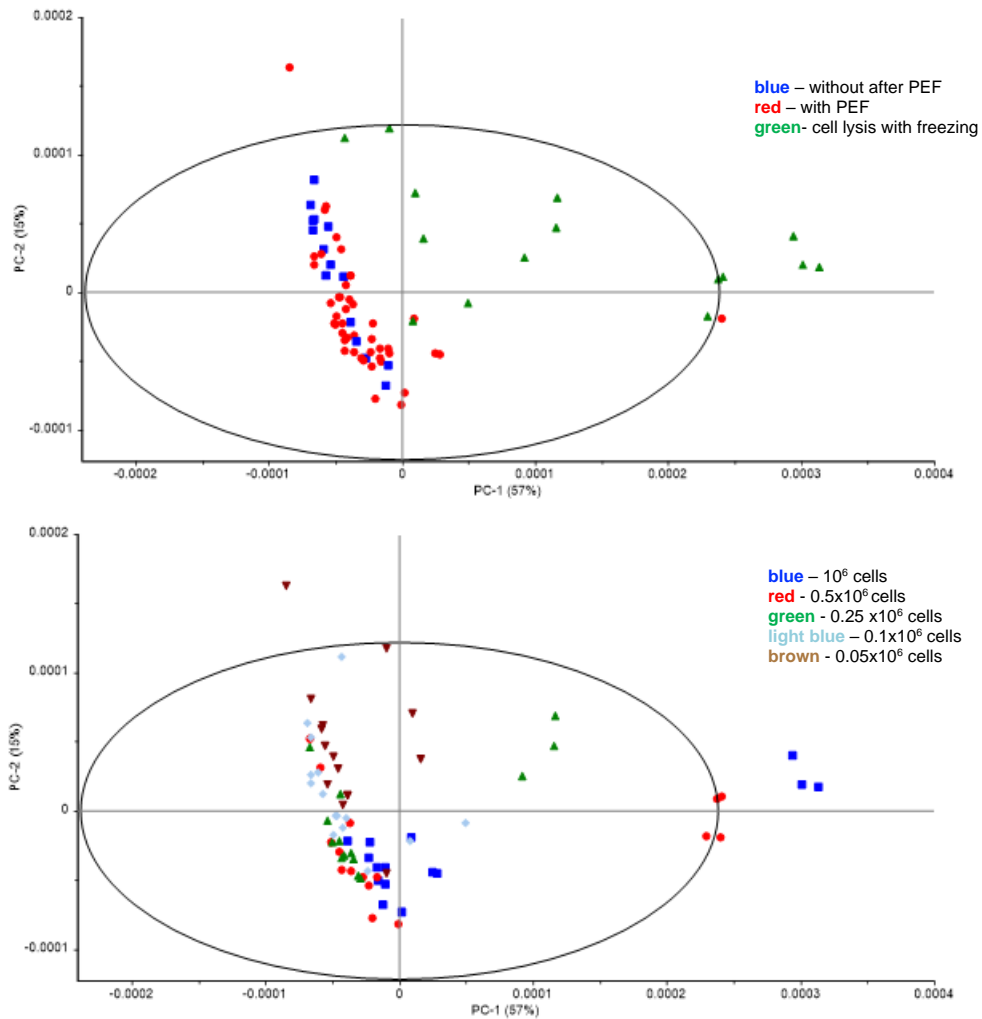


Figure 5.24. PCA of normalized second derivative spectra of culture media from cultures grown for 72hrs after PEF in function if cells were submitted or not to PEF or lysed through cycles of freezing and defrost (A) or in function of the number of cells considered in the PEF assay (B). The Hotelling's ellipse at 5% is represented.

5.3.5. Conclusions on Experiment 2

Experiment 2 came to prove statistically that the cell density inside the electroporation cuvette influences the susceptibility of cells to PEF application. This experiment also showed that, for the conditions evaluated (from cell densities between 1000 000 to 50 000), the higher cells densities (i.e. of 1000 000 and 500 000) were less affected by PEF, i.e. presenting higher viability, less plasma lysis, less temperature increase during PEF. This number is five to ten times more cells that was used in experiment 1.

5.4. Experiment 3 – Effect of repeated PEF applications

Since in the previous section, the best result was obtained with the maxima cell densities evaluated (i.e. 500,000 and 1,000,000 cells per 800 μ L), in the present section was evaluated these two cell densities and a third one of 1,500,000 cells.

5.4.1. Overview

Experiment 3 was based on the following electrical parameters: $t_{on}=5\mu s$, $f=1Hz$, $U=4kV$, $P=5$, $E=10kV/cm$. In this experiment, the main goal was to assess how long could cells endure, when exposed to three consecutive PEF applications, with 48h interval. The 48h gap between applications was stipulated by the availability of the equipment although it was observed before (in experiment 1) that cells full recovery is reached only at 72h. The first assay corresponded to the first PEF application, and was designated as $t=0h$, the second assay that corresponds to the second PEF application conducted after 48h and a third assay, which corresponds to the third PEF application after a total time of 96h after the first PEF application. A negative control (i.e. without PEF exposure) was used for all groups. Experiments were conducted in triplicate. FTIR spectroscopic analysis was conducted in 384-well microplate, enabling triplicate analysis of each sample.

It was considered 3 groups in each assay, A with 1,500,000 cells, B with 1,000,000 cells and C with 500,000 cells. The first assay was based on cells at the 4th passage. For all the three assays ($t=0$, 48 and 96hrs), the theoretical number of cells used to start each culture was defined with the objective of having after 48hrs: for group A, was seeded 28,500 cells (7,500 cells per cm^2 in wells of $3.8cm^2$) to reach 1,500,000 cells; For group B was seeded 19,000 cells (5,000 cells per cm^2 in wells of $3.8cm^2$) in order to have 1,000,000 after 48h. And for group C, 9,500 cells were seeded (2,500 cells per cm^2 in wells of $3.8cm^2$) to have 500,000 per well after 48h.

For trypan blue exclusion assays, the DF remained the same as in experiment 2, for the group of 1,000,000 cells a DF of 5, for the group of 500,000 cells a DF of 2.5, and for the new group, 1,500,000 cells a DF of 10 was chosen.

FTIR spectroscopic analysis of DPBS (conductive solution) and pellet (separately) was performed at $t=0h$, $t=48h$ and $t=96h$, and for culture medium was performed at $t=48h$, $t=96h$ and $t=144h$.

5.4.2. First Assay ($t=0h$)

5.4.2.1. Variations in electrical current and temperature increase during PEF application

Group A to C present similar small fluctuations in temperature increase, between $4^{\circ}C$ and $5^{\circ}C$ (table 5.11). The group with a larger number of cells, is the one that have a lower increase of temperature, and as the number of cells decreases, the temperature increases, this can be explained due to cellular ionic charge, that influences the electrical field, thus influencing PEF application results (also as verified in experiment 2).

Table 5.11. First Assay. Groups A; B; C (1,500,000; 1,000,000; 500,000 cells/800 μ L PBS)

Group	Pulses (P)	Current (A)	Voltage (V)	t_{on} (μ s)	Frequency (Hz)	Energy Field (kV/cm)	W (J)	Wt (J)	Ws (kJ/kg)	ΔT (C°)	ΔT (C°) average
A ₁	1°	11	4000	5	1	10 KV/cm	0.2	0.2	0.3	0.1	4.56
	2°	260	4000	5	1	10 KV/cm	5.2	10.4	13.1	3.1	
	3°	268	4000	5	1	10 KV/cm	5.4	16.1	20.1	4.8	
	4°	269	4000	5	1	10 KV/cm	5.4	21.5	26.9	6.4	
	5°	270	4000	5	1	10 KV/cm	5.4	27.0	33.8	8.1	
A ₂	1°	11	4000	5	1	10 KV/cm	0.2	0.2	0.3	0.1	
	2°	263	4000	5	1	10 KV/cm	5.3	10.5	13.2	3.1	
	3°	274	4000	5	1	10 KV/cm	5.5	16.4	20.6	4.9	
	4°	282	4000	5	1	10 KV/cm	5.6	22.6	28.2	6.7	
	5°	284	4000	5	1	10 KV/cm	5.7	28.4	35.5	8.5	
A ₃	1°	13	4000	5	1	10 KV/cm	0.3	0.3	0.3	0.1	
	2°	262	4000	5	1	10 KV/cm	5.2	10.5	13.1	3.1	
	3°	263	4000	5	1	10 KV/cm	5.3	15.8	19.7	4.7	
	4°	273	4000	5	1	10 KV/cm	5.5	21.8	27.3	6.5	
	5°	275	4000	5	1	10 KV/cm	5.5	27.5	34.4	8.2	
B ₁	1°	13	4000	5	1	10 KV/cm	0.3	0.3	0.3	0.1	
	2°	272	4000	5	1	10 KV/cm	5.4	10.9	13.6	3.3	
	3°	274	4000	5	1	10 KV/cm	5.5	16.4	20.6	4.9	
	4°	281	4000	5	1	10 KV/cm	5.6	22.5	28.1	6.7	
	5°	283	4000	5	1	10 KV/cm	5.7	28.3	35.4	8.5	
B ₂	1°	12	4000	5	1	10 KV/cm	0.2	0.2	0.3	0.1	
	2°	276	4000	5	1	10 KV/cm	5.5	11.1	13.8	3.3	
	3°	277	4000	5	1	10 KV/cm	5.5	16.6	20.8	5.0	
	4°	287	4000	5	1	10 KV/cm	5.7	23.0	28.7	6.9	
	5°	290	4000	5	1	10 KV/cm	5.8	29.0	36.3	8.7	
B ₃	1°	12	4000	5	1	10 KV/cm	0.2	0.2	0.3	0.1	
	2°	259	4000	5	1	10 KV/cm	5.2	10.4	13.0	3.1	
	3°	269	4000	5	1	10 KV/cm	5.4	16.1	20.2	4.8	
	4°	270	4000	5	1	10 KV/cm	5.4	21.6	27.0	6.5	
	5°	274	4000	5	1	10 KV/cm	5.5	27.4	34.3	8.2	
C ₁	1°	11	4000	5	1	10 KV/cm	0.2	0.2	0.3	0.1	
	2°	279	4000	5	1	10 KV/cm	5.6	11.2	14.0	3.3	
	3°	281	4000	5	1	10 KV/cm	5.6	16.9	21.1	5.0	
	4°	283	4000	5	1	10 KV/cm	5.7	22.6	28.3	6.8	
	5°	291	4000	5	1	10 KV/cm	5.8	29.1	36.4	8.7	
C ₂	1°	12	4000	5	1	10 KV/cm	0.2	0.2	0.3	0.1	
	2°	274	4000	5	1	10 KV/cm	5.5	11.0	13.8	3.3	
	3°	281	4000	5	1	10 KV/cm	5.6	16.9	21.1	5.0	
	4°	283	4000	5	1	10 KV/cm	5.7	22.6	28.3	6.8	
	5°	284	4000	5	1	10 KV/cm	5.7	28.4	35.5	8.5	
C ₃	1°	12	4000	5	1	10 KV/cm	0.2	0.2	0.3	0.1	
	2°	272	4000	5	1	10 KV/cm	5.4	10.9	13.6	3.3	
	3°	276	4000	5	1	10 KV/cm	5.5	16.6	20.7	5.0	
	4°	280	4000	5	1	10 KV/cm	5.6	22.4	28.0	6.7	
	5°	286	4000	5	1	10 KV/cm	5.7	28.6	35.8	8.6	

5.4.2.2. Cells counting and cell viability

From table 5.12, Like in experiment 2, there are few discrepancies between the total number of cells counted and the theoretical number of cells aimed at the assay, most probably due to counting errors.

For negative control samples, viability varied between 92% and 100%, most probably due to the cell's manipulation outside the CO₂ cabinet, as cells were manipulated the same way as the cells submitted to PEF, apart from PEF exposure.

It was observed that PEF application to group A (with 1500 000 cells), B (with 1000 000 cells) and C (with 500 000 cells), lead immediately to 25.3%, 12% and 56% cell lysis, respectively, and from the cells that were not lysed to 81.6%, 61.3% and 36% cells viability, respectively. Therefore, the higher cells density, the final higher cell viability. After 48hr of culture of PEF application, group A, B and C resulted in 35%, 56.7% and 66.7% lower cell counting in relation to desired.

After 48hrs of culture of PEF, group A, B and C presented 79%, 73% and 70% cells viability, respectively, pointing that PEF affected the recovery of cells along the culture in function of the cells density, were the higher the cell density during the PEF assay the lower its effect on the cells capability of recover.

Table 5.12. Cell counting by a trypan blue exclusion method, immediately after PEF and 48h after.

Trypan Blue exclusion method (Hemacytometer – Neubauer chamber – counting)													
Experimenta I Groups		Dilution			Before PEF (t=0h)	After 1 st PEF application (t=0h)				48h after 1 st PEF application (C _{culture} =48h)			
		DF	Cellular volume (μ L)	Trypan Blue volume (μ L)		Total number of viable cells	Total number of cells (in 800 μ L)	Number of viable cells (in 800 μ L)	Number of dead cells (in 800 μ L)	Number of completed lysed cells (in 800 μ L)	Total number of cells (in 1000 μ L)	Number of viable cells (in 1000 μ L)	Number of dead cells (in 1000 μ L)
A	A1	10	10	90	1.5x10 ⁶	1,120,000	880,000	240,000	380,000	1,000,000	800,000	200,000	79.3
	A2					1,680,000	1,360,000	320,000	0	800,000	600,000	200,000	
	A3					1,120,000	960,000	160,000	380,000	1,100,000	900,000	200,000	
	A-					1,600,000	1,440,000	160,000	0	1,200,000	1,110,000	90,000	
B	B1	5	20	80	1x10 ⁶	800,000	560,000	240,000	200,000	350,000	300,000	50,000	73.1
	B2					840,000	600,000	240,000	160,000	250,000	100,000	150,000	
	B3					1,040,000	880,000	160,000	0	700,000	550,000	150,000	
	B-					960,000	960,000	0	0	800,000	750,000	50,000	
C	C1	2.5	40	60	5x10 ⁵	200,000	140,000	60,000	300,000	150,000	125,000	25,000	70.0
	C2					240,000	160,000	80,000	260,000	200,000	125,000	75,000	
	C3					280,000	240,000	40,000	220,000	150,000	100,000	50,000	
	C-					360,000	340,000	20,000	140,000	400,000	400,000	0	

5.4.2.3. FTIR Spectroscopy

The FTIR spectra of supernatant (Fig. 5.25), presents a significant difference between the group with 1,500,000 cells submitted to PEF in relation to the negative control group. For the spectra of culture medium at 48h there is no significant difference of all groups between the experiment with PEF in relation to the control samples, indicating that cells needed more time in culture.

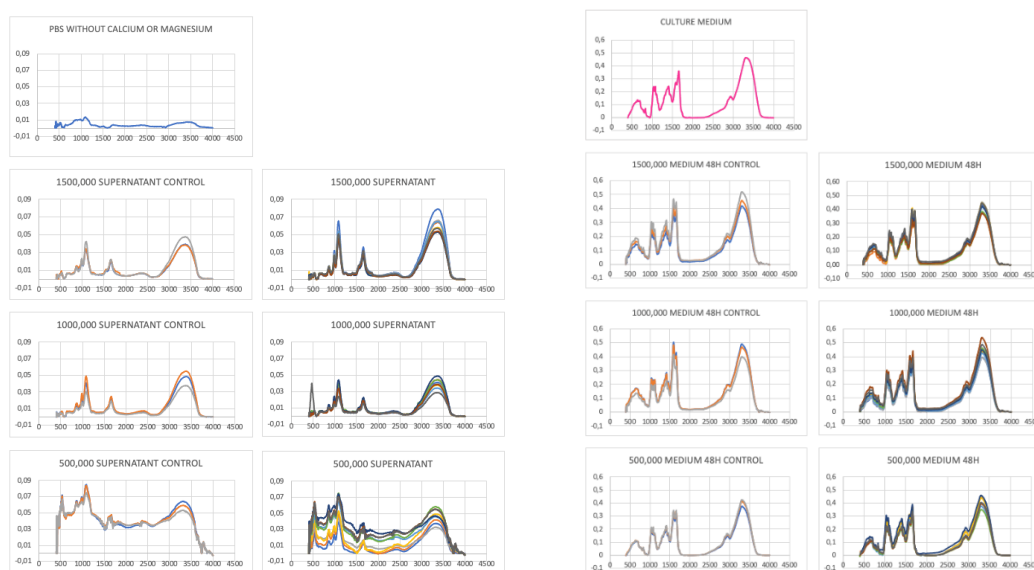


Figure 5.25. Left: Spectra of DPBS immediately after PEF, when compared with the control groups and DPBS not exposed to cells or PEF. Right: Spectra of culture media immediately after PEF, when compared with the control groups and medium not exposed to cells or PEF.

5.4.3. Second Assay (t=48h)

The assay started with the total number counted at 48h in culture as presented in table 5.12, i.e. A1 with 1,000,000 cells, A2 800,000 cells, A3 1,100,000 cells, A- 1,200,000, B1 350,000 cells, B2 250,000 cells, B3 700,000 cells, B- 800,000 cells, C1 150,000 cells, C2 200,000 cells, C3 150,000 cells and C- 400,000 cells.

5.4.3.1. Variations in electrical current and temperature increase during PEF application

In table 5.13, as in the first assay, the groups with most cells are the ones that have a lower increase of temperature, but in the second assay, with greater temperature differences (0.3°C to 0.4°C) between groups.

Table 5.13. Second Assay. Groups A; B; C (1,500,000; 1,000,000; 500,000 cells/800µL PBS)

Group	Pulses (P)	Current (A)	Voltage (V)	t_{on} (µs)	Frequency (Hz)	Energy Field (kV/cm)	W (J)	Wt (J)	Ws (kJ/kg)	ΔT (C°)	ΔT (C°) average	
A1	1°	12	4000	5	1	10 KV/cm	0.2	0.2	0.3	0.1	4.4	
	2°	250	4000	5	1	10 KV/cm	5.0	10.0	12.5	3.0		
	3°	253	4000	5	1	10 KV/cm	5.1	15.2	19.0	4.5		
	4°	256	4000	5	1	10 KV/cm	5.1	20.5	25.6	6.1		
	5°	268	4000	5	1	10 KV/cm	5.4	26.8	33.5	8.0		
A2	1°	12	4000	5	1	10 KV/cm	0.2	0.2	0.3	0.1		
	2°	251	4000	5	1	10 KV/cm	5.0	10.0	12.6	3.0		
	3°	256	4000	5	1	10 KV/cm	5.1	15.4	19.2	4.6		
	4°	265	4000	5	1	10 KV/cm	5.3	21.2	26.5	6.3		
	5°	265	4000	5	1	10 KV/cm	5.3	26.5	33.1	7.9		
A3	1°	12	4000	5	1	10 KV/cm	0.2	0.2	0.3	0.1		
	2°	256	4000	5	1	10 KV/cm	5.1	10.2	12.8	3.1		
	3°	257	4000	5	1	10 KV/cm	5.1	15.4	19.3	4.6		
	4°	262	4000	5	1	10 KV/cm	5.2	21.0	26.2	6.3		
	5°	270	4000	5	1	10 KV/cm	5.4	27	33.8	8.1		
B1	1°	11	4000	5	1	10 KV/cm	0.2	0.2	0.3	0.1		
	2°	271	4000	5	1	10 KV/cm	5.4	10.8	13.6	3.2		
	3°	272	4000	5	1	10 KV/cm	5.4	16.3	20.4	4.9		
	4°	280	4000	5	1	10 KV/cm	5.6	22.4	28.0	6.7		
	5°	283	4000	5	1	10 KV/cm	5.7	28.3	35.4	8.5		
B2	1°	13	4000	5	1	10 KV/cm	0.3	0.3	0.3	0.1	4.7	
	2°	271	4000	5	1	10 KV/cm	5.4	10.8	13.6	3.2		
	3°	276	4000	5	1	10 KV/cm	5.5	16.6	20.7	5.0		
	4°	281	4000	5	1	10 KV/cm	5.6	22.5	28.1	6.7		
	5°	288	4000	5	1	10 KV/cm	5.8	28.8	36	8.6		
B3	1°	12	4000	5	1	10 KV/cm	0.2	0.2	0.3	0.1		
	2°	271	4000	5	1	10 KV/cm	5.4	10.8	13.6	3.2		
	3°	281	4000	5	1	10 KV/cm	5.6	16.9	21.1	5.0		
	4°	283	4000	5	1	10 KV/cm	5.7	22.6	28.3	6.7		
	5°	291	4000	5	1	10 KV/cm	5.8	29.1	36.4	8.7		
C1	1°	264	4000	5	1	10 KV/cm	5.3	5.3	6.6	1.6		5.1
	2°	270	4000	5	1	10 KV/cm	5.4	10.8	13.5	3.2		
	3°	274	4000	5	1	10 KV/cm	5.5	16.4	20.6	4.9		
	4°	280	4000	5	1	10 KV/cm	5.6	22.4	28.0	6.7		
	5°	304	4000	5	1	10 KV/cm	6.1	30.4	38.0	9.1		
C2	1°	11	4000	5	1	10 KV/cm	0.2	0.2	0.3	0.1		
	2°	292	4000	5	1	10 KV/cm	5.8	11.7	14.6	3.5		
	3°	293	4000	5	1	10 KV/cm	5.9	17.6	22.0	5.3		
	4°	301	4000	5	1	10 KV/cm	6.0	24.1	30.1	7.2		
	5°	310	4000	5	1	10 KV/cm	6.2	31.0	38.8	9.3		
C3	1°	13	4000	5	1	10 KV/cm	0.3	0.3	0.3	0.1		
	2°	290	4000	5	1	10 KV/cm	5.8	11.6	14.5	3.5		
	3°	294	4000	5	1	10 KV/cm	5.9	17.6	22.1	5.3		
	4°	301	4000	5	1	10 KV/cm	6.0	24.1	30.1	7.2		
	5°	304	4000	5	1	10 KV/cm	6.1	30.4	38.0	9.1		

5.4.3.2. Cells counting and viability

Table 5.14 shows cell counting by trypan blue exclusion method, for the second assay. For group A, immediately after PEF application, the average cells viability was 68.8% and the cell lysis was 55.9%, for group B, the average viability was 55% and the cell lysis was 38.5%, for group C the cell cells viability was 17.6% and the cell lysis was 32%. Higher cell viability was observed again in groups with higher cells concentrations.

After 48hrs of the 2nd PEF application (i.e. at 96h since the first assay), the total number of cells were 64.4%, 76.7% and 73.3% lower for gr After 48hrs of the 2nd PEF application (i.e. at 96h since the first assay), the total number of cells were 64.4%, 76.7% and 73.3% lower for group A, B and C, respectively. Average cells viability at 96h were higher in groups with higher cells concentrations, existing a significant difference between viability between 1,500,000 cells and 500,000 cells.

Table 5.14. Cell counting by a trypan blue exclusion method, immediately after PEF and 48h after.

Trypan Blue exclusion method assay (Hemocytometer – Neubauer chamber – counting)													
Experimental Groups		Dilution			Before PEF (t=0h)	After 2 nd PEF application (t=48h)				48h after 2 nd PEF application (t _{culture} =96h)			
		DF	Cellular volume (μL)	Trypan Blue volume (μL)		Total number of viable cells	Total number of cells (in 800μL)	Number of viable cells (in 800μL)	Number of dead cells (in 800μL)	Number of completed lysed cells (in 800μL)	Total number of cells (in 1000μL)	Number of viable cells (in 1000μL)	Number of dead cells (in 1000μL)
A	A1	10	10	90	1.5x10 ⁶	320,000	240,000	80,000	680,000	400,000	300,000	100,000	56.3
	A2					480,000	320,000	160,000	320,000	400,000	400,000		
	A3					480,000	320,000	160,000	620,000	400,000	200,000	200,000	
	A-					1,120,000	1,040,000	80,000	80,000	500,000	500,000	0	
B	B1	5	20	80	1x10 ⁶	320,000	160,000	160,000	30,000	100,000	100,000	0	50
	B2					120,000	40,000	80,000	130,000	300,000	150,000	150,000	
	B3					360,000	240,000	120,000	340,000	300,000	100,000	200,000	
	B-					760,000	720,000	40,000	40,000	450,000	400,000	50,000	
C	C1	2.5	40	60	5x10 ⁵	120,000	80,000	40,000	30,000	150,000	50,000	100,000	37.5
	C2					100,000	40,000	60,000	100,000	150,000	75,000	75,000	
	C3					120,000	60,000	60,000	30,000	100,000	25,000	75,000	
	C-					420,000	380,000	40,000	0	475,000	425,000	50,000	

5.4.3.3. FTIR spectroscopy

The FTIR spectra of supernatant was different between the assay with 500,000 cells relatively to the corresponding control and to the other two groups, indicating a higher susceptibility of this group to PEF application.

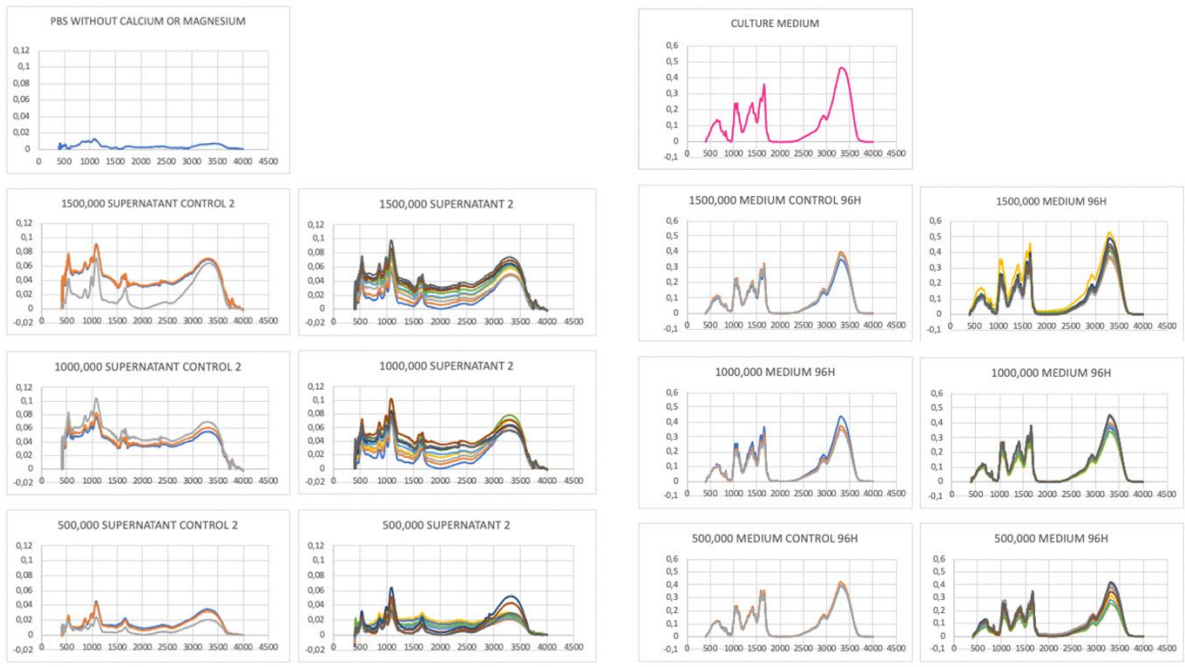


Figure. 5.26. Left: Spectra of DPBS immediately after the 2nd repetition of PEF, when compared with the control groups and DPBS not exposed to cells or PEF. Right: Spectra of culture media of the 2nd assay, when compared with the control groups and medium not exposed to cells or PEF.

5.4.4. Third Assay

The assay started with the total number counted at 96h in culture represented in table 5.12, i.e. A1 with 400,000 cells, A2 800,000 cells, A3 400,000 cells, A- 500,000, B1 100,000 cells, B2 300,000 cells, B3 300,000 cells, B- 450,000 cells, C1 150,000 cells, C2 150,000 cells, C3 100,000 cells and C- 475,000 cells.

5.4.4.1. Variations in electrical current and temperature increase during PEF application

The third assay has unexpected results (table 5.15), due to plasma membrane lysis. So, it is not so visible the difference of temperature increase like is seen in the first and second trial. As such, it could be concluded that PEF exposure for more than three repetitions in intervals less than 48h has major effects on cell viability and proliferation and in cell overheating.

Table 5.15. Third Assay. Groups A; B; C (1,500,000; 1,000,000; 500,000 cells/800µL PBS)

GROUP	PULSES (P)	CURRENT (A)	VOLTAGE (V)	T _{ON} (µS)	FREQUENCY (HZ)	ENERGY FIELD (KV/CM)	W (J)	WT (J)	WS (KJ/KG)	ΔT (C°)	ΔT (C°) average
A ₁	1°	13	4000	5	1	10 KV/cm	0.3	0.3	0.3	0.1	4.9
	2°	268	4000	5	1	10 KV/cm	5.4	10.7	13.4	3.2	
	3°	275	4000	5	1	10 KV/cm	5.5	16.5	20.6	4.9	
	4°	276	4000	5	1	10 KV/cm	5.5	22.1	27.6	6.6	
	5°	286	4000	5	1	10 KV/cm	5.7	28.6	35.8	8.6	
A ₂	1°	13	4000	5	1	10 KV/cm	0.3	0.3	0.3	0.1	
	2°	276	4000	5	1	10 KV/cm	5.5	11.0	13.8	3.3	
	3°	282	4000	5	1	10 KV/cm	5.6	16.9	21.2	5.1	
	4°	284	4000	5	1	10 KV/cm	5.7	22.7	28.4	6.8	
	5°	286	4000	5	1	10 KV/cm	5.7	28.6	35.8	8.6	
A ₃	1°	283	4000	5	1	10 KV/cm	5.7	5.7	7.1	1.7	
	2°	284	4000	5	1	10 KV/cm	5.7	11.4	14.2	3.4	
	3°	293	4000	5	1	10 KV/cm	5.9	17.6	22.0	5.3	
	4°	295	4000	5	1	10 KV/cm	5.9	23.6	29.5	7.1	
	5°	295	4000	5	1	10 KV/cm	5.9	29.5	36.9	8.8	
B ₁	1°	11	4000	5	1	10 KV/cm	0.2	0.2	0.3	0.1	
	2°	280	4000	5	1	10 KV/cm	5.6	11.2	14.0	3.4	
	3°	282	4000	5	1	10 KV/cm	5.6	16.9	21.2	5.1	
	4°	286	4000	5	1	10 KV/cm	5.7	22.9	28.6	6.8	
	5°	293	4000	5	1	10 KV/cm	5.9	29.3	36.6	8.8	
B ₂	1°	13	4000	5	1	10 KV/cm	0.3	0.3	0.3	0.1	
	2°	280	4000	5	1	10 KV/cm	5.6	11.2	14.0	3.3	
	3°	282	4000	5	1	10 KV/cm	5.6	16.9	21.2	5.1	
	4°	291	4000	5	1	10 KV/cm	5.8	23.3	29.1	7.0	
	5°	293	4000	5	1	10 KV/cm	5.9	29.3	36.6	8.8	
B ₃	1°	11	4000	5	1	10 KV/cm	0.2	0.2	0.3	0.1	
	2°	284	4000	5	1	10 KV/cm	5.7	11.4	14.2	3.4	
	3°	287	4000	5	1	10 KV/cm	5.7	17.2	21.5	5.2	
	4°	293	4000	5	1	10 KV/cm	5.9	23.4	29.3	7.0	
	5°	296	4000	5	1	10 KV/cm	5.9	29.6	37.0	8.9	
C ₁	1°	11	4000	5	1	10 KV/cm	0.2	0.2	0.3	0.1	
	2°	260	4000	5	1	10 KV/cm	5.2	10.4	13.0	3.1	
	3°	279	4000	5	1	10 KV/cm	5.6	16.7	20.9	5.0	
	4°	285	4000	5	1	10 KV/cm	5.7	22.8	28.5	6.8	
	5°	291	4000	5	1	10 KV/cm	5.8	29.1	36.4	8.7	
C ₂	1°	12	4000	5	1	10 KV/cm	0.2	0.2	0.3	0.1	
	2°	260	4000	5	1	10 KV/cm	5.2	10.4	13.0	3.1	
	3°	274	4000	5	1	10 KV/cm	5.5	16.4	20.6	4.9	
	4°	276	4000	5	1	10 KV/cm	5.5	22.1	27.6	6.6	
	5°	288	4000	5	1	10 KV/cm	5.8	28.8	36	8.6	
C ₃	1°	12	4000	5	1	10 KV/cm	0.2	0.2	0.3	0.1	
	2°	279	4000	5	1	10 KV/cm	5.6	11.2	14.0	3.3	
	3°	288	4000	5	1	10 KV/cm	5.8	17.3	21.6	5.2	
	4°	296	4000	5	1	10 KV/cm	5.9	23.7	29.6	7.1	
	5°	300	4000	5	1	10 KV/cm	6.0	30.0	37.5	9.0	

5.4.4.2. Cells counting and viability

Cell viability after immediately after the third assay decreased significantly for group A, with 36.4% of viable cells and 45% of cell lysis after PEF application (table 5.16). For group B average viability was 33.3% and cell lysis was 40%. For group C the average viability was 18.2% and cell lysis 45%.

Table 5.16. Cell counting by a trypan blue exclusion method, immediately after PEF and 48h after.

Trypan Blue exclusion method assay (Hemocytometer – Neubauer chamber – counting)													
Experimental Groups		Dilution			Before PEF	After 3 rd PEF application (t _{culture} =96h)				48h after 3 rd PEF application (t _{culture} =144h)			
		DF	Cellular volume (μL)	Trypan Blue volume (μL)		Total number of viable cells	Total number of cells (in 800μL)	Number of viable cells (in 800μL)	Number of dead cells (in 800μL)	Number of completed lysed cells (in 800μL)	Total number of cells (in 1000μL)	Number of viable cells (in 1000μL)	Number of dead cells (in 1000μL)
A	A1	10	10	90	1.5x10 ⁶	240,000	80,000	160,000	160,000	200,000	150,000	50,000	50
	A2					240,000	160,000	80,000	560,000	200,000	100,000	100,000	
	A3					400,000	80,000	320,000	0	300,000	100,000	200,000	
	A-					480,000	240,000	240,000	200,000	500,000	500,000	0	
B	B1	5	20	80	1x10 ⁶	160,000	40,000	120,000	0	100,000	50,000	150,000	33.3
	B2					240,000	80,000	160,000	60,000	150,000	25,000	125,000	
	B3					80,000	40,000	40,000	220,000	200,000	75,000	125,000	
	B-					320,000	160,000	160,000	130,000	400,000	400,000	0	
C	C1	2.5	40	60	5x10 ⁵	80,000	20,000	60,000	70,000	50,000	15,000	35,000	20
	C2					100,000	20,000	80,000	50,000	25,000	0	25,000	
	C3					40,000	0	40,000	60,000	0	0	0	
	C-					220,000	200,000	20,000	225,000	425,000	400,000		

As in the other assays, cell viability remains to decrease as smaller numbers of cells are electroporated.

Cell proliferation was studied at 144h after the first assay, and 48h after the third assay. The total number of cells were 84.4% lower than the expected number of 1,500,000 cells for group A, group B was 85% lower than 1,000,000 cells, and group C was 95% lower than 500,000 cells. These results show the impact of PEF in cell proliferation. Every time PEF is applied in sequential repetitions there are significant changes in the cell.

Cell viability of cells in culture was also lower when compared to the first assay.

5.4.4.3. FTIR spectroscopy

The FTIR spectra of supernatant of the group with 1,500,000 cells and 1,000,000 cells, after the third PEF application, did not present significant difference between them and the control, being the most noticeable differences observed in the FTIR spectra of the culture at 144h relative to the group with 1,500,000 cells.

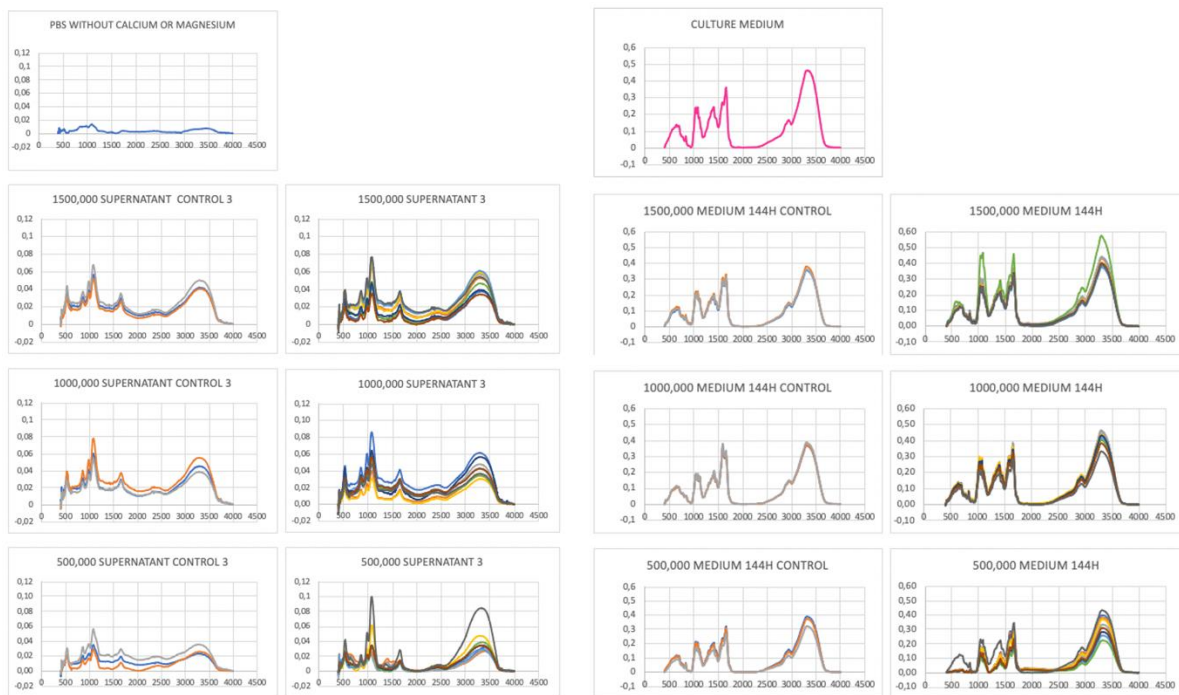


Figure 5.27. Left: Spectra of DPBS immediately after the 3rd repetition of PEF, when compared with the control groups and DPBS not exposed to cells or PEF. Right: Spectra of culture media of the 3rd assay, when compared with the control groups and medium not exposed to cells or PEF.

5.4.5. Conclusions

Experiment 3 has interesting results that allows to study the impact of repeated PEF on cell metabolism and proliferation. It could be inferred a direct link between cell number and repeated PEF in temperature increase, in cell metabolism and consequent proliferation.

Table 5.17 represents the percentage of number of cells and cells viability of each group of experience in relation to the negative control experiment. It was observed that a higher cells number and cells viability was observed with groups of experiments with the highest cell's densities. This was independent of the number of PEF applications. It was also observed that along the successive PEF experiments, and due to cells lysis, the number of cells reduced and were progressively lower than theoretically aimed. For example, for group A1, the 1st, 2nd and 3rd PEF assays were applicable to a cell density of 1500000, 1000000 and 400000, respectively. Consequently, part of the results is also due to the decrease cells density along consecutive PEF assays.

Table 5.17. Percentage of average number of cells and cells viability in relation to the control assay, of group of experiments with different cells density in relation to the assay without PEF and along three consecutive PEF applications.

Cells used in the assay	Average cells (n=3) after PEF	Standard deviation (n=3) of cells after PEF	Average cells viability (n=3) after PEF	Standard deviation of cells viability (n=3) after PEF
1st Assay				
1500 000	82	20	91	4
1000 000	89	13	78	8
500 000	67	11	78	11
2nd Assay				
1500 000	38	8	75	5
1000 000	35	17	53	18
500 000	27	3	57	15
3rd Assay				
1500 000	61	19	80	48
1000 000	50	25	72	25
500 000	33	14	17	15

Concerning the ANOVA of the sum of absorbance of spectra between a defined group and its control experiment, the following significative differences at 5% were observed:

- In the first assay, was significative different the supernatant analysis of the assays based on 1,500,000 and 500,000 cells in relation to the corresponding controls; the pellet analysis resulted in all assays being significant different in relation to the corresponding control; after 48 h of culture, only the assay based on 1,500,000 cells was significantly different in relation to its control;
- In the second assay, was significative different the supernatant analysis of the assays based on 1,000,000 in relation to the corresponding control; the pellet analysis resulted in all assays being significant different in relation to the corresponding control; after 48 h of culture, only the assay based on 1,500,000 cells was significantly different in relation to its control; after 48 h of culture, no assay was significantly different in relation to the corresponding control;
- In the third assay, only the pellet spectra of the assay with 1,500,000 was significantly different in relation to the control.

The influence of PEF application according to the cell's concentration on the assay, was also observed along PCA of spectra (Fig. 5.29). It was observed that results obtained along the diverse assays conducted with the lowest cells concentration (i.e. 500,000) presented in a totally different cluster than experiments conducted with higher cells concentrations.

The PCA also highlighted the PEF effect on the experiments, as clusters of data from samples submitted to PEF were in a different space that its corresponding assay without submitted to PEF (Fig. 5.29). These results were highlighted with pellet spectra. It was also observed that the differences of cells concentration were not so visible after 3 PEF applications, most probably reflecting either the cumulative effect of PEF application either the limitations associated to obtain the desired cells concentration on the PEF assay. These observations were according to ANOVA of the sum of absorbances.

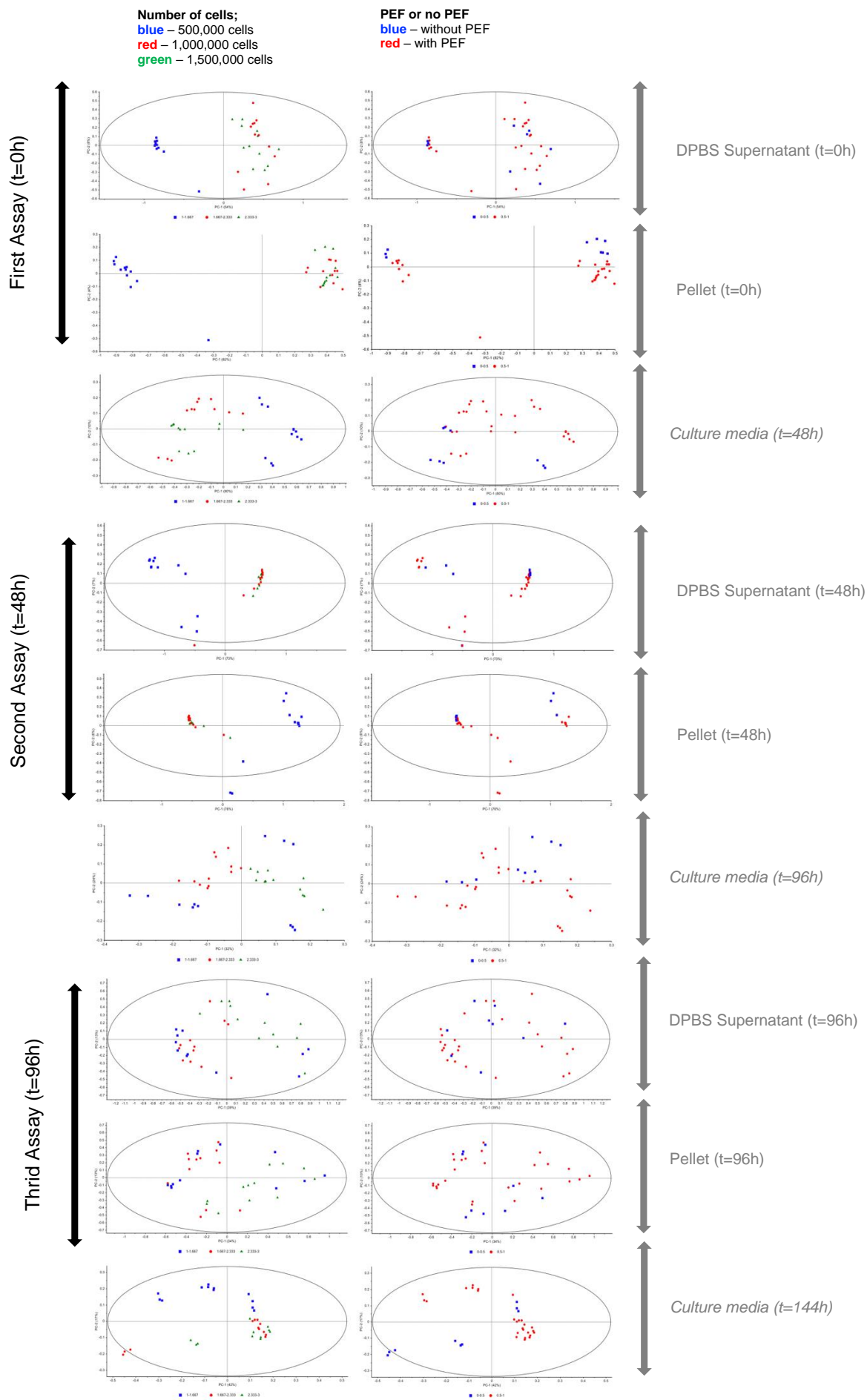


Figure 5.28. PCA of normalized second derivative FTIR spectra of supernatant DPBS, pellet and Culture medium of 1st assay, 2nd assay and 3rd assay.

[This page is intentionally left blank]

Chapter 6

6. Conclusions & Future Work

Conclusions and future work

The present work is highly interdisciplinary, including electrical and biological engineering, and consequently presents several challenges. The main goal was to study the influence of applying pulsed electric fields, PEF, to *in vitro* fibroblast cells, considering different conditions, to observe if there was, in the one hand a cell lysis and consequently death or, in the other hand, survival of cells and changes in their metabolic status and proliferation. The first experiment intended to explore four conditions of PEF with varied pulses and energy fields when compared to the negative control group, the second experiment intended to understand the influence of the number of cells in the electrical field, and the third experiment aimed to evaluate the impact of repeated PEF application to the same cells.

For all PEF experiments the same solution was chosen to resuspend the cells and electroporate, Dulbecco-PBS without magnesium or calcium, due to its conductivity that is similar to water (5.5 mS/cm), while enabling an isotonic environment for fibroblasts. It was also decided to place the samples at 4°C, 10 minutes before each test, to standardize the metabolism and partially inhibit the cells metabolism to reduce the impact of having cells outside the CO₂ cabinet.

All PEF experiments seemed to be unrelated but ultimately each experiment influenced the experiment that followed.

With experiment 1, where the same number of fibroblasts, i.e. 100,000, was used for all groups, it was possible to draw important connections about the energy field and also about the number of impulses to be applied to this biological sample. The number of pulses significantly influences the specific energy and, consequently, the temperature increase of the sample, when at (or above) 20 pulses, the cells media increases 26.7°C and leads to an average viability of 14.2% and 51.2% immediately or 72hrs after PEF application. In turn, it was also observed that the energy field also influences the temperature of the sample, were above 15kV/cm, the temperature increase of 13.8°C, lead to cells average viability of 9.9% and 46.9%, immediately or after 72hrs of PEF application, respectively. It was also noticed that the acceptable energy field in relation to the temperature increase is 10kV/cm, with a number of pulses between 2 and 10P, with a viability between 80.8% and 94.3% for these groups immediately after PEF application. It was observed that all PEF conditions evaluated had an impact on cells metabolism, resulting even in some cases in whole cell lysis or even impairing the cells viability and metabolism with high impact on cells proliferation.

Thus, based on experiment 1, an energy field of 10kV/cm and a number of pulses of 5P (value between 2 and 10P) were chosen for the other two experiments, and some other conditions had to change, like the volume of solution to electroporate, that passed from 1000µL to 800µL, since there was a small cell volume that was not exposed to the electric field because it overlapped the electrodes of the electroporation cuvette. The plate used for FTIR analysis also changed, from 96 wells to 384 wells, since it allows to save biological sample and to make triplicates measurements of each sample.

In experiment 2, diverse cells concentrations were evaluated, with a corresponding negative (i.e. not submitted to PEF) and a positive (i.e. with cell lysis by cycles of thermal shock) control groups. Regarding the heating of the it, it was noticed that it decreases as the number of cells per cuvette increases, being the groups with higher cells densities, i.e. of 1,000,000 and 500,000 cells the least affected with temperature increase. According to data, these cells groups were also the less affected by PEF concerning cells lysis and cell viability and cells proliferation after 72h oof PEF application.

Based on experiment 2, in experiment 3, was evaluated 1,000,000 and 500,000 cells, and a higher density group with 1,500,000 cells, and the corresponding negative controls. It was observed that cell metabolism undergoes drastic changes when it comes to PEF repetitions with intervals of only 48h. The ideal time between PEF applications should be of 72h or above because it was observed in the previous experiments that cells started to recover after 48h, and their metabolism restored at 72h.

Due to the variability associated to the present biological system (i.e. the cell line and cell culture protocol) a higher number of replicate experiments, including the control groups, should have been conducted. The third experiment should be repeated to ensure the application of successive PEF with the same cell densities.

Regarding statistical data, *p-values* inferior to 10% were present in most experiments, validating this way the initial hypothesis. To support the conclusion, PCA of all experiments showed the scores of the triplicate samples are near each other and apart from other assays samples, implying that the assays are reproducible.

The study itself presented the limitations and bias of an *in vitro* research and the surprise factor of an innovative research. Innovation meets the unexpected, but it is also in innovation that the collected data allow not only the present works but also the starting point for future works.

In the future, these *in vitro* studies could be optimised in terms of protocol and explored using other type of connective tissue cells.

Personal Reflexion and turning points

The learning curve for working with animal cells and mastering cell culture took some time. Unlike microorganisms as *Escherichia coli* and *Saccharomyces cerevisiae*, animal cells do not have a cell wall - they only have the plasma membrane in direct contact with the extracellular medium - and as such they are more susceptible to mechanical shocks. Besides the longer period of growth also increases the contamination risk.

When I started this work, the initial idea was to study the reaction of chondrocytes when exposed to an electric field and see if there were significant changes in their metabolic status, for the future purpose of regenerating chondral lesions. However, this initial idea will undergo several metamorphoses throughout the investigation process, as new data also emerge. The final work is distant from what I initially projected, but this does not prevent it from serving as a base or reference for future studies with chondrocytes.

During research, I came across a new way of delivering energy, very specific and with a more controlled application, which implied less heating of biological samples. This process is called Pulsed Power and consists of storing energy for a large amount of time and applying controlled impulses in a small amount of time. This allows an application of electric fields with less overheating, which makes it ideal for experiments with cells. Fortunately, this is a type of technology that is manufactured in Portugal and the equipment was available for this research.

Since chondrocytes are difficult lines to obtain and to maintain, I chose to reformulate the initial idea, choosing, then, another type of cell of the connective tissue, highly producer of extra cellular matrix, less demanding in culture, more resistant and with greater predominance in the mammalian organism - the Fibroblast.

I hope that this work represents the basis for many future works, and that I and others can learn from my failures. I've learned a lot from the breakthroughs, but I learned so much more from my mistakes and frustrations.

Chapter 7

7. Bibliography

1. Seeley RR, Stephens TD, Tate P. *Anatomy & Physiology*. McGraw-Hill, 2017.
2. Junqueira L, Carneiro J. *Basic Histology: Text & Atlas*. McGraw-Hill, 2018.
3. Ovalle W, Nahirney P. *Netter's Essential Histology*. Elsevier Saunders, 2013.
4. Lautenschlaeger F. Cell compliance: cytoskeletal origin and importance for cellular function. PhD dissertation, University of Cambridge, 2011.
5. Kozlov MM. Some aspects of membrane elasticity. *Soft Condensed Matter Physics in Molecular and Cell Biology*. Poon WCK and Andelman D eds. CRC Press, 2006.
6. Whalley NA, Walters S, Hammond K. *Molecular Cell Biology. Molecular Medicine for Clinicians*, Wits Univ. Press, 2018.
7. Takahashi K, Tanabe K, Ohnuki M, Narita M, Ichisaka T, Tomoda K, et al. Induction of Pluripotent Stem Cells from Adult Human Fibroblasts by Defined Factors. *Cell*, 131:861-72, 2007.
8. Dick MK, Limaie F. *Histology, Fibroblast*. StatPearls Publishing, 2020.
9. [Internet]. Chemistry Libretexts™ - Lipid bilayer membrane [cited August 2019]. Available from: [https://chem.libretexts.org/Bookshelves/Biological_Chemistry/Supplemental_Modules_\(Biological_Chemistry\)/Lipids/Applications_of_Lipids/Lipid_Bilayer_Membranes/](https://chem.libretexts.org/Bookshelves/Biological_Chemistry/Supplemental_Modules_(Biological_Chemistry)/Lipids/Applications_of_Lipids/Lipid_Bilayer_Membranes/)
10. Robert A, Freitas J. *Nanomedicine, Volume I: Basic Capabilities*, Landes Bioscience, Georgetown, TX, 1999.
11. Alberts B, Johnson A, Lewis J, et al. *Fibroblasts and Their Transformations: The Connective - Tissue Cell Family*. *Molecular Biology of the Cell*. 4th edition. Garland Science, New York, 2002.
12. [Internet]. Fibroblast Cell Applications. [cited February 2020]. Available from: <https://cellapplications.com/fibroblast/>
13. Darby IA, Hewitson TD. Fibroblast Differentiation in Wound Healing and Fibrosis. *Int Rev Cyt*, 257:143-179, 2007.
14. Redondo LM, Silva JF. Repetitive high-voltage solid state Marx modulator design for various load conditions. *IEEE Trans Plasma Sci*, 37(8):1632-1637, 2009.
15. Redondo LM, Silva JF, Margato E. Analysis of a modular generator for high-voltage, high-frequency pulsed applications, using low voltage semiconductors (1kV) and series connected step-up (1:10) transformers. *Rev Sci Instrum*, 78(3):034702, 2007.
16. Redondo LM. *Basic Concepts of High-Voltage Pulse Generation*. Springer International Publishing AG, 1-19, 2017.
17. Kotnik T, Kramar P, Pucihar G, Miklavčič D, Tarek M. Cell membrane electroporation - Part 1: The phenomenon. *IEEE Electr Insul Mag*, 255:14-23, 2012.
18. [Internet]. LUMEN Anatomy and Physiology, I [cited February 2020]. Available from: <https://courses.lumenlearning.com/cuny-csi-ap-1/chapter/membranes/>
19. Kotnik T, Frey W, Sack M, Meglič SH, Peterka M, Miklavčič D. Electroporation-based applications in biotechnology. *Trends Biotechnol*, 33, 480–488, 2015.
20. Ivorra A, Rubinsky B. Historical Review of Irreversible Electroporation in Medicine. In: Rubinsky B. (eds) *Irreversible Electroporation*. Series in Biomedical Engineering. Springer, Berlin, Heidelberg, 2010.
21. Mahnič-Kalamiza S, Vorobiev E, Miklavčič D. Electroporation in Food Processing and Biorefinery. *J. Membr. Biol.* 247:1279-1304, 2014.
22. Freshney RI. *Culture of animal cells. A manual of basic technique and specialized applications*. 6 ed. New Jersey: John Wiley & Sons, 2010.
23. Rebello MA. *Fundamentos da Cultura de Tecido e Células Animais*. 1st ed. Rio de Janeiro: Rubio, 41-52, 2014.
24. [Internet]. ATCC ® In partnership with LGC standards [cited April 2019]. Available from: <https://www.lgcstandards-atcc.org/>

25. Slack JMW. Molecular Biology of the Cell. Principles of Tissue Engineering, 4th edition, Elsevier Inc., 127–145, 2013.
26. Driskell RR, Lichtenberger BM, Hoste E, Kretzschmar K, Simons BD, Charalambous M, et al. Distinct fibroblast lineages determine dermal architecture in skin development and repair. *Nature*, 504:277-281, 2013.
27. Sanford KK, et al. The growth in vitro of single isolated tissue cells. *J Natl Cancer Inst*, 9:229-246, 1948.
28. Schafer KA. The cell cycle: a review. *Vet Pathol*, 35(6):461-78,1998.
29. [Internet]. Phosphate-buffered saline (PBS). Cold Spring Harb Protoc, 2006 [cited May 2019]. Available from: <http://cshprotocols.cshlp.org/content/2006/1/pdb.rec8247/>
30. Philippeos C, Hughes RD, Dhawan A, Mityr RR. Introduction to Cell Culture. Mityr R, Hughes R (eds) *Human Cell Culture Protocols. Methods in Molecular Biology (Methods and Protocols)*, vol 806. Humana Press. 2012.
31. Chua F, Laurent GJ. Fibroblasts. *Encyclopedia of Respiratory Medicine, Four-Volume*, Elsevier Saunders, 2006.
32. Villegas J, McPhaul M. Establishment and culture of human skin fibroblasts. *Curr Protoc Mol Biol*, Chapter 28: Unit 28.3, 2005.
33. [Internet]. Eppendorf Handling Solution [cited 2019 April]. Available from: <https://handling-solutions.eppendorf.com/sample-handling/centrifugation/safe-use-of-centrifuges/basics-in-centrifugation/>
34. Redondo LM, Silva JF. Chapter 26: Solid state pulsed power electronics. *Power Electronics Handbook*, 3rd ed. Butterworth-Hinemann Publishing, Elsevier, USA, pp 669-710, 2010.
35. Redondo LM, Silva JF. Flyback versus forward switching power supply topologies for unipolar pulsed power applications. *IEEE Trans Plasma Sci* 37(1):171-178, 2009.
36. [Internet]. Breathing Labs [cited May 2020]. Available from: <https://www.breathinglabs.com/monitoring-feed/electroporation/electroporation-ewrs2018-org/>
37. VWR Part of avantor [cited 2020 April]. Available from: <https://pt.vwr.com/>
38. Haberl S, Miklavčič D et al. Cell membrane electroporation - Part 2: The Applications. *IEEE Electr. Insul. Mag.* 29(1):29-37, 2013.
39. Rocha CMR, Genisheva Z, Ferreira-Santos P, Rodrigues R, Vicente AA, Teixeira JA, Pereira RN. Electric field-based technologies for valorization of bioresources. *Bioresource Technology*, 254:325–339, 2018.
40. Pereira MT, Rego DS, Redondo LMS. Advantages of Pulsed Electric Field Use for Treatment of Algae. Miklavcic D. (eds) *Handbook of Electroporation*. Springer, Cham, 2016.
41. Campbell KH, McWhir J, Ritchie WA, Wilmut I. Sheep cloned by nuclear transfer from a cultured cell line. *Nature*, 380, 64-66, 1996.
42. Napotnik TB, Miklavčič D. *In vitro* electroporation detection methods – An overview. *Bioelectchem*, 120:166–182,2017.
43. Sherba JJ, Hogquist S, Lin H, Shan JW, Shreiber DI, Zahn JD. The effects of electroporation buffer composition on cell viability and electro-transfection efficiency. *Scient Rep*, 10(1):3053, 2020.
44. Napotnik TB, Reberšek M, Miklavčič D et al. Effects of high voltage nanosecond electric pulses on eukaryotic cells (*in vitro*): A systematic review. *Bioelectchem*, 110:1–12, 2016.
45. Xiao S, Guo S, Nesin V, Heller R, Schoenbach KH. Subnanosecond Electric Pulses Cause Membrane Permeabilization and Cell Death. *IEEE Trans Biomed Eng*, 58(5):1239-1245, 2011.
46. Golberg A, Bei M, Sheridan RL, Yarmush ML. Regeneration and control of human fibroblast cell density by intermittently delivered pulsed electric fields. *Biotechnol Bioeng*, 110(6):1759-68, 2013.
47. Schoenbach KH, Peterkin FE, Alden RW, Beebe SJ. The effect of pulsed electric fields on biological cells: experiments and applications. *IEEE Trans Plasma Sci*, 25(2):284-292, 1997.
48. Xiao S, Semenov I, Petrella R, Pakhomov AG, Schoenbach KH. A subnanosecond electric pulse exposure system for biological cells. *Med Biol Eng Comput*, 55(7):1063–1072, 2017.
49. Vadlamani RA, Nie Y, Detwiler DA, Dhanabal A, Kraft AM, Kuang S, et al. Nanosecond pulsed electric field induced proliferation and differentiation of osteoblasts and myoblasts. *J R Soc Interface*, 16(155):20190079, 2019.

50. Soueid M, Dobbelaar MCF, Bentouati S et al. Delivery devices for exposure of biological cells to nanosecond pulsed electric fields. *Med Biol Eng Comput*, 56(1):85–97, 2017.
51. Frey W, White JA, Price RO, Blackmore PF, Joshi RP, Nuccitelli R, Beebe SJ, Schoenbach KH, Kolb JF. Plasma membrane voltage changes during nanosecond pulsed electric field exposure. *Biophys J*, 90(10):3608–3615, 2006.
52. Mi Y, Li P, Liu Q et al. Multi-Parametric Study of the Viability of *in Vitro* Skin Cancer Cells Exposed to Nanosecond Pulsed Electric Fields Combined with Multi-Walled Carbon Nanotubes. *Technol Cancer Res Treat*, 18:1-10, 2019.
53. Corovic S, Lackovic I, Miklavčič D et al. Modeling of electric field distribution in tissues during electroporation. *Biomed Eng Online*, 12:16, 2013.
54. Pintar M, Langus J, Miklavčič D et al. Time-Dependent Finite Element Analysis of *In Vivo* Electrochemotherapy Treatment. *Technol Cancer Res Treat*, 17:1-9, 2018.
55. Martin LY, Alexander G, Gregor S, Tadej K, Damijan M. Electroporation-Based Technologies for Medicine: Principles, Applications, and Challenges. *Annual Rev Biomed Eng*, 16(1):295-320, 2014.
56. Rosazza C, Meglic SH, Zumbusch A, Rols MP, Miklavcic D. Gene Electrotransfer: A Mechanistic Perspective. *Curr Gene Ther*, 16(2):98-129, 2016.
57. Neumann E. Membrane electroporation and direct gene transfer. *J Electroanal Chem*, 28:247-267, 1992.
58. Sharma A. Electroporative transdermal drug delivery: Optimization and safety. ProQuest Dissertations and Theses. Pharmacy, Memorial University of Newfoundland, 1998.
59. Zhao Y, Liang R, Yang Y, Lin S. The mechanism of pulsed electric field (PEF) targeting location on the spatial conformation of pine nut peptide. *J Theor Biol*, 492:110195, 2020.
60. Hsu PD, Lander ES, Zhang F. Development and applications of CRISPR-Cas9 for genome engineering. *Cell*, 6:1262-1278, 2014.
61. Dong S, Wang H, Zhao Y, Sun Y, Yao C. First Human Trial of High-Frequency Irreversible Electroporation Therapy for Prostate Cancer. *Technol Cancer Res Treat*, 17:1-9, 2018.
62. Chung TH, Stancampiano A, Sklias K, Gazeli K, André FM, Dozias S, et al. Cell electropermeabilisation enhancement by non-thermal-plasma-treated PBS. *Cancers*, 12(1):2019, 2020.
63. Kirson ED, Gurvich Z, Schneiderman R, Dekel E, Itzhaki A, Wasserman Y, et al. Disruption of Cancer Cell Replication by Alternating Electric Fields. *Cancer Res*, 64:3288-3295, 2004.
64. Rego D, Redondo L et al. Application of pulsed electric fields for the valorization of platelets with no therapeutic value for transfusion medicine. *Technology*, 7(01n02): 40-45, 2019.
65. Stoddart MJ. Cell viability assays: introduction. *Methods in molecular biology* 740:1-6, 2011.
66. Strober, Warren. Trypan Blue Exclusion Test of Cell Viability. *Curr Protoc Immunol*, 111:A3.B.1-A3.B.3, 2019.
67. [Internet]. Michigan State University [cited March 2019]. Available from: <https://www2.chemistry.msu.edu/faculty/huang/Standard%20Operating%20Procedures.pdf/>
68. Cell S. Hemocytometer Protocol. *Natl Sci Found*, 2006.
69. Mascotti K, McCullough J, Burger SR. HPC viability measurement: Trypan blue versus acridine orange and propidium iodide. *Transfusion*, 40(6):693-6, 2000.
70. Kowalczyk D, Pitucha M. Application of FTIR Method for the Assessment of Immobilization of Active Substances in the Matrix of Biomedical Materials. *Materials*, 12(18):2972, 2019.
71. Zhang Q, Zhu Y, Tian Y, et al. Induced Self-Aspiration Electrospray Ionization Mass Spectrometry for Flexible Sampling and Analysis. *Anal Chem*, 92:4600-4606, 2020.
72. Bellisola G, Sorio C. Infrared spectroscopy and microscopy in cancer research and diagnosis. *Am J Cancer Res*, 2(1):1–21, 2012.